The role of CADM1 in energy and glucose homeostasis

Dissertation

Zur Erlangung des akademischen Grades

d o c t o r r e r u m n a t u r a l i u m

(Dr. rer. nat)

im Fach Biologie

eingereicht an der

Mathematisch-Naturwissenschaftliche Fakultät I

der Humboldt-Universität zu Berlin

von

Dipl. Ern.wiss. Dörte Matthäus, geb. Wissmann

Präsident der Humboldt-Universität zu Berlin

Prof. Dr. Jan-Hendrik Olbertz

Dekan der Mathematisch-Naturwissenschaftlichen Fakultät I

Prof. Stefan Hecht, Ph.D.

Gutachter

1.) Prof. Thomas Sommer

2.) Prof. Mathias Treier

3.) Prof. Susanne Klaus

Tag der mündlichen Prüfung: 06.11.2013

Die Arbeit wurde von 11/2008 bis 02/2013 unter der Leitung von Matthew N. Poy, Ph.D. am Max-Delbrück-Centrum für Molekulare Medizin Berlin-Buch durchgeführt.

Table of contents

Abstract

More than 300 million people world-wide are affected by diabetes, the majority suffering from type 2 diabetes. Type 2 diabetes is characterized by insulin resistance, usually caused by obesity and overweight. Enhanced pancreatic insulin secretion largely compensates insulin resistance for years. A failure of pancreatic β-cells to meet increased insulin demands drastically increases blood glucose levels and marks the onset of type 2 diabetes. Besides environmental influences, mainly elevated food intake and reduced physical activity, also genetic mutations are important factors in the pathophysiology of type 2 diabetes.

Recent literature highlights the role of microRNA 375 (miR-375) in the growth and function of pancreatic insulin-producing β-cells. *MiR-375* gene expression is regulated in diabetic humans and rodents, suggesting that this microRNA is involved in the pathogenesis of type 2 diabetes. Genes regulated by miR-375 have been described in pancreatic β-cells. Nevertheless, the exact mechanisms how miR-375 regulates β-cell growth and insulin secretion have not been understood.

Cell adhesion molecule 1 (CADM1) is a known target of miR-375 and has mainly been described as regulator of synapse number and synaptic function in the brain. CADM1 is also expressed in pancreatic β-cells and might regulate β-cell growth and function and might be involved in the control of glucose and energy homeostasis. The aim of this work was to investigate whether CADM1 in pancreatic β-cells or neuronal tissue contributes to the regulation of energy and glucose homeostasis by using total and conditional *Cadm1* deficient mice.

Total *Cadm1* deficient (*Cadm1*KO) mice showed increased sensitivity to glucose and insulin as well as enhanced glucose-stimulated insulin secretion compared to littermate control mice. Elevated glucose-stimulated insulin secretion after *Cadm1* depletion could be confirmed in an *in vitro* β-cell model. In addition, enhanced insulin sensitive was evident in diet and genetic-induced obese *Cadm1*KO mice. Furthermore, *Cadm1*KO mice

showed significantly reduced body weight during postnatal development and adulthood, which was already apparent at four days of age. However, body weight increase of adult *Cadm1*KO mice was unchanged under CHOW diet as well as in diet and genetic-induced obese *Cadm1*KO mice. Male *Cadm1*KO mice further displayed reduced relative body fat content and increased relative lean body mass. Analysis of energy homeostasis yielded increased locomotor activity in male *Cadm1*KO mice. Enhanced insulin and glucose sensitivity as well as reduced body weight and altered body composition could be confirmed in mice with conditional *Cadm1* deficiency only in neuronal and glia cells (*Cadm1NesCre*KO). From these data we conclude that *Cadm1* deficiency enhances β-cell insulin secretion and whole body insulin sensitivity. In addition, CADM1 influences locomotor activity and body composition in male mice, while susceptibility to obesity is not influenced by CADM1 action. Alterations in insulin sensitivity, body weight and body composition are caused by CADM1 action in neuronal or glia cells. The described results indicate that CADM1 might contribute to the development of type 2 diabetes by influencing β-cell insulin secretion and insulin sensitivity.

Zusammenfassung

Mehr als 300 Millionen Menschen sind weltweit von Diabetes betroffen, die Mehrheit davon leidet an Typ-2-Diabetes. Typ-2-Diabetes ist durch eine Insulinresistenz charakterisiert, welche meistens durch Übergewicht und Adipositas verursacht wird. Diese Insulinresistenz kann zunächst durch eine erhöhte pankreatische Insulinsekretion kompensiert werden, jedoch können langfristig die pankreatischen β-Zellen den erhöhten Insulinbedarf nicht mehr decken. Dies verursacht einen starken Anstieg der Blutglucosespiegel und stellt den Beginn der Typ-2-Diabetes Erkrankung dar. Neben genetischen Veränderungen sind Umweltfaktoren, wie erhöhte Nahrungsaufnahme und reduzierte Bewegung, wichtige Faktoren in der Pathogenese des Typ-2-Diabetes.

Frühere Forschungsergebnisse zeigten eine wichtige Rolle von microRNA 375 (miR-375) im Wachstum und in der Funktion der Insulin produzierenden β-Zellen. Die Genexpression von *miR-375* ist in diabetischen Nagetieren und Menschen verändert, was auf eine wichtige Rolle dieser microRNA in der Pathogenese des Typ-2-Diabetes hindeutet. Gene, die durch miR-375 reguliert werden, wurden in den pankreatischen β-Zellen beschrieben, jedoch ist der Mechanismus wie miR-375 das Wachstum und die Funktion der pankreatischen β-Zellen beeinflusst noch nicht im Detail verstanden.

Das Cell Adhesion Molecule 1 (CADM1) ist ein bekanntes Zielgen der miR-375 und vor allem im Gehirn als Regulator von Anzahl und Funktion der Synapsen bekannt. Da es außerdem in den pankreatischen β-Zellen exprimiert ist, könnte es auch dort an der Regulation von β-Zellwachstum und –funktion beteiligt sein und die Glucose- und Energiehomöostase verändern. Ziel dieser Arbeit war es, in vollständig oder konditionell *Cadm1*-defizienten Mäusen den Einfluss von CADM1 in pankreatischen β-Zellen und neuronalem Gewebe an der Regulation von Glucose- und Energiehomöostase zu untersuchen.

Vollständig *Cadm1*-defiziente (*Cadm1*KO)-Mäuse zeigten eine erhöhte Glucose- und Insulinsensitivität, sowie eine vermehrte glucosestimulierte Insulinsekretion im

Vergleich zu Geschwisterkontrolltieren. Eine erhöhte glucosestimulierte Insulinsekretion nach *Cadm1*-Defizienz konnte auch in einem *in vitro* β-Zellmodell gezeigt werden. Eine vermehrte Insulinsensitivität war auch in nahrungs- und genetisch induzierten übergewichtigen *Cadm1*KO-Mäusen nachzuweisen. Außerdem zeigten *Cadm1*KO-Mäuse signifikant reduziertes Körpergewicht im Erwachsenenalter und während der postnatalen Entwicklung, was bereits im Alter von vier Tagen messbar war. Die Körpergewichtszunahme von adulten *Cadm1*KO-Mäusen war jedoch unter CHOW-Fütterung sowie in nahrungs- und genetisch induzierten übergewichtigen *Cadm1*KO-Mäusen unverändert. Männliche *Cadm1*KO-Mäuse hatten zudem einen reduzierten relativen Körperfettgehalt und eine erhöhte relative Muskelmasse. Die Analyse der Energiehomöostase ergab eine erhöhte lokomotorische Aktivität von männlichen *Cadm1*KO-Mäusen. Eine gesteigerte Insulin- und Glucosesensitivität sowie reduziertes Körpergewicht und veränderte Körperzusammensetzung konnte auch in Mäusen mit konditioneller *Cadm1*-Defizienz in Neuronal- und Gliazellen (*Cadm1NesCre*KO) bestätigt werden. Aus diesen Daten kann geschlussfolgert werden, dass *Cadm1*-Defizienz die β-Zellen-Insulinsekretion und die Insulinsensitivität im Körper erhöht. Zudem beeinflusst CADM1 die lokomotorische Aktivität und die Körperzusammensetzung in männlichen Mäusen, während die Prädisposition gegenüber Übergewicht durch CADM1 in beiden Geschlechtern nicht beeinflusst wird. Veränderungen in Insulinsensitivität, Körpergewicht und Körperzusammensetzung werden anscheinend durch den Einfluss von CADM1 in Neuronal- oder Gliazellen verursacht. Diese Ergebnisse deuten darauf hin, dass CADM1 in der Pathogenese von Typ-2-Diabetes beteiligt sein könnte, indem es die Insulinsekretion der β-Zellen und die Insulinsensitivität beeinflusst.

List of Figures

List of Tables

Abbreviations

aCSF ..... Artificial cerebrospinal fluid

ADP ..... Adenosine diphosphate

AGRP ..... Agouti-related protein

AKT ..... V-akt murine thymoma viral oncogene homolog

AMPK ..... 5' Adenosine monophosphate-activated protein kinase

ANCOVA ..... Analysis of covariance

ANOVA ..... Analysis of variance

ARC ..... Arcuate nucleus

AS160 ..... AKT substrate of 160 kDa

ASD ..... Autism spectrum disorder

ATP ..... Adenosine-5'-triphosphate

BCA ..... Bicinchoninic acid

BSA ..... Bovine serum albumin

CADM ..... Cell Adhesion Molecule

Cadm1/ob ..... *Cadm1* and leptin deficient

*Cadm1*KO ..... Total *Cadm1* knock-out

*Cadm1LeprCre*KO ..... *Cadm1* knock-out in *leptin receptor*-expressing cells

*Cadm1NesCre*KO ..... *Cadm1* knock-out in neuronal and glia cells

CASK ..... Calcium/calmodulin-dependent serine protein kinase

CNS ..... Central nervous systems

Cre ..... Causes recombination

db. ..... *Diabetes*

DIO ..... Diet-induced obesity

DMEM ..... Dulbecco's Modified Eagle's medium

DMN ..... Dorsomedial nucleus

DNA ..... Desoxyribonucleic acid

DPH ..... Dulbeco’s PBS-HEPES-BSA

EDTA ..... Ethylenediaminetetraacetic acid

EE ..... Energy expenditure

EGF ..... Epidermal growth factor

eGFP ..... Enhanced green fluorescent protein
ELISA ..... Enzyme-linked immunosorbent assay
EPSC ..... Excitatory postsynaptic potential
FA. .....Fatty acid
FADH2 .....Flavine adenine dinucleotide
FBS ..... Fetal bovine serum
F*IR*KO ..... Fat-specific *insulin receptor* knock-out
FOX..... Forkhead box protein
FTO.....Fat mass and obesity associated
GABA ..... γ-aminobutyric acid
GABAR..... GABA receptor
GABBR2..... GABA B receptor 2
GH… ..... Growth hormone
Ghr ..... Growth hormone receptor
GHRH.....Growth hormone-releasing hormone
GLUT ..... Glucose transporter
GnRH .....Gonadotropin-releasing hormone
GRB2 ..... Growth factor receptor-bound protein 2
GSK.....Glycogen synthase kinase
GTP.....Guanosine-5'-triphosphate
GTT.....Glucose tolerance test
GWAS ..... Genome-wide association studies
HEPES.....4-(2-hydroxyethyl)-1-piperazineethanesulfonic acid
HFD ..... High fat diet
HGP .....Hepatic glucose production
i.p…. .....Intraperitoneal
Ig.....Immunoglobulin
IGF-1.....Insulin-like growth factor 1
IGF1R.....Insulin-like growth factor 1 receptor
IgSF.....Immunoglobulin superfamily
IKK ..... Inhibitor of kappaB kinase beta
IPSC ..... Inhibitory postsynaptic potential
IRS .....Insulin receptor substrate

ITT ..... Insulin tolerance test
JAK2..... Janus kinase 2
JNK .....c-Jun NH(2)-terminal kinase
KO. .....Knock-out
LatH..... Lateral hypothalamus
Lepr ..... Leptin receptor
LepRCre ..... Cre recombinase under the control of the *leptin receptor* promoter
L*IR*KO..... Liver-specific *insulin receptor* knock-out
lox ..... *Lox P* (locus of X-over P1), recognition site for cre recombinase
M3..... Muscarinic cholinergic receptor 3
MAPK ..... Mitogen-activated protein kinase
MDC ..... Max-Delbrück-Centrum für Molekulare Medizin
MIN6 ..... Mouse insulinoma cells
MINT1 ..... Munc-18-interacting protein 1
miR-375..... microRNA-375
*miR-375*KO ..... *MiR-375* knock-out
M*IR*KO .....Muscle-specific *insulin receptor* knock-out
miRNA ..... microRNA
MODY..... Maturity Onset Diabetes of the You
mTOR ..... Mechanistic target of rapamycin
MUNC18-1 .....Mammalian uncoordinated-18-1
Mupp1 ..... Multiple PDZ domain protein 1
NADH .....Nicotinamide adenine dinucleotide
NAFLD ..... Non-alcoholic fatty liver disease
NECL.....Nectin-like protein
NesCre ..... Cre recombinase under the control of the *nestin* promoter
NMR ..... Nuclear magnetic resonance
NPY..... Neuropeptide Y
ob. ..... *Obese*
p38 MAPK ..... Mitogen-activated protein kinase p38
PBS .....Phosphate buffered saline
PCR.....Polymerase chain reaction
PDK..... 3-phosphoinositide-dependent protein kinase

PDK1 ..... Pyruvate dehydrogenase kinase 1
PDX1 ..... Pancreatic and duodenal homeobox 1
PDZ ..... Post synaptic density-95/Disc large/Zonula occludens-1
PH ..... Pleckstrin homology
PI3K ..... Phosphatidylinositol 3-kinase
PIP2 ..... Phosphatidylinositol-4,5-disphosphate
PIP3 ..... Phosphatidylinositol-3,4,5-trisphosphate
PKB ..... Protein Kinase B
PKCζ ..... Protein kinase C zeta
POMC ..... *Pro-opiomelanocortin*
PPARG2 ..... Peroxisome proliferator-activated receptor G2
PSNS ..... Parasympathetic nervous system
PTEN ..... Phosphatase and tensin homologue deleted on chromosome 10
PVN ..... Paraventricular nucleus
qRT-PCR ..... Quantitative real time polymerase chain reaction
RER ..... Respiratory rate
RIA ..... Radioimmunoassay
RNA ..... Ribonucleic acid
ROS ..... Reactive oxygen species
RT-PCR ..... Reverse transcription polymerase chain reaction
SDS ..... Sodium dodecyl sulfate
Ser ..... Serine
SgIgSF ..... Spermatogenic immunoglobulin superfamily
SH2 ..... Src homology 2
SHC ..... Src homology 2 domain-containing
SNP ..... Single-nucleotide polymorphism
SNS ..... Sympathetic nervous system
SOCS3 ..... Suppressor of cytokine signaling 3
SREBP ..... Sterol regulatory element binding protein
STAT ..... Signal transducer and activator of transcription
SynCAM ..... Synaptic cell adhesion molecule
TBST ..... Tris-buffered saline with Tween 20
TCA ..... Tricarboxylic acid

TCF7L2 ..... Transcription factor 7-like 2

Thr ..... Threonine

TNF-α ..... Tumor necrosis factor α

TSLC ..... Tumor suppressor in lung cancer

USV ..... Ultrasonic vocalization

VMH ..... Ventromedial hypothalamus

VMN ..... Ventromedial nucleus

YFP ..... Yellow fluorescent protein

*βIR*KO ..... β-cell-specific *insulin receptor* knock-out

1 Introduction

Diabetes is characterized by chronic hyperglycemia caused by insufficient release of insulin or insufficient response to insulin. The consequences of chronically elevated blood glucose levels are cardiovascular disease, neuropathy and retinopathy (Stolar 2010). Currently, diabetes affects 346 million people world-wide. It is estimated that in 2004 3.4 million people died from diabetes-related diseases. 90 % of diabetic patients world-wide are affected by type 2 diabetes (WHO 2012). Unlike type 1 diabetes, which is an auto-immune disease causing deficient insulin production, type 2 diabetes is characterized by an insulin resistant state and subsequent β-cell failure to meet high insulin demands of the body by increased insulin production (Skyler 2004). Obesity is a major cause of insulin resistance and therefore largely contributes to the development of type 2 diabetes (Kahn and Flier 2000).

The step from obesity-induced insulin resistance to type 2 diabetes is largely dependent on the ability of the pancreas to meet increased insulin demands by induction of islet hyperplasia. MicroRNA-375 (miR-375) is the highest expressed microRNA (miRNA*)* in the pancreas and recent investigations highlighted the importance of miR-375 in the control of islet hyperplasia as well as insulin secretion (Poy, Eliasson et al. 2004; Poy, Hausser et al. 2009). These studies suggested that miR-375 influences the development of type 2 diabetes. However, the molecular mechanisms of how miR-375 regulates β-cell mass and β-cell function could not be established. Nevertheless, several genes targeted by this microRNA were identified. One of these genes is *cell adhesion molecule 1* (*Cadm1*) (Poy, Hausser et al. 2009).

In order to address whether CADM1 is involved in β-cell growth and β-cell function, we investigated mice with a complete deletion of *Cadm1* (*Cadm1*KO) for changes in glucose homeostasis. During the course of our studies we also observed changes in insulin sensitivity and body weight in *Cadm1*KO mice. Body weight is a major determent in the development of insulin resistance and therefore in the pathogenesis of type 2 diabetes (Kahn 2003). We therefore extended our studies to understand how CADM1 regulates

body weight by investigating the influence of CADM1 on energy homeostasis. Taken together, our studies are the first step in uncovering the role of CADM1 in the pathogenesis of type 2 diabetes.

1.1 Regulation of glucose and energy homeostasis

1.1.1 Regulation of blood glucose homeostasis by insulin

Carbohydrates and especially glucose are important energy sources for several tissues. In particular, blood cells derive fuel only from glucose and the brain relies mainly on glucose (Biesalski and Grimm 2002). In an acute state, absolute or relative insulin deficiency can lead to life threatening hyperglycemic crises caused by diabetic ketoacidosis or a hyperglycemic hyperosmolar state (Chaithongdi, Subauste et al. 2011). Chronic insulin deficiency causes glucose toxicity, leading to nephropathy, retinopathy, neuropathy and atherosclerosis (Stolar 2010). A tight regulation of blood glucose homeostasis to avoid hyper- or hypoglycemia is therefore important.

Blood glucose homeostasis is mainly maintained by insulin. The hormone is produced in pancreatic β-cells where its release is initiated by increased postprandial blood glucose levels **(Figure 1)** (Felig, Wahren et al. 1976). Insulin-stimulated decrease of blood glucose levels is mediated by glucose uptake in skeletal muscle and adipose tissue (Klip and Paquet 1990). In addition, hepatic glucose production (HGP) is inhibited by insulin directly through decreasing glycolytic enzymes and increasing gluconeogenic enzymes. Furthermore, insulin inhibits HGP indirectly through stimulation of agouti-related protein (AGRP)-expressing neurons in the hypothalamus of the brain and subsequent innervation of the liver and inhibition of gluconeogenic enzymes (1.1.4) (Pilkis and Granner 1992; Konner, Janoschek et al. 2007). While insulin lowers blood glucose levels, α-cell-produced glucagon increases blood glucose levels by stimulating HGP (Felig, Wahren et al. 1976; Pilkis and Granner 1992; Shah, Vella et al. 2000). Glucagon release is inhibited by high postprandial blood glucose levels and stimulated when blood glucose levels are too low (Weir, Knowlton et al. 1974).

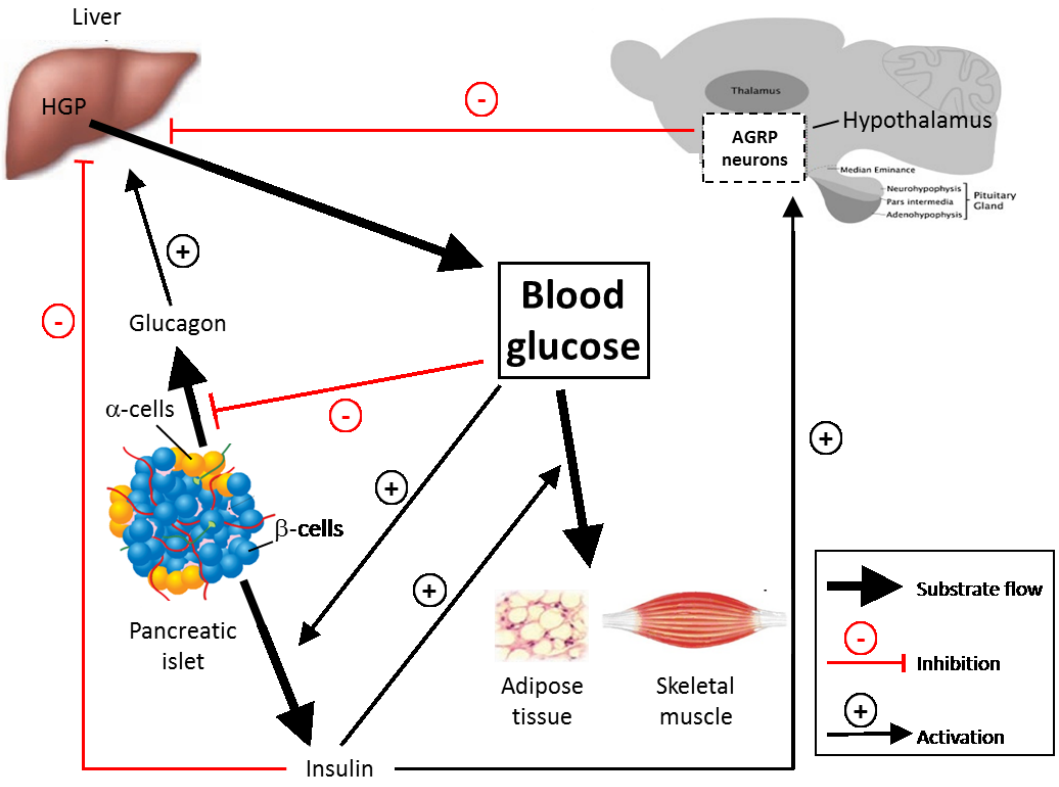

Figure 1: Regulation of blood glucose homeostasis
Blood glucose levels are mainly determined by HGP and glucose uptake in skeletal muscle and adipose tissue. High blood glucose levels stimulate insulin release from pancreatic β-cells and inhibit glucagon release from α-cells. Insulin in turn stimulates insulin-dependent glucose uptake in skeletal muscle and adipose tissue. In addition, insulin inhibits HGP in liver directly and indirectly through stimulation of *AGRP*-expressing neurons in the hypothalamus. In total, insulin-mediated effects decrease blood glucose levels. Glucagon released from pancreatic α-cells stimulates HGP, increasing blood glucose levels.
Abbreviations: Agouti-related protein (AGRP); Hepatic glucose production (HGP)
Modified from (Saltiel and Kahn 2001)

1.1.2 Mechanisms of insulin release from pancreatic β-cells

The pancreas is mainly comprised of an enzyme-producing exocrine portion and a hormone-producing endocrine portion, the islets of Langerhans or simply called pancreatic islets. These islets are built of different cell types such as insulin-producing β–cells, glucagon-producing α-cells, somatostatin-producing δ-cells and pancreatic

polypeptide (PP)-producing PP cells. In addition, neuronal and vascular cells highly infiltrate pancreatic islets (Halban 2004).

Glucose is specifically transported into β-cells by the insulin-independent glucose transporter (GLUT)2, a transporter with high capacity and low affinity that facilitates the glucose transport in direct proportion to blood glucose concentrations **(Figure 2)** (Johnson, Newgard et al. 1990). The following glucokinase-mediated phosphorylation of glucose to glucose-6-phosphate is the rate-limiting step of glucose uptake (De Vos, Heimberg et al. 1995). Mutations in the *glucokinase* gene lead to maturity-onset diabetes of the young (MODY), emphasizing this gene as essential for insulin release from pancreatic β-cells (Froguel, Vaxillaire et al. 1992). The glycolytic break-down of glucose produces nicotinamide adenine dinucleotide (NADH), which is transported into mitochondria by the glycerol phosphate-dihydroxyacetone phosphate and the malate-aspartate shuttles (Dukes, McIntyre et al. 1994; Mertz, Worley et al. 1996). In addition, pyruvate produced through glycolysis is metabolized to acetyl-coenzyme A, generating NADH and flavine adenine dinucleotide ($FADH_2$) via the tricarboxylic acid (TCA) cycle in mitochondria (MacDonald 1993). The electron transport chain converts NADH and $FADH_2$ to adenosine-5'-triphosphate (ATP), increasing cytosolic ATP/adenosine diphosphate (ADP) ratio. ATP released into the cytosol blocks ATP-sensitive K^+-channels, leading to membrane depolarization (Cook and Hales 1984; Rorsman and Trube 1985) und subsequent opening of voltage-sensitive calcium channels (Keahey, Rajan et al. 1989). The influx of calcium ions triggers docking and release of insulin-containing secretory vesicles (Ashby and Speake 1975).

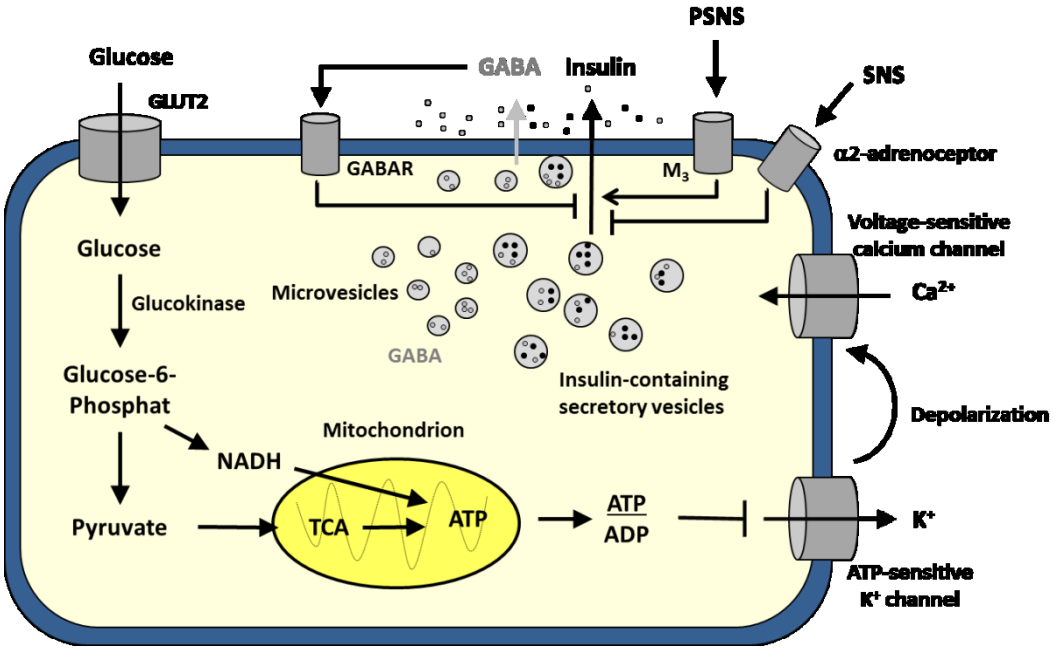

Figure 2: Model of insulin secretion in pancreatic β-cells
Glucose is taken up by insulin-independent GLUT2 and metabolized to NADH and pyruvate through glycolysis. Pyruvate is fueled into the TCA cycle, generating $FADH_2$ and NADH. The electron transport chain in mitochondria converts NADH and $FADH_2$ to ATP, increasing cytosolic ATP/ADP ratio. Enhanced ATP/ADP ratio closes ATP sensitive K^+-channels, which depolarizes the membrane and opens voltage-gated Ca^{2+}-channels. Increased cytosolic Ca^{2+} concentrations trigger docking of insulin-containing secretory vesicles and insulin release. Furthermore, GABA contained in secretory vesicles and synaptic like microvesicles is secreted similarly to insulin. Autocrine GABA signaling and sympathic innervation negatively regulate insulin secretion. Parasympathic innervation positively regulates insulin secretion.
Abbreviations: Adenosine diphosphate (ADP); Adenosine-5'-triphosphate (ATP); γ-aminobutyric acid (GABA); γ-aminobutyric acid receptor (GABAR); Glucose transporter 2 (GLUT2); Muscarinic acetylcholine receptor 3 (M3); Nicotinamide adenine dinucleotide (NADH); Sympathetic nervous system (SNS); Parasympathetic nervous system (PSNS); Tricarboxylic acid cycle (TCA)

Glucose functions as the main secretagogue for insulin secretion but the mechanism of insulin secretion is sensitive to nutrients such as fatty acids (FAs) (Dobbins, Chester et al. 1998), autocrine γ-aminobutyric acid (GABA) signaling (Braun, Wendt et al. 2004; Dong, Kumar et al. 2006) or autonomic innervations (Conaway, Griffey et al. 1975) **(Figure 2)**. Autonomic innervations of pancreatic β-cells increase insulin secretion through the

parasympathic muscarinic acetylcholine receptor 3 (M3), while blocking of M3 reduces insulin secretion in mice (Gautam, Han et al. 2006). Autonomic innervations through sympathic innervations inhibit glucose-mediated insulin release through activation of α2-adrenoceptors (Skoglund, Lundquist et al. 1988; Kurose, Seino et al. 1990). GABA is released from secretory vesicles, in parallel to insulin, and from synaptic-like microvesicles **(Figure 2)** (Reetz, Solimena et al. 1991; Gammelsaeter, Froyland et al. 2004). Both types of vesicles secret GABA in a glucose-dependent manner (Thomas-Reetz, Hell et al. 1993; MacDonald, Obermuller et al. 2005). In the presence of high glucose concentrations, GABA inhibits insulin secretion in an autocrine manner (Braun, Wendt et al. 2004; Dong, Kumar et al. 2006).

1.1.3 Molecular mechanisms of insulin signaling

Insulin signaling in insulin sensitive tissues is activated by binding of insulin to the insulin receptor **(Figure 3)** or by binding of insulin-like growth factor 1 (IGF-1) to the insulin-like growth factor-1 receptor (IGF1R) or to the insulin receptor (Steele-Perkins, Turner et al. 1988). The insulin receptor belongs to the growth factor receptor tyrosine kinase superfamily (McInnes, Wang et al. 1998) and is located at the plasma membrane as a dimer to control several signaling cascades (Freychet, Roth et al. 1971; Boni-Schnetzler, Rubin et al. 1986). Insulin receptors can be found in many different tissues, including skeletal muscle, liver, adipose tissue, different brain areas and pancreas (Havrankova, Roth et al. 1978; Watanabe, Hayasaki et al. 1998). Upon binding of insulin or IGF-1, the insulin receptor undergoes a conformational change followed by autophosphorylation of distinct tyrosine residues of the β subunit (Kasuga, Zick et al. 1982; Kasuga, Zick et al. 1982), which results in a second conformational change (Donner and Yonkers 1983). The second conformational change activates the receptor protein tyrosine kinase activity, enabling recruitment of ATP and tyrosine phosphorylation of recruited substrates (Rosen, Herrera et al. 1983; Cobb, Sang et al. 1989). These substrates include insulin receptor substrate (IRS)1-6 and Src homology 2-containing (SHC) protein (Shoelson, Chatterjee et al. 1992) **(Figure 3)**.

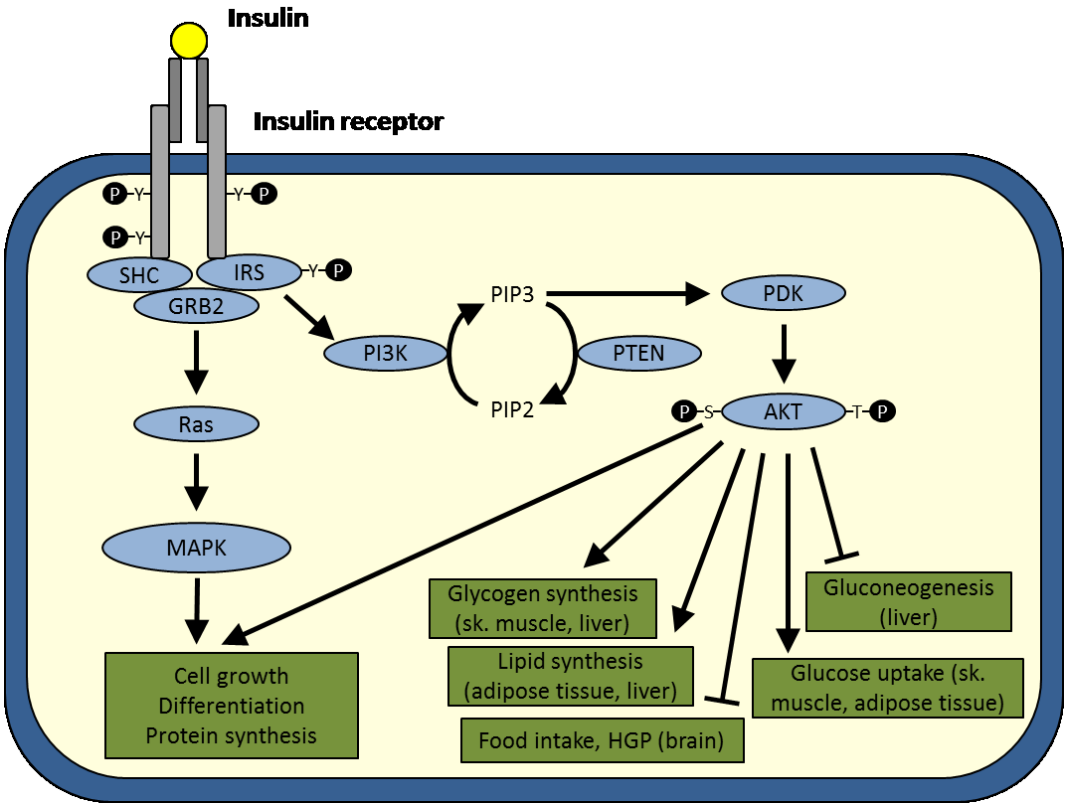

Figure 3: The insulin signaling pathways
The insulin signaling cascade is activated by binding of insulin to its receptor, leading to conformational changes and autophosphorylation on tyrosine (Y) residues of the insulin receptor. Recruited substrates, such as SHC and IRS, are tyrosine phosphorylated by the insulin receptor tyrosine kinase activity. SHC is an activator of the MAPK pathway, which is responsible for insulin-mediated effects on cell growth, differentiation and protein synthesis. IRS proteins facilitate activation of PI3K, which phosphorylates PIP2 to PIP3. PIP3 is an activator of PDK, which further phosphorylates AKT on serine (S) and threonine (T) residues. AKT-regulated downstream targets are responsible for glycogen synthesis, lipid synthesis, glucose uptake, cell growth, differentiation and protein synthesis, inhibition of gluconeogenesis and food intake.
Abbreviations: V-akt murine thymoma viral oncogene homolog (AKT); Growth factor receptor bound 2 (GRB2); Hepatic glucose production (HGP); Insulin receptor substrate (IRS); Mitogen-activated protein kinase (MAPK); Phosphoinositide-dependent kinase (PDK); Phosphatase and tensin homologue deleted on chromosome 10 (PTEN); Phosphatidylinositol 3-kinase (PI3K); Serine (S); Src-homology-2-containing (SHC); Threonine (T); Tyrosine (Y)

Six different IRS isoforms have been identified so far. IRS1 and IRS2 are ubiquitously expressed (Araki, Sun et al. 1993; Sun, Wang et al. 1995). IRS1 knock-out (*Irs1*KO) mice are growth retarded pre- and postnatal. Furthermore, resistance to insulin occurs in adipocytes but not in skeletal muscle and liver in *Irs1*KO mice. Serum insulin levels in these mice are high in order to compensate for insulin resistance (Araki, Lipes et al. 1994; Tamemoto, Kadowaki et al. 1994). These data showed that IRS1 is important in insulin-stimulated somatic growth and glucose uptake but its effects can be compensated in skeletal muscle, liver and pancreatic β-cells. This compensation is thought to be facilitated by IRS2. Unlike *Irs1*KO mice, *Irs2*KO mice do not show compensation for insulin resistance and develop β-cell dysfunction and diabetes. Insulin resistance occurs in skeletal muscle and liver of *Irs2*KO mice. Somatic growth is only slightly reduced in these mice (Withers, Gutierrez et al. 1998). These data showed that IRS1 mainly regulates somatic growth and insulin-stimulated glucose uptake in adipose tissue. IRS2 is essential for β-cell growth regulation as well as insulin signaling in skeletal muscle and liver. IRS3 occurs in many rodent tissues, especially in liver, lung and adipocytes (Sciacchitano and Taylor 1997; Liu, Wang et al. 1999), but is absent in human tissues (Bjornholm, He et al. 2002). *Irs3*KO mice do not show alterations in glucose homeostasis and somatic growth, suggesting that IRS3 is not involved in these processes (Liu, Wang et al. 1999). IRS4 is mainly detected in pituitary and thyroid glands but absent in insulin-sensitive tissues, indicating that IRS4 does not play a major role in insulin signaling (Uchida, Myers et al. 2000). IRS5 and IRS6 have truncated c-terminals and do not bind to proteins involved in the regulation of glucose homeostasis, suggesting that these two IRS isoforms do not contribute to the control of glucose homeostasis (Cai, Dhe-Paganon et al. 2003).

The IRS proteins bind to src homology 2 (SH2) domains of recruited proteins, such as phosphatidylinositol 3-kinase (PI3K) (Backer, Myers et al. 1992; Lavan, Kuhne et al. 1992; Myers, Backer et al. 1992) and growth factor receptor-bound protein 2 (GRB2) (Skolnik, Lee et al. 1993; Tobe, Matuoka et al. 1993) **(Figure 3)**. GRB2, together with SHC, activates the Ras–mitogen-activated protein kinase (MAPK) pathway (Skolnik, Lee et al. 1993), promoting cell growth, differentiation and protein synthesis in several different

tissues (Bonni, Brunet et al. 1999). PI3K is responsible for phosphorylation of phosphatidylinositol-4,5-disphosphate (PIP2), generating phosphatidylinositol-3,4,5-trisphosphate (PIP3) as important second messenger (Ruderman, Kapeller et al. 1990; Hawkins, Jackson et al. 1992). This reaction can be reversed by phosphatase and tensin homologue deleted on chromosome 10 (PTEN), one mechanism to inhibit the insulin signal (Maehama and Dixon 1998). PIP3 activates proteins via pleckstrin homology (PH) domains, with 3-phosphoinositide-dependent protein kinase (PDK) 1 and 2 being the most important PH domain-containing proteins. PDK then activates v-akt murine thymoma viral oncogene homolog (AKT), also called protein kinase B (PKB), a group of kinases that phosphorylate other kinases, proteins or transcription factors (Anderson, Coadwell et al. 1998). Insulin-mediated AKT activation is facilitated by phosphorylation of threonine (Thr)308 and serine (Ser)473 (Alessi, Andjelkovic et al. 1996). Knock-out studies in mice identified the role of each AKT isoform. AKT1 was shown to be dispensable for the regulation of glucose homeostasis but facilitates somatic growth in mice (Cho, Thorvaldsen et al. 2001). Contrary, *Akt2* knock-out (*Akt2*KO) mice are born with mild growth deficiency, loss of pancreatic β-cells and adipose tissue and develop severe insulin resistance in liver and skeletal muscle (Cho, Mu et al. 2001; Garofalo, Orena et al. 2003). These studies showed that AKT2 is the dominant AKT isoform regulating glucose homeostasis through control of insulin sensitivity and maintenance of tissue mass in organs involved in glucose homeostasis. AKT1 is the major form regulating organismal growth. AKT3 does not play a role in regulating glucose homeostasis but controls brain development by influencing cell size and number (Easton, Cho et al. 2005; Tschopp, Yang et al. 2005).

In skeletal muscle, insulin-mediated AKT activation increases glucose uptake and induction of glucose storage **(Figure 3)**. Signaling for glucose uptake is facilitated by the AKT effector AKT substrate of 160 kDa (AS160) (Bruss, Arias et al. 2005). AKT signaling induces phosphorylation of AS160 and subsequent translocalization of GLUT4 to the plasma membrane (Sano, Kane et al. 2003). GLUT4 is the major insulin responsive glucose transporter in heart, skeletal muscle and adipose tissue (Bell, Murray et al. 1989). Glucose storage in skeletal muscle is induced through signaling of glycogen

synthase kinase (GSK)3. GSK3 is phosphorylated and inactivated by AKT, increasing glycogen synthesis in skeletal muscle (Cross, Alessi et al. 1995).

Similar to skeletal muscle, insulin-mediated AKT activation phosphorylates AS160 and subsequent translocates GLUT4 to the plasma membrane in adipocytes (Sano, Kane et al. 2003) **(Figure 3)**. However, this tissue contributes only to 3 – 5 % to the whole body insulin-dependent glucose uptake (James, Burleigh et al. 1985). The most important function of insulin signaling in adipocytes is the induction of lipogenesis and inhibition of lipolysis. This could be shown in animals with *insulin receptor* knock-out in white adipose tissue (F*IR*KO) (Bluher, Michael et al. 2002). These animals are resistant to obesity and obesity-induced glucose intolerance, since lipid synthesis in white adipose tissue is largely impaired. Insulin regulates lipid metabolism in adipocytes by controlling important enzymes, such induction of lipogenesis through AKT-dependent activation of fatty acid synthase (FAS) (Wang and Sul 1998) or inhibition of lipolysis through reduction of adipose triglyceride lipase (ATGL) or hormone sensitive lipase (HSL) (Kralisch, Klein et al. 2005).

Insulin signaling in the liver is highly relevant for the control of blood glucose levels. This could be shown in mice with liver-specific *insulin receptor* knock-out (L*IR*KO) (Michael, Kulkarni et al. 2000). L*IR*KO mice exhibit severe glucose intolerance due to unsuppressed HGP. Circulating insulin levels of these mice are increased due to a combination of insulin resistance and impaired insulin clearance, showing that the liver is also responsible for insulin uptake and degradation. Hepatic AKT targets include GSK3, increasing glycogen synthesis in liver (Cross, Alessi et al. 1995) **(Figure 3)**. Furthermore, AKT inhibits the transcription factors forkhead box protein (FOX)O1 and peroxisome proliferator-activated receptor-γ coactivator (PGC)1α, leading to inhibition of gluconeogenic genes in the liver (Puigserver, Rhee et al. 2003). In addition, insulin stimulated AKT signaling is responsible for increased lipid synthesis through activation of sterol regulatory element binding protein (SREBP)-1c in the liver (Foretz, Pacot et al. 1999; Yecies, Zhang et al. 2011).

Last, AKT facilitates growth and proliferation signals of insulin **(Figure 3)**. Especially pancreatic islets show increased β-cell growth in response to AKT activation (Tuttle, Gill et al. 2001). Conversely, β-cell-specific *insulin receptor* knock-out (β*IR*KO) decreases β-cell mass in aged mice, showing that autocrine insulin signaling in β-cells is necessary for increased β-cell mass in response to insulin resistance (Kulkarni, Bruning et al. 1999). In addition, β*IR*KO mice showed reduced glucose-stimulated insulin release (Kulkarni, Bruning et al. 1999), since insulin induces transcription of the *insulin* and *glucokinase* genes (Leibiger, Leibiger et al. 2001; Meur, Qian et al. 2011). These genes are responsible for glucose utilization in β-cells.

1.1.4 Effects of neuronal insulin signaling

Insulin was the first described peripheral hormone with catabolic effects in the brain (Woods, Lotter et al. 1979). Insulin receptors are widely distributed in the brain, including areas such as olfactory bulb, cerebellum, hippocampus and hypothalamus (Havrankova, Roth et al. 1978; van Houten, Posner et al. 1979; Marks, Porte et al. 1990). Deletion of the *insulin receptor* in neuronal tissues leads to hypertriglyceridemia, hyperinsulinemia, hyperphagia, diet-induced obesity and reduced fertility, suggesting that central insulin signaling regulates glucose homeostasis, energy homeostasis and fertility (Bruning, Gautam et al. 2000).

Early studies indicated that insulin exerts its effects at least partially through increasing expression of melanocortins in the hypothalamus (Benoit, Air et al. 2002). Melanocortins are transcribed from a single precursor gene, called *pro-opiomelanocortin (Pomc)* (Nakanishi, Inoue et al. 1979). Besides the pituitary gland, also the hypothalamus is a known site of strong *Pomc* expression (Gee, Chen et al. 1983). *Pomc* deletion in mice and *POMC* mutations in humans induce severe obesity, emphasizing the role of *POMC* in the regulation of energy homeostasis (Krude, Biebermann et al. 1998; Yaswen, Diehl et al. 1999). Besides insulin, also leptin is a potent inducer of *Pomc* expression (Schwartz, Seeley et al. 1997; Mizuno, Kleopoulos et al. 1998) (1.1.6). Insulin signaling induces *Pomc* expression through phosphorylation and inhibition of FOXO1, which is an inhibitor of the

Pomc promoter (Kitamura, Feng et al. 2006) **(Figure 4)**. Dissection of insulin-mediated effects on energy and glucose homeostasis showed that insulin signaling in hypothalamic *Pomc*-expressing neurons increases locomotor activity (Lin, Plum et al. 2010). Nevertheless, insulin signaling in *Pomc*-expressing neurons does not affect body weight regulation (Konner, Janoschek et al. 2007; Lin, Plum et al. 2010).

Further studies indicated that hypothalamic insulin signaling regulates whole body glucose homeostasis through inhibition of HGP (Obici, Feng et al. 2002; Obici, Zhang et al. 2002). These studies also showed that antagonism of melanocortins does not influence insulin-mediated effects on glucose homeostasis, suggesting that other genes than *Pomc* are involved in this process. Early studies showed that insulin decreases expression of *neuropeptide Y* (*Npy*) (Schwartz, Sipols et al. 1992; Sipols, Baskin et al. 1995) and insulin-mediated effects on HGP involve reduction of *Npy* expression (van den Hoek, Voshol et al. 2004). *Npy* is an inducer of obesity by stimulating food intake and decreasing energy expenditure (Stephens, Basinski et al. 1995) and insulin as well as leptin negatively regulate expression of *Npy* (Schwartz, Seeley et al. 1996; Korner, Savontaus et al. 2001). Insulin-mediated effects on HGP involve opening of ATP-sensitive K^+-channels, leading to hyperpolarization of *Agrp*-expressing neurons (Konner, Janoschek et al. 2007; Lin, Plum et al. 2010) **(Figure 4)**. *Agrp* is coexpressed with *Npy* in the same *Agrp*/*Npy*-expressing neurons (Hahn, Breininger et al. 1998). Insulin-mediated hyperpolarization decreases AGRP release from *Agrp*/*Npy*-expressing neurons and leads to innervation of the liver (Konner, Janoschek et al. 2007). Insulin-mediated innervation of the liver activates signal transducer and activator of transcription (STAT)3 and inhibits hepatic *glucose-6-phosphatase* and subsequent hepatic gluconeogenesis. *Agrp*/*Npy*-expressing neurons inhibit *Pomc*-expressing neurons through GABA-mediated innervation (Cowley, Smart et al. 2001; Tong, Ye et al. 2008), suggesting that insulin-mediated hyperpolarization of *Agrp*/*Npy*-expressing neurons activates *Pomc*-expressing neurons **(Figure 4).** Similar to *Pomc*-expressing neurons, also insulin signaling in *Agrp*/*Npy*-expressing neurons does not affect body weight regulation (Konner, Janoschek et al. 2007; Lin, Plum et al. 2010), indicating that body weight regulation is

mediated by insulin signaling in other neurons, such as dopaminergic neurons (Konner, Hess et al. 2011).

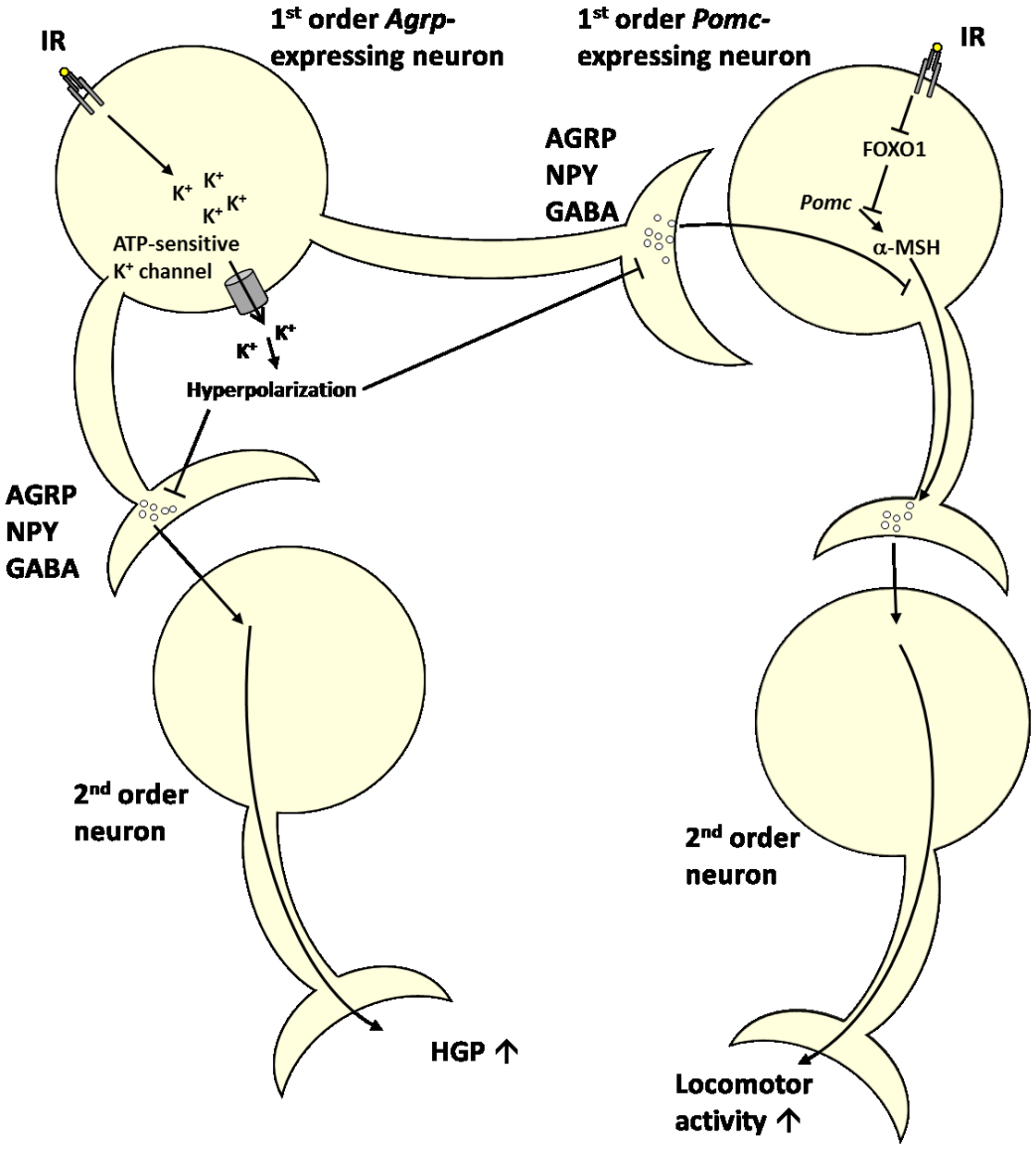

Figure 4: Effects of hypothalamic insulin signaling on energy and glucose homeostasis
Insulin signaling in 1st order neurons expressing *insulin receptor* and *Agrp* (left) leads to opening of ATP-sensitive K^+-channels and subsequent hyperpolarization. Insulin-mediated hyperpolarization of *Agrp*-expressing neurons represses release of neurotransmitters, such as NPY, AGRP and GABA. Reduced neurotransmitter release signals through 2nd order neurons and hepatic innervation and results in decreased HGP.

In *Pomc*-expressing neurons (right), insulin signaling causes release of α-MSH, a transcribed protein of the *Pomc* gene, directly through inhibition of FOXO1 and indirectly through inhibited release of NPY, AGRP and GABA. Insulin-mediated α-MSH release promotes locomotor activity.
Abbreviations: Agouti-related protein (AGRP); Forkhead box protein O1 (FOXO1); γ-aminobutyric acid (GABA); Hepatic glucose production (HGP); Insulin receptor (IR); α-Melanocyte-stimulating hormone (α-MSH); Neuropeptide Y (NPY); *Pro-opiomelanocortin (Pomc)*

1.1.5 Components and regulation of energy homeostasis

Energy homeostasis is regulated by different tissues controlling uptake, digestion, circulation and break-down of nutrients. Digested nutrients can be stored for later use or broken-down, while exergonic energy is stored and transported in small metabolites, such as ATP, guanosine-5'-triphosphate (GTP) and NADH, for short term usage. The energy is used for maintaining basal metabolic rate, physical activity and diet-induced thermogenesis (Biesalski 2004; Pinheiro Volp, Esteves de Oliveira et al. 2011). The basal metabolic rate is the energy necessary for maintenance of all body functions at rest, such as chemical reactions, transport processes or involuntary movements. Diet-induced thermogenesis includes energy that is used for digestion, absorption and converting of nutrients. Physical activity can be separated into exercise and non-exercise activity, called non-exercise activity thermogenesis (Levine 2004).

Since the early 1940s, it became apparent that energy homeostasis is strongly regulated by the brain (Brobeck 1946), a picture that was quickly defined by the notion that also peripheral signals produced by fat tissue play a role in this regulation (Kennedy 1953). The occurrence of genetic mutations in laboratory mice, such as *obese* (*ob*) (Ingalls, Dickie et al. 1950) and *diabetes* (*db*) (Hummel, Dickie et al. 1966), helped to identify leptin as an important adipose-derived hormone regulating energy homeostasis (Zhang, Proenca et al. 1994) and its regulated networks (Leibel, Chung et al. 1997). Leptin as well as insulin are the major hormones regulating energy homeostasis in the brain. The brain is responsible for short-term and long-term regulation of food intake and energy expenditure **(Figure 5)**. Short-term afferent signals include chemical signals, such as

cholecystokinin (CCK), ghrelin and gastrin-releasing peptide (Baile and Della-Fera 1985; Figlewicz, Stein et al. 1985; Nakazato, Murakami et al. 2001). Short-term afferent signals also include mechanical signals released from the digestive system upon gastrointestinal loads. Mechanical signals are transported by vagal afferent neuronal signaling to the brain (Schwartz and Moran 1996). In addition, long-term signals, including leptin and insulin, modulate food intake as well as energy expenditure by stimulating neurons, which mainly originate in the arcuate nucleus (ARC) of the hypothalamus (van Houten, Posner et al. 1980; McGowan, Andrews et al. 1992; Satoh, Ogawa et al. 1997). Furthermore, cytokines, neuropeptides, circadian rhythms and visceral sensory input have been described in regulating energy homeostasis (Larue and Le Magnen 1972; Plata-Salaman 1995; Hillebrand, de Wied et al. 2002; Turek, Joshu et al. 2005). These afferent signals are detected and processed in multiple areas of the brain, with hypothalamus playing a crucial role in regulating energy and glucose homeostasis **(Figure 5)**. Further integrating areas include telencephalic, hippocampus and brain stem structures (Berthoud 2002). Efferent signals then coming from the brain include neuroendocrine responses through hormone release from hypothalamus and pituitary gland, autonomic responses via sympathic and parasympathic nerves and cognitive responses (Berthoud 2002) **(Figure 5).** Insulin and leptin are key components of this complex neuronal network and development of resistance to these hormones is a crucial step in the pathogenesis of obesity and type 2 diabetes (Schwartz and Porte 2005) (1.2.1).

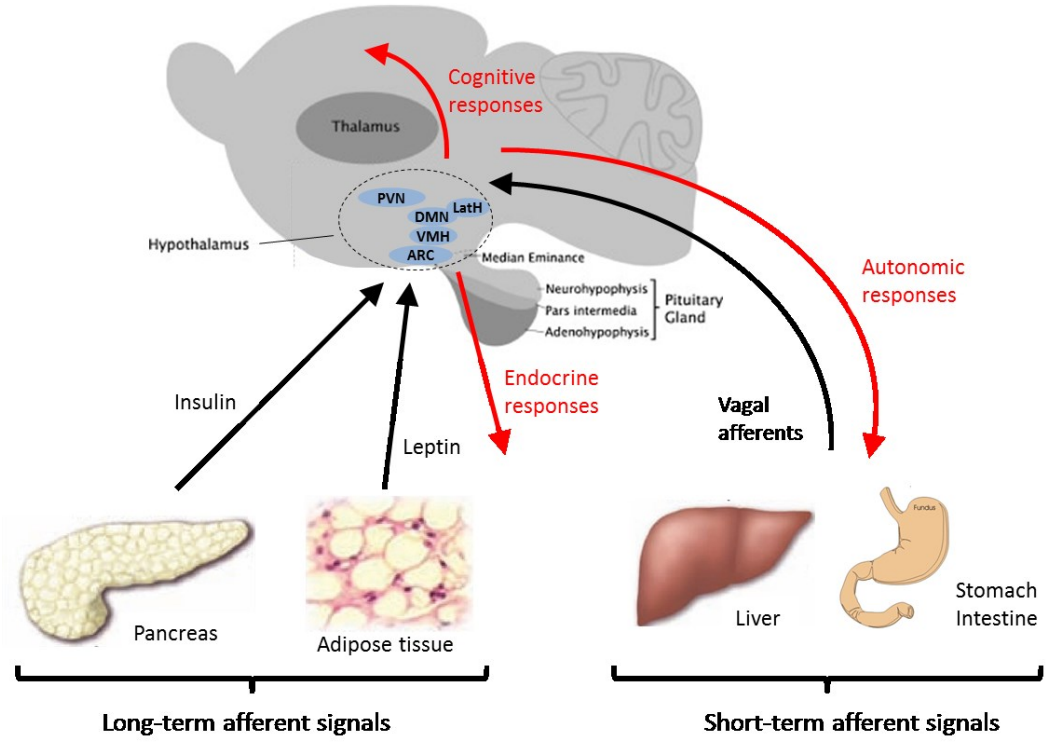

Figure 5: Afferent and efferent hypothalamic signals controlling energy homeostasis
Afferent signals (black) influence the brain to regulate energy homeostasis. Long-term afferent signals include leptin and insulin (left). Short-term afferent signals are food-related chemical and mechanical signals sensed by the digestive system and transported to the brain through vagal afferents (right). All signals are integrated by activation of neuropeptides and neurotransmitters in different areas of the hypothalamus, such as ARC, VMN, DMN, LatH and PVN, and non-hypothalamic areas including brain stem and spinal cord. Efferent signals from the brain (red) include endocrine responses, cognitive responses and autonomic control. Efferent signals regulate energy expenditure, glucose homeostasis and food intake.
Abbreviations: Arcuate nucleus (ARC); Dorsomedial nucleus (DMN); Lateral hypothalamus (LatH); Paraventricular nucleus (PVN); Ventromedial nucleus (VMN). Modified from (Szarek, Cheah et al. 2010)

1.1.6 Leptin signaling in the brain regulates energy homeostasis

In 1950, the spontaneous *ob* mutation occurred in an inbred mouse strain of the Jackson Laboratory, which led to sever obesity and infertility (Ingalls, Dickie et al. 1950). It was the first description of a gene associated with obesity. Despite the discovery of more genetic mutations leading to obesity in mice (Friedman and Leibel 1992), it was not until

1994 that the *ob* gene was identified to be expressed in white adipose tissue of humans and rodents by the group of Jeffrey Friedman (Zhang, Proenca et al. 1994). Later on, the *ob* protein product was termed leptin. Leptin is secreted relative to body fat mass and signals for the amount of body fat (Maffei, Halaas et al. 1995). The hormone decreases food intake and increase energy expenditure, therefore having negative impact on body fat storages (Halaas, Gajiwala et al. 1995). Leptin mediates its effects on energy homeostasis through regulation of neuronal networks mainly in the hypothalamic ARC (Campfield, Smith et al. 1995; Satoh, Ogawa et al. 1997).

In 1966, the spontaneous mutation *db* occurred in the Jacksons Laboratory, leading to obesity in mice (Hummel, Dickie et al. 1966). Mice carrying this mutation express an abnormally spliced *leptin receptor* (*Lepr*) variant, leading to LEPR deficiency (Maffei, Fei et al. 1995). Different LEPRs isoforms were identified in several tissues with functions in metabolism, angiogenesis, immunity, reproduction and blood pressure regulation (Fruhbeck 2001). LEPRs belong to the group of the cytokine receptor superfamily (Tartaglia, Dembski et al. 1995). All LEPRs isoforms carry the same extracellular sequence but differ in the length of the intracellular domain, which is important for the signaling properties of the receptors (Lee, Proenca et al. 1996). The longest isoform, LEPRb, plays the most important role in regulating energy and glucose homeostasis in the brain with little involvement of the short LEPR isoforms (LEPRa, LEPRc and LEPRd) (Osborn, Sanchez-Alavez et al. 2010). The short LEPR isoforms have an important role in leptin uptake by the brain and the impairment of leptin uptake into the brain during obesity (Hileman, Pierroz et al. 2002).

LEPRs exist as preformed dimer at the plasma membrane **(Figure 6)**. Binding of leptin leads to subsequent conformational changes of the receptor dimers (Devos, Guisez et al. 1997; Couturier and Jockers 2003). Like all members of the cytokine receptor superfamily, LEPRs lack an intrinsic tyrosine kinase domain (Kaczmarski and Mufti 1991). The recruitment of intracellular kinases to the LEPRs is therefore necessary for leptin receptor signaling. Janus kinase 2 (JAK2) is the main intracellular kinase that autophosphorylates upon conformational changes of the LEPRs and phosphorylates

tyrosine residues on the LEPRs (Ghilardi and Skoda 1997). This receptor tyrosine phosphorylation allows proteins with SH2 domains to bind to the LEPRs (Heim, Kerr et al. 1995). The transcription factor STAT3 is one of the most important SH2 domain-containing proteins binding to the LEPRs at tyrosine residues (Baumann, Morella et al. 1996; Ghilardi, Ziegler et al. 1996; Vaisse, Halaas et al. 1996). STAT3 is phosphorylated by JAK2, dimerizes and translocates to the nucleus, inducing expression of target genes such as *Pomc* (Schwartz, Seeley et al. 1997) and *suppressor of cytokine signaling 3* (*Socs3),* an inhibitor of leptin receptor signaling (Bjorbaek, El-Haschimi et al. 1999; Bjorbak, Lavery et al. 2000). Besides the JAK/STAT signaling pathway, leptin also activates other signaling pathways, such as insulin signaling (Kellerer, Koch et al. 1997; Zhao, Shinohara et al. 2000; Kitamura, Feng et al. 2006) and MAPK signaling, facilitating cell growth, protein synthesis and differentiation (Takahashi, Okimura et al. 1997) **(Figure 6)**.

The most important leptin targets in the regulation of energy homeostasis are cells expressing *Pomc* or *Agrp*, which are mainly situated in the hypothalamic ARC (Jacobowitz and O'Donohue 1978; Pelletier and Desy 1979; Haskell-Luevano, Chen et al. 1999). In *Pomc*-expressing neurons, leptin activates STAT3 and inactivates FOXO1 through phosphorylation of FOXO1 (Kitamura, Feng et al. 2006; Ernst, Wunderlich et al. 2009) **(Figure 6)**. FOXO1 is an inhibitor of *Pomc* expression (Kitamura, Feng et al. 2006). Leptin-mediated increased expression of *Pomc* induces expression of the anorexic neuropeptide α-MSH, the most relevant protein product of the *Pomc* gene in regards to food intake (Tung, Piper et al. 2006). In addition, leptin-mediated STAT3 activation and FOXO1 inactivation represses *Agrp* in *Agrp*-expressing neurons, inhibiting the expression of the orexic neuropeptides AGRP and coexpressed NPY (Muraoka, Xu et al. 2003; Kitamura, Feng et al. 2006). Leptin signaling in *Pomc*- and *Agrp*-expressing neurons reduces food intake and increases energy expenditure. However, mutations of *leptin* or *Lepr* also affects glucose homeostasis and fertility, showing that leptin also has important roles in other than *Pomc*- and *Agrp*-expressing neurons (Coleman 1978; van de Wall, Leshan et al. 2008).

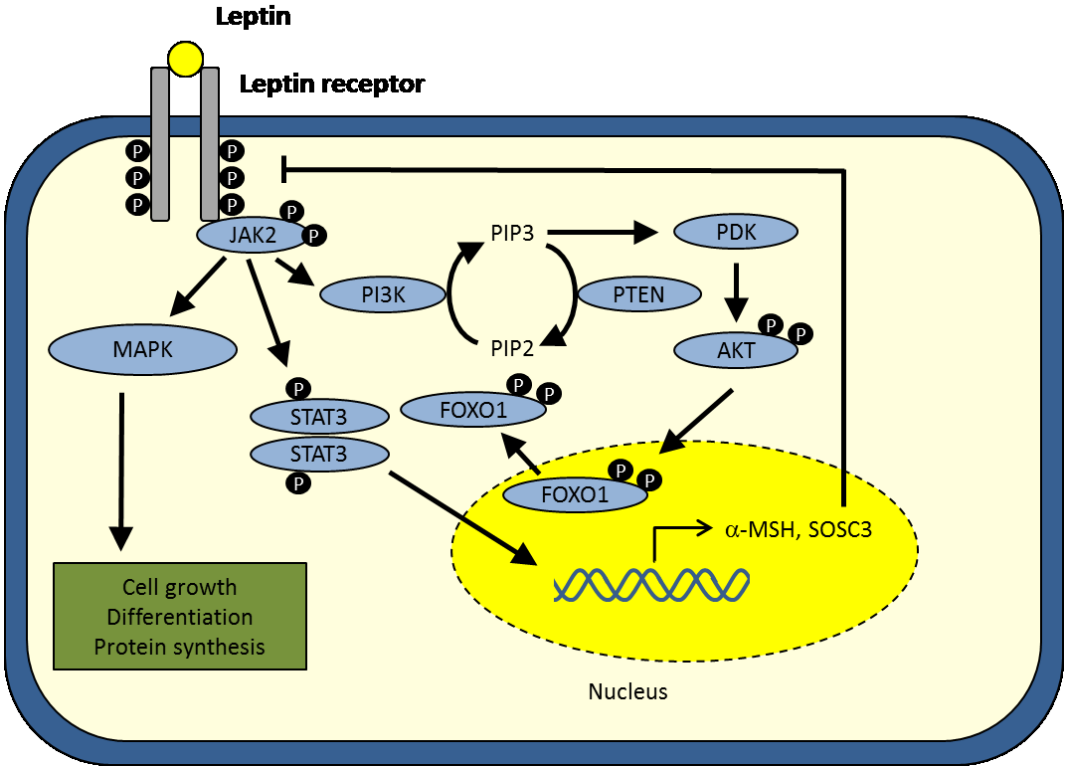

Figure 6: Leptin signaling pathways
Leptin binds to its preformed receptor dimers in order to recruit intracellular JAK2 tyrosine kinase. JAK2 autophosphorylates and induces phosphorylation (P) of tyrosine residues on the intracellular tail of the leptin receptor, activating the transcription factor STAT3. STAT3 is responsible for most of the leptin-induced effects by activating genes such as *Pomc*, translating into the protein product α-MSH, and *Socs3*. SOCS3 represses leptin signaling, providing a negative feedback for the leptin signaling pathway. JAK2 furthermore activates the insulin signaling pathway by activating PI3K and the MAPK pathway, facilitating cell growth and differentiation. In addition, leptin-induced PI3K activation inhibits FOXO1 through phosphorylation and translocation to the nucleus. FOXO1 is an inhibitor of *Pomc* expression and an inducer of *Agrp* expression.
Abbreviations: Melanocyte-stimulating hormone (α-MSH); V-akt murine thymoma viral oncogene homolog (AKT); Forkhead box protein 01 (FOXO1); Janus kinase (JAK); Mitogen-activated protein kinase (MAPK); Phosphoinositide-dependent kinase (PDK); Phosphatidylinositol 3-kinase (PI3K); Phosphatidylinositol-4,5-diphosphate (PIP2); Phosphatidylinositol-3,4,5-trisphosphate (PIP3); Phosphatase and tensin homologue deleted on chromosome 10 (PTEN); Suppressors of cytokine signaling 3 (SOSC3); Signal transducer and activator of transcription 3 (STAT3)

1.2 Type 2 diabetes: mechanisms of insulin resistance and β-cell failure

The first clinical symptom of type 2 diabetes is impaired glucose tolerance due to insulin resistance (Osei, Rhinesmith et al. 2004; Hong, Gui et al. 2008; Cali, Man et al. 2009). Main consequences of insulin resistance are reduced suppression of hepatic gluconeogenesis and decreased peripheral glucose uptake in skeletal muscle (DeFronzo, Gunnarsson et al. 1985; Consoli, Nurjhan et al. 1989). Elevated pancreatic insulin production, reflected in islet hyperplasia, compensates insulin resistance for years before the onset of type 2 diabetes (LeRoith 2002). Obesity-induced lipo- and glucotoxicity can lead to stress in pancreatic β-cells (Robertson, Harmon et al. 2004). Eventually, pancreatic β-cells fail to produce sufficient amounts of insulin and plasma glucose levels dramatically increase, marking the onset of type 2 diabetes (Prentki and Nolan 2006).

1.2.1 Obesity as a major cause for insulin resistance

Obesity is associated with increased intra-abdominal fat content and decreased insulin sensitivity, showing that fat tissue-derived factors are major determents of whole body insulin sensitivity (Park, Rhee et al. 1991; Carey, Jenkins et al. 1996). Adipose tissue-derived factors, which have been implicated to correlate with insulin sensitivity or insulin resistance, include FAs and adipokines such as leptin, adiponectin, resistin, tumor necrosis factor α (TNF-α) or interleukin 6 (IL-6) (Hotamisligil, Shargill et al. 1993; Carey, Jenkins et al. 1996; Barzilai, Wang et al. 1997; Bastard, Maachi et al. 2002; Kubota, Terauchi et al. 2002; Satoh, Nguyen et al. 2004; Yang, Graham et al. 2005). In addition, cytokines released from macrophages attracted to adipocytes contribute to obesity-caused insulin resistance (Weisberg, McCann et al. 2003). Furthermore, ectopic lipid accumulation in muscle and liver enhances local cytokine production in these tissues (Pan, Lillioja et al. 1997; Fabbrini, Magkos et al. 2009). The increased expression of cytokines from adipose tissue, macrophages, liver and skeletal muscle is responsible for

a chronic local and systemic inflammation in obesity (Saghizadeh, Ong et al. 1996; Cai, Yuan et al. 2005; Wellen and Hotamisligil 2005).

Gene variations, also called single-nucleotide polymorphisms (SNPs), which have been identified to contribute to the development of insulin resistance in type 2 diabetes are often associated with their effect on obesity (Li, Zhao et al. 2011). One of the strongest associations with obesity has the genetic variation rs9939609 of the *fat mass and obesity associated (FTO)* gene. 16 % of the European and Asian populations are homozygous for this SNP and have a 30 % increased risk to become obese or overweight (Frayling, Timpson et al. 2007; Zhou, Liu et al. 2012). However, the *FTO* polymorphism exclusively affects type 2 diabetes by influencing obesity (Frayling, Timpson et al. 2007). Recent studies implicated that FTO regulates food intake by controlling oxytocin (Olszewski, Fredriksson et al. 2009; Tung, Ayuso et al. 2010; Olszewski, Fredriksson et al. 2011), a protein with previously described functions in food intake (Kublaoui, Gemelli et al. 2008). One of the most common risk alleles affecting release of adipose-derived factors is an alanine to proline substitution in codon 12 of the gene *peroxisome proliferator-activated receptor G2* (*PPARG2)*. Around 85 % of the population are carriers of the proline allele of PPARγ2, which is associated with a 1.25 fold risk increase for type 2 diabetes (Altshuler, Hirschhorn et al. 2000). *PPARG2* is exclusively expressed in adipocytes and the low risk alanine allele of PPARγ2 suppresses insulin-mediated release of FAs and secretion of TNF-α, resistin and adiponectin (Stumvoll and Haring 2002).

Cytokines and FAs derived from adipose tissue are inducers of serine/threonine kinases **(Figure 7)** (Hotamisligil, Peraldi et al. 1996; Paz, Hemi et al. 1997). Phosphorylation of serine residues on IRS1 and IRS2 through serine/threonine kinases is a central step in the development of insulin resistance. Serine phosphorylation of IRS1 and IRS2 inhibits tyrosine phosphorylation of both IRS isoforms and subsequent insulin signaling (Paz, Hemi et al. 1997). Serine phosphorylation of IRS is mediated by serine/threonine kinases like c-Jun NH(2)-terminal kinase (JNK) (Aguirre, Uchida et al. 2000), protein kinase C zeta (PKCζ) (Liu, Paz et al. 2001), inhibitor of kappaB kinase beta (IKK) (Gao, Hwang et al. 2002), mitogen-activated protein kinase p38 (p38 MAPK) (de Alvaro, Teruel et al. 2004)

or mechanistic target of rapamycin (mTOR) (Ozes, Akca et al. 2001). SOCS3 is a target of cytokine signaling with inhibitory function on tyrosine IRS phosphorylation (Emanuelli, Peraldi et al. 2001). IRS1 activity can also be influenced by genetic variations (Ohshige, Iwata et al. 2011). The most common risk locus for *IRS1* is rs2943641, situated 500 kb upstream of *IRS1* (Rung, Cauchi et al. 2009). The risk cytosine allele of *IRS1* is associated with decreased IRS1 protein expression and reduced insulin-mediated PI3K activation (Rung, Cauchi et al. 2009). The cytosine allele increases the risk for type 2 diabetes about 15 - 35 % (Rung, Cauchi et al. 2009; Ohshige, Iwata et al. 2011).

Reduced insulin signaling causes hyperglycemia in type 2 diabetic patients mainly by decreasing suppression of hepatic gluconeogenesis (Consoli, Nurjhan et al. 1989; Mitrakou, Kelley et al. 1990; Meyer, Woerle et al. 2004) **(Figure 7)**. In accordance, L*IR*KO mice are severely insulin resistant and hyperglycemic (Michael, Kulkarni et al. 2000). Although hepatic gluconeogenesis is increased by reduced insulin signaling, insulin-mediated stimulation of hepatic fatty acid synthesis is maintained through induction of the transcription factor SREBP-1c (Shimomura, Matsuda et al. 2000). Increased hepatic fatty acid synthesis can lead to non-alcoholic fatty liver disease (NAFLD), a disease often diagnosed in obese and diabetic patients (Angulo and Lindor 2002). In skeletal muscle, type 2 diabetes patients show normal or increased glucose uptake compared to non-diabetic patients despite an insulin resistant state (DeFronzo, Gunnarsson et al. 1985; Consoli, Nurjhan et al. 1989; Mitrakou, Kelley et al. 1990; Meyer, Woerle et al. 2004). These studies are in line with studies on mice with muscle-specific *insulin receptor* knock-out (M*IR*KO) (Bruning, Michael et al. 1998). M*IR*KO mice are normoglycemic and have normal glucose tolerance and circulating insulin levels. However, in skeletal muscle from type 2 diabetes patients, glucose uptake is not appropriate for increased plasma glucose concentrations (DeFronzo, Gunnarsson et al. 1985; Cusi, Maezono et al. 2000). Therefore, insulin resistance in hepatic and non-hepatic tissues contributes to the development of hyperglycemia in type 2 diabetes **(Figure 7)**.

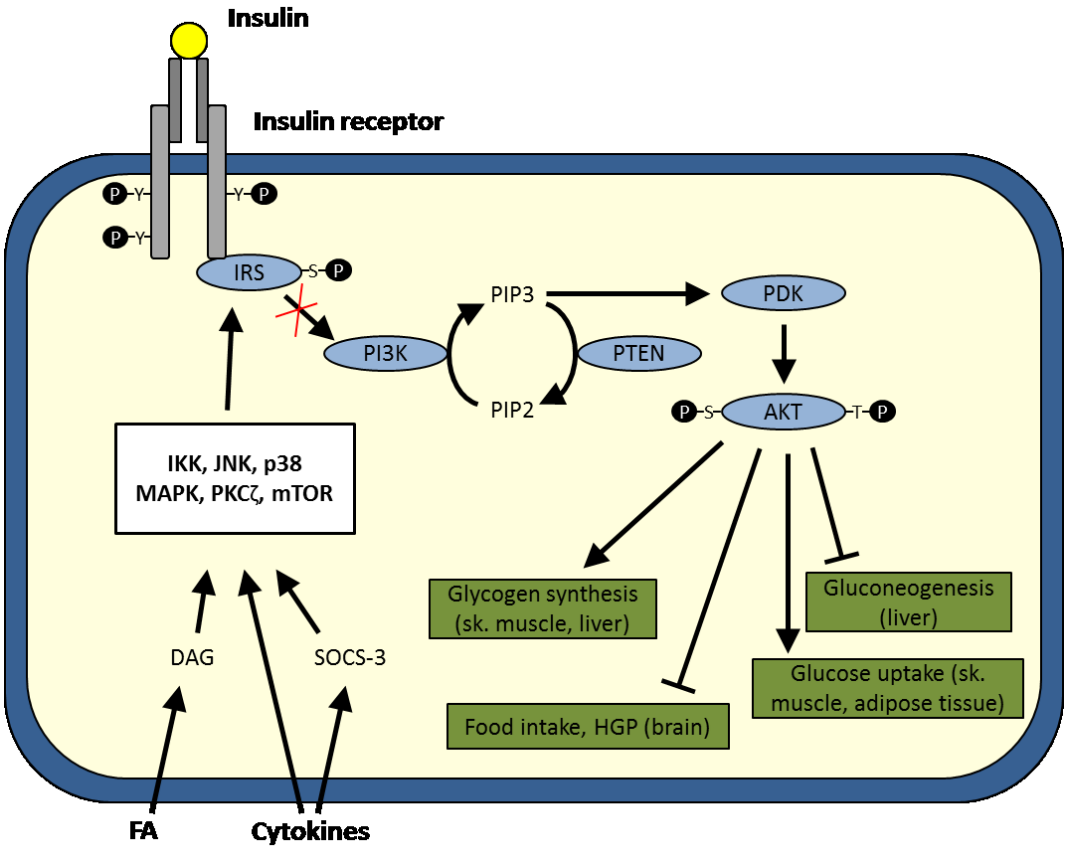

Figure 7: Serine phosphorylation of IRS causes insulin resistance
The above explained insulin cascade (Figure 3) is inhibited by FAs and cytokines derived from adipose tissue, macrophages and ectopic lipid accumulation in muscle and liver. Cytokines and FAs activate serine/threonine kinases, such as IKK, JNK, p38 MAPK, PKCζ or mTOR. Serine/threonine kinases phosphorylate serine (S) residues on IRS1 and IRS2, inhibiting tyrosine (Y) phosphorylation of IRS. Subsequent insulin signaling cascades are impaired, resulting in decreased glucose uptake and glycogen synthesis and enhanced food intake, HGP and hepatic gluconeogenesis. Resulting hyperglycemia can partially be rescued by increased insulin secretion from pancreatic β-cells until β-cells fail to produce sufficient amounts of insulin and type 2 diabetes develops.
Abbreviations: V-akt murine thymoma viral oncogene homolog (AKT); Diacylglycerol (DAG); Fatty acids (FA); Hepatic glucose production (HGP); Inhibitor of kappaB kinase beta (IKK); Insulin receptor substrate (IRS); c-Jun NH(2)-terminal kinase (JNK); Mitogen-activated protein kinase p38 (p38 MAPK); Mechanistic target of rapamycin (mTOR); Phosphoinositide-dependent kinase (PDK); Protein kinase C zeta (PKCζ); Phosphatase and tensin homologue deleted on chromosome 10 (PTEN); Phosphatidylinositol 3-kinase (PI3K); Serine (S); Suppressor of cytokine signaling 3 (SOCS3); Threonine (T); Tyrosine (Y)

Obesity-induced insulin resistance is also evident in the central nervous systems (CNS), mainly in the hypothalamus (De Souza, Araujo et al. 2005; Zhang, Zhang et al. 2008; Posey, Clegg et al. 2009). Similar to peripheral insulin resistance, hypothalamic insulin resistance is induced by local cytokine production and subsequent activation of serine/threonine kinases (De Souza, Araujo et al. 2005; Posey, Clegg et al. 2009). Impaired hypothalamic insulin signaling increases food intake, further worsening the progression of obesity-caused insulin resistance and type 2 diabetes (De Souza, Araujo et al. 2005; Posey, Clegg et al. 2009) **(Figure 7)**. Furthermore, hypothalamic insulin resistance is associated with impaired regulation of glucose homeostasis through induction of hepatic insulin resistance (Belgardt, Mauer et al. 2010; Purkayastha, Zhang et al. 2011) and impaired pancreatic insulin release (Calegari, Torsoni et al. 2011).

1.2.2 Obesity and genetic predispositions cause β-cell failure

Insulin resistance, the failure of the body to react to insulin appropriate, is usually induced by obesity and is the first step in the development of type 2 diabetes (1.2.1). Enhanced insulin release from pancreatic β-cells compensates obesity-induced insulin resistance for years (Rhodes 2005). Increased β-cell growth, called islet hyperplasia, caused by mechanisms such as enhanced β-cell survival and proliferation, is essential for compensation of insulin resistance (Jetton, Lausier et al. 2005). Elevation of insulin release per β-cell, through mechanisms such as increased glucose sensitivity or increased glucose metabolism, further plays an important role in insulin resistance compensation (Chen, Hosokawa et al. 1994; Liu, Jetton et al. 2002). β-cell compensation of insulin resistance normalizes blood glucose concentration completely or almost completely (LeRoith 2002; Poitout, Amyot et al. 2010). However, β-cell compensation fails in obese patients with susceptible pancreatic β-cells (Osei, Rhinesmith et al. 2004; Hong, Gui et al. 2008; Cali, Man et al. 2009).

In susceptible pancreatic β-cells, obesity-induced elevated circulating FAs and glucose concentrations induce gluco- and lipotoxicity. Glucotoxicity is caused by enhanced intracellular glucose levels, which are metabolized through anaerobic glycolysis,

glycosylation, glucose autoxidation and the glucosamine pathway (Robertson, Harmon et al. 2003). These processes form reactive oxygen species (ROS), which have a high potential for cellular damage. Similar, also metabolism of FAs, which are elevated in the blood stream of obese patients (1.2.1), cause the production of ROS, a process called lipotoxicity (Robertson, Harmon et al. 2004). Low levels of antioxidant enzymes in pancreatic β-cells make the insulin release process vulnerable for oxidative stress (Robertson, Harmon et al. 2003). The loss of pancreatic and duodenal homeobox 1 (PDX1), an important transcription factor regulating the *insulin* gene, and increased apoptosis through increased nuclear factor kappa B (NFκB) activity are two of many possible molecular consequences of glucose toxicity and lipotoxicity (Robertson, Harmon et al. 2003). Eventually, glucolipotoxicity enhances apoptosis and leads to β-cell failure and subsequently dramatically increased blood glucose levels, marking the onset of type 2 diabetes (Butler, Janson et al. 2003).

Susceptibility to β-cell failure is largely influenced by genetic predisposition, accounting for more than 50 % (Nolan, Damm et al. 2011). Most of the gene variations involved in the pathogenesis of type 2 diabetes regulate pancreatic β-cell maturation or insulin secretion (Bonnefond, Froguel et al. 2010; Nolan, Damm et al. 2011; Ashcroft and Rorsman 2012). Through employment of large-scale, high-resolution genome-wide association studies (GWAS), risk SNPs in many human genes have been identified, such as *KCNJ11, TCF7L2, WFS1, HNF1B, SLC30A8, CDKAL1* or *IGF2BP2* (Nolan, Damm et al. 2011). One of the strongest risk alleles for type 2 diabetes was found in the gene *transcription factor 7-like 2 (TCF7L2*). The strongest risk SNP of *TCF7L2*, thymine rs7903146, decreases glucose-mediated insulin secretion, increasing the risk for type 2 diabetes about 50 % (Grant, Thorleifsson et al. 2006; Saxena, Gianniny et al. 2006). *TCF7L2* is an crucial component in the WNT signaling pathway, effecting transcription of many genes during embryogenesis and adulthood (Jin and Liu 2008). *TCF7L2* and other so far identified genetic variations associated with increased type 2 diabetes risk explain only 10 % of the heritability of the disease, leaving room for future investigations aiming

to identify rare genetic variations and genetic variations with small effects on the progression of type 2 diabetes (Herder and Roden 2011).

Type 2 diabetes can also be caused by genetic mutations in one of the essential genes for the insulin release machinery. This monogenic diabetes, called maturity onset diabetes of the young (MODY), effects 1 - 2 % of all diabetic patients and occurs shortly after birth or during childhood (Bonnefond, Froguel et al. 2010). Despite the low relevance for the pathophysiology of type 2 diabetes, human monogenic diabetes helped to improve the understanding of the molecular basis of insulin secretion. These findings include genes responsible for the development of pancreatic β-cells, such as *PDX1* (MODY4) (Stoffers, Zinkin et al. 1997), *neurogenic differentiation 1* (*NeuroD1*, MODY6) (Malecki, Jhala et al. 1999) or *paired box gene 4* (*PAX4*, MODY 9) (Smith, Watada et al. 2000), as well as genes responsible for controlling insulin secretion, such as *hepatocyte nuclear factor 4α* (*Hnf-4α*, MODY1) (Herman, Fajans et al. 1997) or *hepatocyte nuclear factor 1α* (*Hnf-1α*, MODY3) (Shih, Screenan et al. 2001). Also genes for glucose uptake and break-down, such as *glucokinase* (*GCK*, MODY2) (Vionnet, Stoffel et al. 1992), and genes encoding membrane channels, such as *potassium inwardly-rectifying channel* (*KCNJ11*) and *ATP-binding cassette transporter sub-family C member 8* (*ABCC8*) (Gloyn, Weedon et al. 2003), are known to be mutated in diabetic patients and improved the understanding of the mechanisms of insulin release.

1.2.3 **MiR-375-targeted CADM1 expression in type 2 diabetes**

MicroRNAs (miRNAs) are RNAs, consisting of about 21 nucleotides, and are repressors of posttranscriptional gene expression (Bartel 2004; Krol, Loedige et al. 2010). Expression of many miRNAs is regulated in obesity and miRNA-regulated genes contribute to the development of type 2 diabetes (Zhao, Keller et al. 2009), opening the possibility that miRNAs play an essential role in the pathophysiology of type 2 diabetes. So far, many miRNAs have been identified with a role in β-cell apoptosis (miR-34a, miR-146) (Lovis, Roggli et al. 2008), *insulin* expression (miR-24, miR-26, miR-182, miR-148) (Melkman-

Zehavi, Oren et al. 2011) or glucose-stimulated insulin secretion (miR-369-5p, miR-130a, miR-27a, miR-410, miR-200a, miR-337) (Williams and Mitchell 2012).

MiR-375 is the highest expressed miRNA in pancreatic islets (Poy, Eliasson et al. 2004). MiR-375 expression negatively correlates with glucose-induced insulin secretion *in vivo* and *in vitro* (Poy, Eliasson et al. 2004; Poy, Hausser et al. 2009). In addition, *miR-375* knock-out (*miR-375*KO) mice exhibit reduced pancreatic β-cell mass due to impaired proliferation (Poy, Hausser et al. 2009), showing that miR-375 is a regulator of pancreatic β-cell growth and function. *MiR-375* expression is regulated in islets from hyperplastic *ob/ob* mice, diabetic rats and diabetic patients, further emphasizing a possible role of this miRNA in the development of type 2 diabetes (El Ouaamari, Baroukh et al. 2008; Poy, Hausser et al. 2009; Zhao, Guan et al. 2010). Recent investigations showed that pyruvate dehydrogenase kinase 1 (PDK1) is one target of miR-375 (El Ouaamari, Baroukh et al. 2008). Increased miR-375 expression reduces PDK1 expression and subsequent induction of *insulin* gene expression and DNA synthesis. In addition to PDK1, miR-375 also regulates expression of cell adhesion molecule (CADM)1 (Poy, Hausser et al. 2009). The exact role of CADM1 in pancreatic islets has not been fully established (1.3.2). However, the targeting of CADM1 by miR-375 suggests that CADM1 might be involved the miR-375-mediated effects on β-cell growth and pancreatic insulin secretion.

1.3 Cell adhesion molecule 1 (CADM1)

Cell adhesion molecules are proteins targeting cells to their specific locations by facilitating cell to cell or cell to matrix interactions. In addition, cell adhesion molecules have important roles in signaling within and between cells, influencing processes such as growth, cell differentiation or vesicle trafficking. CADM1 belongs to a family of calcium-independent cell adhesion molecules that is characterized by immunoglobulin (Ig)-like domains and therefore called immunoglobulin superfamily (IgSF) (Bork, Holm et al. 1994). The Ig-like domain functions as a binding domain, facilitating protein to protein or protein to ligand interactions, regardless of the function of the protein inheriting the Ig-like domain. The founding members of the IgSF are immunoglobulins, also called antigen receptors or antibodies. Additional, Ig-like domains can be found in a vast amount of protein families, which function as cell surface receptors, matrix proteins, enzymes or cell adhesion molecules.

The CADM protein family consist of four members termed CADM1, CADM2, CADM3 and CADM4 (Biederer 2006). The proteins of the CADM family have been described by several independent groups, giving them different names. Although CADM has been accepted as the official symbol, early names such as synaptic cell adhesion molecule (SynCAM), spermatogenic immunoglobulin superfamily (SgIgSF), tumor suppressor in lung cancer (TSLC), nectin-like protein (NECL) or immunoglobulin superfamily member (IgSF) have still been used in recent publications. The individual names for each CADM protein are referenced elsewhere (Pietri, Easley-Neal et al. 2008).

Like other IgSF proteins, the proteins of the CADM family contain three Ig-like domains at the extracellular N-terminus **(Figure 8).** These Ig-like domains are formed by repetitive antiparallel β-strands in a loop-like structure and stabilized by sulphydryl bridges (Gomperts, Kramer et al. 2003). The Ig-like domains facilitate homophilic binding between each CADM protein to itself or heterophilic binding between CADM1 and 2 or CADM3 and 4. The binding affinity between the CADM proteins is regulated by the degree of N-glycosylation of the Ig-like domains (Fogel, Akins et al. 2007). Furthermore, the Ig-like domains allow a lateral self-assembly of CADM1 as *cis* oligomers, which

enhances *trans*-binding of CADM1 from cell to cell (Fogel, Stagi et al. 2011). Lastly, the Ig-like domains have been described in mediating binding of CADM proteins to growth factor receptors, such as epidermal growth factor receptors (EGFR) (Kawano, Ikeda et al. 2009).

The first description of CADM1 as a cell adhesion molecule came from *in vitro* cell studies, where CADM1 was found to be expressed at boundaries between non-polarized cells as well as at the basolateral membrane of polarized cells (Masuda, Yageta et al. 2002). Later on, these results could be confirmed *in vivo* in murine lung and gall bladder epithelium (Fujita, Soyama et al. 2003; Shingai, Ikeda et al. 2003). In addition, these studies showed that CADM1 is expressed outside of specialized cell to cell junctions, such as tight-, adherens- and gap junctions. In the following years, CADM1 expression was confirmed between several different cell types such as nerve to nerve (Biederer, Sara et al. 2002), nerve to mast cell (Ito, Hagiyama et al. 2008), nerve to astrocytes (Sandau, Mungenast et al. 2011), smooth to mast cell (Ito, Hagiyama et al. 2008), mast cell to fibroblasts (Ito, Jippo et al. 2003), epidermal to epidermal cells (Giangreco, Jensen et al. 2009), spermatogenic cells to Sertoli cells (van der Weyden, Arends et al. 2006) and tumor cells to lymphocytes (Boles, Barchet et al. 2005). The respective functions of CADM1 seems to be largely dependent on the expressing cell type and include roles in synaptogenesis, tumor suppression, fertility, epithelial structure formation and cytotoxicity (Murakami 2005). The most relevant CADM1 functions for this work are explained in the following sections.

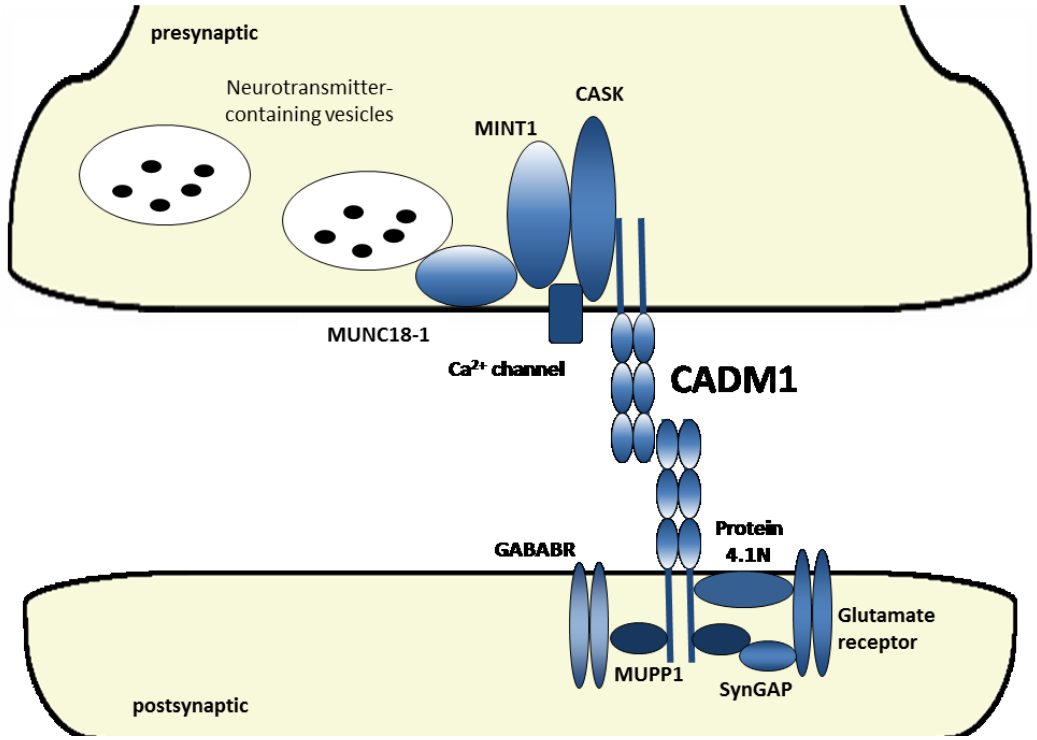

Figure 8: CADM1 protein interactions at the synapse

CADM1 (blue) is expressed at the pre- (top) and postsynaptic (bottom) membrane spanning the synaptic cleft. Each CADM1 molecule is clustered to itself in *cis*-binding, enhancing binding to CADM1 molecules bound to the opposing cell type in *trans*-conformation. *Cis*- and *trans*-binding is facilitated by immunoglobulin (Ig)-like domains (blue ovals) at the extracellular part of CADM1. The intracellular PDZ-binding domain of CADM1 can bind to proteins with corresponding PDZ domains, such as MUPP1. MUPP1 binds to GABBR2 in inhibitory neurons or SynGAP in excitatory neurons. SynGAP further binds to glutamate receptors in excitatory neurons. Other binding partners of CADM1 with PDZ domains include CASK and MINT1. MINT1 and CASK recruit Ca^{2+} channels which are important for release of synaptic vesicles. MINT1 can also bind to MUNC18-1, which is directly involved in synaptic vesicle fusion. The intracellular part of CADM1 can bind to protein 4.1N via its protein 4.1-binding domain to recruit glutamate receptors at the postsynaptic membrane.

Abbreviations: Cell adhesion molecule 1 (CADM1); Calcium/calmodulin-dependent serine protein kinase (CASK); γ-aminobutyric acid receptor B receptor 2 (GABBR2); Munc-18-interacting protein (MINT1); Mammalian uncoordinated-18-1 (MUNC18-1); Multiple PDZ domain protein 1 (MUPP1); Synaptic Ras GTPase activating protein 1 (SynGAP)

1.3.1 **CADM1 as an enhancer of synaptic function**

All four CADM proteins are highly expressed during embryonic and postnatal development in several parts of the nervous system. In addition, CADM1 shows a lower expression in peripheral tissues, such as lung and testis (Fogel, Akins et al. 2007). Early studies identified CADM1 as inducer of synaptic transmissions when being overexpressed together with the glutamate receptor 2 (GluR2) (Biederer, Sara et al. 2002). Later on, it was shown that the CADM proteins are highly enriched in pre- and postsynaptic membranes especially two weeks after birth, when synapse formation peaks (Fogel, Akins et al. 2007). In addition, CADM1 negatively regulates the structural complexity and number of synapses during postnatal synaptogenesis (Stagi, Fogel et al. 2010). It is therefore thought that regulation of synaptogenesis in the nervous system during development is one of the main functions of the CADM family. It was furthermore shown that adult *Cadm1* deficient mice have increased spatial learning and altered synaptic plasticity (Robbins, Krupp et al. 2010). Synaptic plasticity is a process altering synaptic strength and efficacy in response to synaptic activity and is important for cognitive tasks, such as spatial learning. The studies by Robbins *et al.* also showed that CADM1 influences the number of excitatory synapses, while inhibitory synapses are not regulated by this protein. CADM1 therefore plays an important role in regulating synaptic connections and synaptic efficacy also in adult rodents, mainly by regulating excitatory synapses.

Several putative binding partners of CADM1 have been identified, which might explain how CADM1 influences synaptic formation and function. The cytoplasmic tail of CADM1 contains a post synaptic density-95/disc large/zonula occludens-1 (PDZ)-binding domain (Biederer, Sara et al. 2002; Fogel, Akins et al. 2007). Putative CADM1 binding partners with PDZ domains include multiple PDZ domain protein 1 (MUPP1) (Fujita, Tanabe et al. 2012) **(Figure 8)**. MUPP1 interacts with GABA B receptor 2 (GABBR2) in postsynaptic inhibitory neurons or synaptic Ras GTPase activating protein 1 (SynGAP) in postsynaptic excitatory neurons (Krapivinsky, Medina et al. 2004; Balasubramanian, Fam et al. 2007). SynGAP further binds to glutamatergic *N*-methyl-D-aspartate receptors (NMDAR).

Although the exact physiological role of CADM1 binding to MUPP1 has not been established, CADM1 might positively regulate neurotransmitter receptor signaling at postsynaptic membranes by stabilizing the respective receptor complexes. Other putative CADM1 binding partners with PDZ domains include calcium/calmodulin-dependent serine protein kinase (CASK) and munc-18-interacting protein 1 (MINT1) (Biederer, Sara et al. 2002) **(Figure 8)** . MINT1 displays one possible link between CADM1 and its function as enhancer of synaptic activity, since MINT1 binds to mammalian uncoordinated-18-1 (MUNC18-1), an essential protein in synaptic neurotransmitter release (Biederer and Sudhof 2000). Furthermore, VELI, CASK and MINT1 form a tripartite complex, which localizes and stabilizes cell surface and signaling proteins, such as β-neurexins. The β-neurexins-neuroligins binding is known to facilitate synaptogenesis at the postsynaptic membrane (Graf, Zhang et al. 2004). In addition, MINT1 and CASK are known to recruit Ca^{2+} channels, which are important for synaptic vesicle release (Maximov, Sudhof et al. 1999) **(Figure 8)**.

Besides the PDZ-binding domain, the intracellular c-terminus of CADM1 contains a highly conserved protein 4.1-binding domain (Biederer 2006), which might be involved in the CADM1-mediated regulation of synaptic growth and function. The protein 4.1-binding domain binds to protein 4.1N, which recruits excitatory glutamate receptors *in vitro* (Hoy, Constable et al. 2009) **(Figure 8).** In addition, FERM, RhoGEF (Arhgef) and pleckstrin domain protein 1 (Farp1), a regulator of synapse complexity and number, was recently identified to bind to the protein 4.1-binding domain of CADM1 (Cheadle and Biederer 2012).

1.3.2 CADM1 and type 2 diabetes

A role of CADM1 in type 2 diabetes has not been investigated yet. However, recent investigation highlighted a potential role of CADM1 in pancreatic islets. Obesity-induced insulin resistance is compensated by enhanced insulin secretion and the failure of β-cells to produce sufficient insulin amounts marks the onset of type 2 diabetes (1.2). In pancreatic α-cells, insulin resistance increases glucagon production, which contributes

to hyperglycemia of diabetic patients through enhanced HGP (Hamaguchi, Fukushima et al. 1991).

CADM1 was detected in all four cell types of the pancreatic islet in humans, whereas murine islets were reported to express CADM1 in α- and δ-cells only (Koma, Furuno et al. 2008). In contrast, other studies identified CADM1 in murine β-cells, although to a lesser degree than in non β-cells (Suckow, Comoletti et al. 2008; Shimada, Tachibana et al. 2012). In human β-cells, CADM1 seems to be involved in insulin secretion, since CADM1 expression correlates with hormone function in human islet cell tumors (Koma, Furuno et al. 2008). In addition, CADM1 was proposed in these studies to be important in cell to cell contact within pancreatic islets. In rodent α-cells, recent studies identified CADM1 as inhibitor of glucagon release through mediation of communication between α-cells (Ito, Ichiyanagi et al. 2012).

Furthermore, CADM1 expression was identified in neuronal crest cells in pancreatic islets (Shimada, Tachibana et al. 2012). Neuronal crest cells are important for the maturation of pancreatic β-cells and they are progenitors of the nervous system, such as autonomic nerves (Shimada, Tachibana et al. 2012). α- and β-cells expressing CADM1 were found in close proximity to CADM1 expressing neuronal crest cells, suggesting that CADM1 facilitates binding between endocrine and neuronal cells in pancreatic islets. However, the exact role of CADM1 mediating these interactions has not been established.

1.3.3 CADM1 and its role in autism

Two missense mutations in the *CADM1* gene were found in patients with autism spectrum disorder (ASD) (Zhiling, Fujita et al. 2008). ASD is an inherited neurodevelopmental disorder characterized by impaired social interaction and impaired communication as well as repetitive behavior (American Psychiatric Association 2011). The disease is linked to mutations in many different genes causing alterations in synaptogenesis and neuronal development (Persico and Bourgeron 2006). The missense

mutations in the *CADM1* gene translate into mutations in the Ig-like domain of CADM1, weakening its extracellular binding and leading to increased intracellular CADM1 accumulation and degradation (Zhiling, Fujita et al. 2008).

Features of the human ASD phenotype were observed in *Cadm1* deficient mice. Besides impaired social behavior, *Cadm1*KO mice have increased anxiety behavior and impaired motor function (Takayanagi, Fujita et al. 2010). Furthermore, *Cadm1* deficient pups showed decreased postnatal ultrasonic vocalizations (USVs), a phenotype which resembles language impairments in autistic humans (Boucher 2012; Fujita, Tanabe et al. 2012). CADM1 is well expressed in Purkinje cells of the cerebellum and dendrite development of these cells is impaired in *Cadm1* deficient mice (Thomas, Akins et al. 2008; Fujita, Tanabe et al. 2012). Loss of cerebellar Purkinje cells was also found in ASD patients and in mice with autistic-like behavior (Ritvo, Freeman et al. 1986; Fatemi, Halt et al. 2002; Martin, Goldowitz et al. 2010; Tsai, Hull et al. 2012). CADM1 is furthermore known to bind to MUPP1, which interacts with GABBR2, in the cerebellum of mice (Fujita, Tanabe et al. 2012). This interaction is postulated to stabilize the synaptic MUPP1–GABBR2 complex. These studies also showed that GABBR2 expression is altered in the cerebellum of *Cadm1* deficient mice, similar to autistic patients (Fatemi, Folsom et al. 2009). Alterations in GABBR2 expression in the absence of CADM1 are therefore thought to induce autistic-like behavior in humans and mice (Fujita, Tanabe et al. 2012).

1.4 Objectives

The pathogenesis of type 2 diabetes is marked by obesity-induced insulin resistance and β-cell failure. The ability of the pancreas to meet increased insulin demands by induction of islet hyperplasia determines whether type 2 diabetes develops in obese patients. MiR-375, the highest expressed miRNA in the pancreas, is an important regulator of hyperplasia as well as insulin secretion. MiR-375 is therefore expected to influence the pathogenesis of type 2 diabetes. CADM1 is one of the genes targeted by miR-375. Nevertheless, the molecular mechanisms how miR-375 regulates β-cell mass and function and the contribution of miR-375-targeted CADM1 expression to these processes have not been understood yet. The pathogenesis of type 2 diabetes is strongly influenced by the brain through regulation of energy homeostasis and subsequent resistance or susceptibility to obesity as well as through regulation of glucose homeostasis. Besides its expression in pancreatic β-cells, CADM1 is also highly expressed in several parts of the brain. So far, a role of CADM1 in the regulation of energy or glucose homeostasis in the brain or pancreatic β-cells has not been investigated.

The aim of this work is to evaluate the influence of CADM1 in peripheral and central tissues of the body on glucose and energy homeostasis. For this, it will be addressed whether CADM1 influences sensitivity to insulin or leptin, the most important hormones in the regulation of glucose and energy homeostasis. Furthermore, the role of CADM1 in pancreatic insulin release will be investigated. Ultimately, the studies should uncover the role of CADM1 in the development of type 2 diabetes.

First, it will be questioned if CADM1 influences energy and glucose homeostasis by investigating the phenotype of mice completely deficient for *Cadm1* (*Cadm1*KO). These studies include analyses of body weight and body composition as well as measurements of energy intake and energy expenditure. In addition, insulin and glucose sensitivity will be analyzed in *Cadm1*KO mice and glucose sensitivity in *Cadm1*-depleted pancreatic β-cells to evaluate the effects of CADM1 on glucose homeostasis. Second, it will be studied whether CADM1 influences the susceptibility to obesity and insulin resistance by

induction of obesity in *Cadm1* deficient mice through genetic modification or high fed diet feeding and subsequent analyses of energy and glucose homeostasis as above. Third, the role of CADM1 in energy and glucose homeostasis in neuronal tissues will be addressed by analyzing mice with *Cadm1* deficiency specifically in neuronal and glia cells for changes in energy and glucose homeostasis. These studies will help to narrow the mechanisms of CADM1 action on energy and glucose homeostasis.

2 Materials and Methods

2.1 Animal Experiments

2.1.1 Mouse lines

Mice carrying a *Cadm1* null allele and conditional *Cadm1* allele (*Cadm1*$^{lox/lox}$) mice were kindly provided by Allan Bradley (Wellcome Trust Genome Campus, Cambridge, UK) (van der Weyden, Arends et al. 2006). Mice heterozygous for the *Cadm1* null allele on a mixed 129/Sv - C57BL/6 background were backcrossed on C57BL/6N mice (Charles River Laboratories, Inc., Wilmington, USA) for four generations before using them for experiments. Breeding colonies were maintained by intercrossing mice heterozygous for the *Cadm1* null allele. Resulting mice homozygous for the *Cadm1* null allele (*Cadm1*KO) were compared to gender-matched littermates heterozygous or wild-type for the *Cadm1* null allele (control) unless otherwise stated. Multiple litters were analyzed for each experiment in order to reduce background effects.

For generating mice expressing POMC-enhanced green fluorescent protein (eGFP) cells (Cowley, Smart et al. 2001), homozygous mice for the *Cadm1* null allele were crossed to C57BL/6J-Tg(POMC-EGFP)1Low/J mice (The Jackson Laboratory, Bar Harbor, USA). Breeding colonies were maintained by crossing male mice heterozygous for the *Cadm1* null and positive for POMC-eGFP transgene with female mice homozygous for the *Cadm1* null allele. Neurons from resulting mice deficient for *Cadm1* and positive for POMC-eGFP (*Cadm1*KO POMC-eGFP) were compared to neurons from gender-matched, littermate control mice heterozygous for the *Cadm1* null allele and positive for POMC-eGFP (control POMC-eGFP).

To generate mice deficient for *Cadm1* and leptin (*Cadm1/ob*), B6.V-*Lep*^{ob}/J mice were purchased (The Jackson Laboratory, Bar Harbor, USA) and crossed to female *Cadm1*KO mice. Breeding colonies were maintained by crossing male mice heterozygous for the

Cadm1 null and *ob* allele with female mice homozygous for the *Cadm1* null allele and heterozygous for the *ob* allele. Resulting mice deficient for *ob* and *Cadm1* (*Cadm1/ob*) were compared to gender-matched, littermate control mice deficient for *ob* and heterozygous for the *Cadm1* null allele (*ob/ob*).

For generating tissue specific *Cadm1* deficient mice, B6.Cg-Tg(*Nes*-cre)1Kln/J (*NesCre*) and B6.129-*Lepr*tm2(*cre*)Rck/J (*LepRCre*) were purchased (The Jackson Laboratory, Bar Harbor, USA). These lines were crossed to *Cadm1*$^{lox/lox}$ animals. Breeding colonies were maintained by crossing *Cadm1*$^{lox/+}$ cre^{+} with *Cadm1*$^{lox/lox}$ cre^{-} mice. Gender-matched, littermate *Cadm1*$^{+/+}$ and *Cadm1*$^{lox/+}$ mice were used as controls (control) for tissue specific *Cadm1* deficient mice (*Cadm1NesCre*KO, *Cadm1LeprCre*KO). Mice expressing cre recombinase were included as controls to avoid differences due to phenotypic effects of cre expression. For *Cadm1NesCre*KO mice, only control mice carrying cre recombinase were used, since mice carrying the *NesCre* transgene are known to have a hypopituitarism phenotype (Galichet, Lovell-Badge et al. 2010).

To visualize *LeprCre* expression, *LepRCre* mice were crossed to B6.129X1-Gt(ROSA)26Sor$^{tm1(EYFP)Cos}$/J, which carry *yellow fluorescent protein* (*YFP*) under the control of the ubiquitously expressed *Rosa26* promoter (*Rosa26-YFP)* and were kindly provided by Prof. Kai Schmidt-Ott, Max-Delbrück-Centrum (MDC) für Molekulare Medizin, Berlin-Buch. Breeding colonies were maintained by crossing mice carrying *Rosa26-YFP* with mice carrying *LepRCre* and *Rosa26-YFP*. Resulting animals carrying *LepRCre* and *Rosa26-YFP* were used for immunohistochemistry.

All mice were housed in pathogen-free facilities in a 12 h light/dark cycle with light on from 7 am till 7 pm and fed ad libitum on CHOW diet with 11 % of calories from fat (ssniff Spezialdiäten GmbH Soest, Germany; M-Z V1124-0;) unless otherwise stated. For high fat diet (HFD) experiments, control and *Cadm1*KO animals were fed HFD with 56 % of calories from fat (ssniff Spezialdiäten GmbH Soest, Germany; EF R/M acc. D12492 mod.), starting between 4 and 7 weeks of age. Gender-matched littermates heterozygous or wild-type for the *Cadm1* null allele were used as control animals (control) unless otherwise stated.

2.1.2 Collection and analysis of blood parameters

Blood glucose concentrations were determined from whole venous blood from the tail tip using an automated glucose monitor (Glucometer Elite, Bayer) according to manufacturer's guidelines. For fasted blood glucose measurements animals were fasted overnight (16 h) before glucose measurements. Random glucose was measured in the afternoon.

For analyzing blood parameters other than glucose, whole venous blood was taken from the tail vein. For serum blood samples, blood without additions was kept at room temperature for 30 min before centrifuging. For plasma samples, ethylenediaminetetraacetic acid (EDTA) or heparin was added and blood was centrifuged immediately. All samples were centrifuged twice for 5 min at 10.000 rpm and supernatants were stored at -20 °C for short term or -80 °C for long term storage. Insulin, leptin, IGF-1 and growth hormone (GH) concentrations were measured by enzyme-linked immunosorbent assay (ELISA) according to manufacturers' guidelines (Mouse/Rat Insulin ELISA, Crystal Chem, Downers Grove, IL, USA; ELISA Development Kits: Murine Leptin ELISA Development Kit, Murine IGF-I ELISA Development Kit, PeproTech, Hamburg, Germany; Rat/Mouse Growth Hormone ELISA, Millipore, MA, USA).

2.1.3 Glucose tolerance test, insulin tolerance test, *in vivo* insulin release

For glucose tolerance tests (GTT), mice were fasted overnight (16 h). Animals were injected intraperitoneally (i.p.) with glucose (2 g/kg body weight) in phosphate buffered saline (PBS, 136.8 mM NaCl, 2.68 mM KCl, 10 mM Na_2HPO_4, 1.76 mM KH_2PO_4, pH = 7.4). For insulin tolerance tests (ITT) animals were starved for 6 h during the day and injected i.p. with bovine insulin in PBS (0.75 U/kg body weight) (Sigma Aldrich, Seelze, Germany). Plasma glucose was measured before (0 min) and 15, 30, 60, and 120 min after injection as described above. *In vivo* insulin release was determined after overnight fasting by glucose injection (2 g/kg body weight) and determination of blood insulin

concentrations before (0 min) and 2.5, 5, and 15 min after glucose injection as described before (2.1.2).

2.1.4 Growth hormone release challenge

Growth hormone (GH) release challenge was conducted as described by Tennese et al. (Tennese and Wevrick 2011). Briefly, random fed animals were injected i.p. with 120 µg/kg rat ghrelin (Tocris Bioscience, MO, USA Bioscience, MO, USA) in PBS and blood samples were taken 15 min after injections. GH levels were measured as described before (2.1.2).

2.1.5 Measurements of body length

Adult animals were briefly anesthetized with isoflurane (CP-Pharma Handelsgesellschaft mbH, Burgdorf, Germany) and placed on a ruler while being completely relaxed. All animals recovered shortly after anesthesia.

2.1.6 Random body weight measurements and body composition measurements by NMR

Body weight measurements were conducted in random fed mice using standard laboratory scales. Body composition was determined by nuclear magnetic resonance (NMR). NMR measurements were conducted by the Mouse Phenotyping Platform, Dr. Arnd Heuser, AG Thierfelder, Max-Delbrück-Centrum (MDC) für Molekulare Medizin Berlin-Buch. The Minispec Model LF90 II (6.5 mHz) (Bruker Scientific Instruments, Billerica, MA, USA) was used for the measurements. Animals were fasted from 9 am and drinking water was taken away at 12 am. Body composition was measured between 2 and 3 pm.

2.1.7 Measurement of pancreatic insulin content

Whole pancreata were taken from random fed mice. Weights of pancreata were measured immediately and pancreata were stored in acidic ethanol (95 % ethanol, 5 % HCl) at -20 °C until use. Pancreata were homogenized and further incubated for at least 24 h at -20 °C. Insulin content was measured by radioimmunoassay (RIA) (Rat insulin RIA kit, Millipore, MA, USA) according to manufacturer's guidelines and normalized to pancreatic weight.

2.1.8 Refeed experiments and indirect calorimetry

For refeeding experiments, mice were individually housed and given 48 h for acclimation before start of refeeding experiments. Food was taken away in the morning and given back 24 h later. Food intake was measured 3 h after refeeding. Body weight difference was calculated as body weight at the time when food was given back subtracted by body weight at the same time when food was taken away.

Indirect calorimetry, locomotor activity and basal food intake measurements were conducted with the PhenoMaster System (TSE Systems, Bad Homburg, Germany). After 24 h of acclimatization, CO_2 and O_2 respiration, food intake and locomotor activity was measured for three days. Locomotor activity was measured three-dimensionally by infrared-light beams. VCO_2 and VO_2 were calculated as difference between reference and sample cage. Energy expenditure (EE) was calculated using the following equation (Weir 1949):

$$EE\ [kcal] = 3.941 * VO_2[l] + 1.106\ * VCO_2[l]$$

RER was calculated using the following equation:

$$RER = \frac{VCO_2}{VO_2}$$

2.1.9 Collection and homogenization of hypothalami for Western Blotting and qRT-PCR

Tissues were taken at random fed state or after 24 h starvation as indicated. Animals were killed by cervical dislocation and tissues dissected. The limits of the hypothalamus for dissection were the optic chiasma at the anterior border, the mammillary bodies at the posterior border, the lateral ventricles at the position of the optic chiasma at the lateral borders and the ventral end of the lateral ventricles at the position of the optic chiasma at the dorsal border. Tissues were snap frozen in 2-methylbutan (Acros Organics, Geel, Belgium) on dry ice and stored at -80 °C until use. For Western Blotting, tissues were thawed quickly and homogenized in protein lysis buffer containing protease inhibitor (cOmplete, EDTA-free Protease Inhibitor Cocktail Tablets, Roche, Basel, Switzerland) and for measurements of phosphorylated proteins also phosphatase inhibitor (PhosSTOP Phosphatase Inhibitor Cocktail Tablets, Roche, Basel, Switzerland). Samples were homogenized using a dounzer and centrifuged at 10,000 g for 10 min at 4 °C (Ender, Krek et al. 2008). For quantitative real time polymerase chain reaction (qRT-PCR), tissues were thawed and homogenized in TRIzol reagent (Invitrogen, Carlsbad, USA) by pipetting up and down.

2.2 Cell culture

2.2.1 Freezing, thawing and growth of cells

Mouse insulinoma cells (MIN6) cells were washed twice with sterile PBS and harvested with trypsin (0.05 % trypsin-EDTA, Gibco, Billings**,** USA). After centrifuging at 200 g for 3 min, cells were either resuspended in growth medium (89 % Dulbecco's Modified Eagle's medium (DMEM, Gibco, Billings**,** USA), 10 % fetal bovine serum (FBS) heat inactivated (56 °C for 30 min, PAN-Biotech GmbH, Aidenbachove, Germany), 1 % penicillin/streptomycin (Gibco, Billings**,** USA), 5.5 mM 2-mercaptoethanol (Sigma-Aldrich**,** Seelze, Germany)) for splitting or resuspended in freezing medium (10 % DMSO (Sigma-Aldrich**,** Seelze, Germany), 40 % FBS heat inactivated , 50 % DMEM) for freezing. Cells were aliquoted in cryotubes and frozen at – 80 °C overnight and transferred for long-term storage in liquid nitrogen.

After thawing, cells were transferred to growth medium, centrifuged at 200 g for 3 min and resupended in growth medium. Cells were transferred to cell culture plates and incubated at 37 °C and 5 % CO_2. Cells were harvested and split every 2 - 3 days as described before (2.1.9).

2.2.2 Transfection of cells

Transfections were conducted by using Amaxa Nucleofector electroporation kit V (Lonza Cologne GmbH, Cologne, Germany) according to the manufacturer's guidelines and experiments were performed 48 h after electroporation. 0.2 pmol siRNA SMARTpool **(Table 1)** against *Cadm1* (Dharmacon Inc., Chicago, USA) or control (siGENOME Non-Targeting siRNA Pool #2, Dharmacon Inc., Chicago, USA) was used per electroporation. For Western blotting analysis, cell culture plates were washed twice with PBS and stored at -80 °C until use. Cells were lysed with protein lysis buffer containing protease inhibitor as described above.

	Sequence (5'-3')
siRNA 1	CCC AUG UCT UAA AUA CGU AUU
siRNA 2	GUA UAA ACC GCA AGU GCA UUU
siRNA 3	UUU GCA UUC UCU AAA GCT AUU
siRNA 4	CGC AUA GCU ACU AAA AUA AUU

Table 1: siRNA SMARTpool against *Cadm1*

2.2.3 *In vitro* insulin secretion

MIN6 cells were transfected with siRNA against *Cadm1* or control as described before (2.2.2). 48 h after transfections, MIN6 cells were preincubated with 5 mM glucose in Dulbeco's PBS-HEPES-BSA (DPH) (0.90 mM $CaCl_2$, 2.67 mM KCl, 1.47 mM KH_2PO_4, 0.5 mM $MgCl_2$-$6H_20$, 138 mM NaCl, 8.10 mM Na_2HPO_4-$7H_20$, 20 mM HEPES, 0.2 % BSA, pH = 7.4) for 30 min at 37 °C and 5 % CO_2. After washing with DPH, cells were incubated with 2.8 mM or 25 mM glucose in DPH for 1 h at 37 °C and 5 % CO_2. An aliquot of the supernatant was collected and centrifuged at 200 g for 5 min. Supernatants were frozen at - 20 °C until insulin measurements. Plates containing cells were washed with DPH and frozen at - 20 °C until further use. Cells were briefly incubated with cold acidic ethanol (95 % ethanol, 5 % HCl) and cell lysates frozen at -20 °C until insulin measurements. Insulin concentrations were measured by RIA (Rat insulin RIA kit, Millipore, MA, USA) according to manufacturer's guidelines. Insulin content of supernatants was normalized to insulin content of the cells.

2.3 Molecular Biology

2.3.1 Isolation of genomic DNA

Mouse tail tips were incubated in lysis buffer (4 M Urea, 10 mM EDTA pH = 8.0, 0.1 M Tris/HCl pH = 8.0, 0.5 % sodium sarcosyl, 0.2 M NaCl) with 0.18 mg/ml proteinase K (PAN-Biotech GmbH, Aidenbachove, Germany) overnight at 55 °C. Desoxyribonucleic acid (DNA) was precipitated in 60 mM sodium acetate and 75 % (v/v) ethanol, centrifuged for 5 min at maximal speed. Precipitates were washed with 70 % (v/v) ethanol. DNA pellets were dried at room temperature for 30 - 45 min and resuspended in Tris/EDTA-buffer (10 mM Tris-HCl, 1 mM EDTA, pH = 8.0). Isolated genomic DNA was stored at 4 °C.

2.3.2 Quantification of RNA and DNA concentrations

DNA and RNA concentrations were determined at 260 nm with a NanoDrop ND-1000 UV-Vis spectrophotometer (Peqlab, Erlangen, Germany) according to manufacturer's guidelines. The ratio of adsorptions at 260 nm versus 280 nm was used as control for purity of DNA and ribonucleic acid (RNA) samples.

2.3.3 Polymerase chain reaction (PCR)

Polymerase chain reaction (PCR) was used for genotyping of all mouse lines. 50 - 200 ng mouse tail DNA and PCR mastermix (1 x PCR buffer homemade (67 mM Tris-HCl pH = 9.1, 16 mM $(NH_4)_2SO_4$, 3.5 mM $MgCl_2$, 0.15 mg/ml BSA), 25 pmol of each primer **(Table 2)**, 25 µM dNTP Mix (Fermentas GmbH, St. Leon-Rot, Germany), 0.5 units *Taq* DNA Polymerase, Nativ (Invitrogen, Carlsbad, USA)) were made up to 20 µl. PCR programs in a thermocycler T3000 (Biometra, Göttingen, Germany) started with 5 min denaturation at 95°C, followed by 30 cycles consisting of denaturation at 95 °C for 45 sec, annealing at oligonucleotide-specific temperatures **(Table 2)** for 30 sec and elongation at 72 °C for 30 sec. After a final elongation step at 72 °C for 10 min, the PCR product was chilled at 4 –

10 °C. For genotyping of *ob* mutant mice, 10 µl of PCR product was digested with 1 x NEBuffer 3 (New England Biolabs, Ipswich, USA) and 5 units of enzyme Dde1 (New England Biolabs, Ipswich, USA) for at least 6 h at 37 °C. All PCR and digested PCR products were analyzed on agarose gel electrophoresis.

Primer	Sequence (5'-3')	$T_{annealing}$ (°C)	Orientation
Cadm1 wt for	CCA TGC TAT GCT TGC TCA TC	60	sense
Cadm1 wt rev	AAA GAT GAT TGC CCA TCC AG	60	antisense
Cadm1KO for	AGC ATC CCT TTC CAC CAT AGT TTT CTC TCT	65	sense
Cadm1KO rev	TAC CAG GAG GGG AGA AGA GGC CCA GAG C	65	antisense
Cre3 for	ATG CTT CTG TCC GTT TGC CG	55	sense
Cre1 rev	CCT GTT TTG CAC GTT CAC CG	55	antisense
Ob for	TGT CCA AGA TGG ACC AGA CTC	62	sense
Ob rev	ACT GGT CTG AGG CAG GGA GCA	62	antisense
POMC-eGFP for	AAG TTC ATC TGC ACC ACC G	60	sense
POMC-eGFP rev	TCC TTG AAG AAG ATG GTG CG	60	antisense
Rosa26-YFP for	CGT AAA CGG CCA CAA GTT CAG	65	sense
Rosa26-YFP rev	GAA CTC CAG CAG GAC CAT GTG	65	antisense

Table 2: Sequence and orientation of PCR primer

2.3.4 RNA Extraction, RT-PCR and qRT-PCR

Gene expression analysis was conducted by Sudhir Gopal Tattikota, AG Poy, MDC Berlin-Buch. RNA was isolated from homogenized cell lysates or tissues using TRIzol reagent

(Invitrogen, Carlsbad, USA) according to manufacturer's guidelines. 5 µg RNA was reversed transcribed (reverse transcription polymerase chain reaction (RT-PCR)) into cDNA using SuperScript III Reverse Transcriptase (Invitrogen, Carlsbad, USA) according to manufacturer's guidelines. Gene expression analysis was performed by qRT-PCR using FastStart Universal SYBR Green Master (Roche, Mannheim, Germany) with a StepOnePlus Real-Time PCR System (Applied Biosystems, Foster City, USA) according to

Primer	Sequence (5'-3')	Orientation
36B4 for	TCC AGG CTT TGG GCA TCA	sense
36B4 rev	CTT TAT CAG CTG CAC ATC ACT CAG A	antisense
Gh for	TCA GCA GGA TTT TCA CCA	sense
Gh rev	ATC TTC CAG CTC CTG CAT	antisense
Ghrh for	TTG TGA TCC TCA TCC TCA CCA GTG	sense
Ghrh rev	ATG ATG TCC TGG ATC ACT TTC CGG	antisense
Npy for	CTG ACC CTC GCT CTA TCT CTG	sense
Npy rev	AGT ATC TGG CCA TGT CCT CTG	antisense
Pomc for	CCC AAG GAC AAG CGT TAC GG	sense
Pomc rev	GTG CGC GTT CTT GAT GAT GG	antisense
Prkaa1 for	GCA CCC TCA CAT CAT CAA AC	sense
Prkaa1 rev	ATC AAG CAG GAC GTT CTCA G	antisense
Prkaa2 for	TAC GAA CTA GCT GTG GAT CG	sense
Prkaa2 rev	GGA TCT TCT TGA AGA GCG TAG G	antisense

Table 3: Sequence and orientation of qRT-PCR primers

manufacturer's guidelines. Primers were designed to span introns avoiding DNA amplification. The annealing temperature was set to 60 °C for all experiments. *36B4* gene expression was used for normalizing unknown gene expression.

2.3.5 **Western blot analysis**

Frozen protein lysates were thawed and protein concentrations were measured by using bicinchoninic acid (BCA) assay. Per reaction, 200 µl of BCA (Sigma-Aldrich**,** Seelze, Germany) were mixed with 4 µl copper (II) sulfate solution (Sigma-Aldrich**,** Seelze, Germany) and added to a 96- well plate containing equal volumes (5 - 15 µl) of protein lysate. Bovine serum albumin (BSA) (SERVA Electrophoresis GmbH, Heidelberg, Germany) solubilized in lysate buffer at varying concentrations was used as protein standard. Absorptions were read with a photometer Infinite 200 PRO (Tecan Group Ltd., Männedorf, Switzerland) at 562 nm and protein concentrations were calculated in comparison to BSA standard concentrations.

Aliquots of protein lysates containing equal protein amounts (20 - 80 ng) were diluted in 5 x SDS loading buffer (310 mM Tris, 10 % (w/v) sodium dodecyl sulfate (SDS), 50 % (v/v) glycerol, 5 mM EDTA, 0.05 % (w/v) bromophenol blue, 5 % (v/v) 2-mercaptoethanol) and incubated for 5 min at 95 °C. Protein lysates were subjected to SDS polyacrylamide gel electrophoresis (SDS-PAGE) (Bio-Rad Laboratories, CA, USA) on 10 % (v/v) SDS gels in SDS running buffer (25 mM Tris, 192 mM glycine, 0.1 % (w/v) SDS, pH = 8.3) at room temperature. Afterwards, protein lysates were blotted onto 0.2 µm nitrocellulose or polyvinylidenfluorid (PVDF) membranes (Carl Roth GMBH, Karlsruhe, Germany) in mini trans-blot cell system (Bio-Rad Laboratories, CA, USA) in transfer buffer (25 mM Tris-HCl pH = 8.4, 192 mM glycine, 20 % (v/v) methanol) for 100 min at 80 V at 4 °C. Membranes were blocked in blocking buffer (2.5 % dry milk, 20 mM Tris, 137 mM NaCl, pH = 7.6) for at least one hour at room temperature. Primary antibodies **(Table 4)** were diluted in blocking buffer and incubated with membranes at 4 °C overnight. Membranes were finally incubated with secondary antibodies (Calbiochem, La Jolla, USA) diluted 1:10,000

in blocking buffer for at least one hour at room temperature. After 3 x 10 min washing with washing buffer (20 mM Tris, 137 mM NaCl, pH = 7.6), bands were detected with homemade enhanced chemiluminescence (1 ml solution A (0.25 mg/ml luminol in 0.1 M Tris, pH = 8.6), 0.1 ml solution B (1.1 mg/ml in DMSO), 0.3 µl H_2O_2 (Sigma-Aldrich, Seelze, Germany)) or SuperSignal West Femto (Thermo Fisher Scientific, IL, USA) using a CCD-camera (Fujifilm LAS-1000/ Intelligent Dark Box, Fujifilm, Japan).

Densitometry of the protein bands was performed using AIDA Image Analyzer Software (Raytest Straubenhardt, Germany). Background was subtracted of each band and protein expression of each sample was normalized to γ-tubulin as internal loading control.

Antigen	Species	Dilution	Source
CADM1	Polyclonal rabbit	1:2000	Sigma-Aldrich, Seelze, Germany
γ-tubulin	Monoclonal mouse	1:2000	Sigma-Aldrich, Seelze, Germany
p-AMPKα (Thr172)	Polyclonal rabbit	1:1000	Cell Signaling, Danvers, MA, USA
T-AMPKα	Polyclonal rabbit	1:1000	Cell Signaling, Danvers, MA, USA

Table 4: Antibodies for Western blotting and immunocytochemistry

2.4 Cell biology

2.4.1 Immunocytochemistry

MIN6 cells were grown on glass coverslips coated with 0.1 % gelatin in PBS in 24 well plates. Transfection was done as described above (2.2.2). 48 h after transfection, cells were fixed with 4 % formaldehyde in PBS for 10 min at room temperature. After washing with PBS, cells were permeabilized 10 min in 0.25 % (v/v) Triton-X in PBS and blocked with 5 % donkey normal serum in PBS for at least 1 hour at room temperature. Staining was done at 4 °C overnight with primary antibody against CADM1 **(Table 4)** diluted in PBS in a wet chamber. After washing with PBS, cells were incubated for at least 1 hour in Alexa Fluor 488 goat anti-rabbit secondary antibody (Invitrogen, Carlsbad, USA) diluted 1 : 300 in PBS. Finally, cells were incubated with TO-PRO-3 (Invitrogen, Carlsbad, USA) diluted 1 : 5000 in PBS for 5 - 10 min. Glass coverslips were washed intensively with PBS mounted on object holder with mounting medium (DAKO, Glostrup, Denmark). Confocal pictures were taken with a 100 x Plan-Apochromat oil objective on a Zeiss Laser Scanning Microscope (LSM510 Meta, Carl Zeiss AG, Germany).

2.4.2 Immunohistochemistry

Immunostainings from mouse brains were conducted by Kun Song, AG Siemens, MDC Berlin-Buch. Briefly, animals were deeply anesthetized and perfused with PBS followed by 4 % formaldehyde in PBS. Brains were dissected and stored in 30 % glucose (w/v) in PBS at 4 °C overnight. Brains were embedded and cut into free-floating sections using a microtome into 30 µm slices, transferred to a 24 - well plate filled with PBS and stored at 4 °C until further use. Slices containing ARC were stained with DAPI and mounted on glass slides (VECTASHIELD HardSet Mounting Medium with DAPI, Vector Laboratories, Inc., Burlingame). Confocal pictures were taken with a 20 x dry objective on a Leica TCS SP5 Microscope (Leica Microsystems GmbH, Wetzlar, Germany).

2.4.3 **Electrophysiological analyses**

Electrophysiological analyses from mouse brains were conducted by Dr. Mirko Moroni, AG Siemens, MDC Berlin-Buch. Pups between 16 and 21 days of age were subject to cervical dislocation and then decapitated. The entire brain was removed and immediately submerged in ice cold, carbogen-saturated (95 % O_2 / 5 % CO_2) artificial cerebrospinal fluid (aCSF) (2.5 mM NaCl, 126 mM KCl, 1.3 mM $MgCl_2$, 2.0 mM $CaCl_2$, 1.2 mM KH_2PO_4, 21.4 mM $NaHCO_3$, 10 mM glucose). 300 μM coronal sections were cut with a Leica VT1000S Vibratome and then incubated in oxygenated aCSF at room temperature for at least 1 h before recording. Whole-cell voltage-clamp recordings from POMC-eGFP neurons were performed using a Multiclamp 700B amplifier (Molecular Devices) and filtered with an eight-pole Bessel filter at 6 kHz. Both voltage and current signals were sampled at 50 kHz using an Axon 1440A interface device (Molecular Devices, Sunnyvale, USA) and the data were acquired using Clampex 10.2 software (Molecular Devices, Sunnyvale, USA). Electrodes were pulled using a micropipette puller (Sutter Instruments, Novato, USA) from thick-walled borosilicate glass GC150F capillaries (Harvard Apparatus, Massachusetts, USA, Massachusetts, USA) to a resistance of ~ 3 MΩ. Series resistance compensation ranged from 50 - 70 % and recordings were discarded if the series resistance exceeded 10 MΩ. Electrodes were filled with an internal solution (140 mM CsCl, 4 mM NaCl, 0.5 mM $CaCl_2$, 10 mM HEPES, 5 mM EGTA, 2 mM Mg-ATP, QX-315 Br 3, pH 7.3 with CsOH, osmolarity of 290 mOsm). Cells were visualized using an infrared differential interference contrast (DIC) optics equipped with equipped ORCA-R2 camera (Hamamatsu Photonics K.K., Hamamatsu, Japan) mounted on a Slicescope (Multi Channel Systems, Reutlingen, Germany) with a 40 x water-immersion objective. Neurons were voltage clamped at − 70 mV. In order to record inhibitory postsynaptic potentials (IPSC)s, the aCSF composition included 3 mM kynurenic acid (Sigma Aldrich, Seelze, Germany) to block excitatory glutamatergic activity. Excitatory postsynaptic potentials (EPSC)s were recorded in presence of 100 μM picrotoxin (Tocris Bioscience, MO, USA) in order to block both GABA- and glycine-evoked currents. Both experimental conditions included 0.5 μM tetrodotoxin (Tocris Bioscience,

MO, USA) to isolate miniature events. Events were excluded from the analysis if their amplitude was less than 3 standard deviations of the baseline noise and if there were overlapping events within 50 ms for IPSCs or 10 ms for EPSCs. All miniature events were automatically detected with Clampfit 10, followed by manual inspection of single events. For frequency distributions a minimum of 200 events were analyzed.

2.5 Statistical methods

Data sets with two groups were analyzed for statistical significance using one-tailed unpaired student's t-test with unequal variance. For comparing means of more than two groups, one-way analysis of variance (ANOVA) and following Tukey-Kramer test was used with the software GraphPad Prism 5 (GraphPad Prism Software, San Diego, CA/USA). For linear regression analysis GraphPad Prism 5 was used. Analysis of covariance (ANCOVA) was performed with the univariate general linear model module in PASW statistics (IBM, Chicago, IL). Adjusted average values were analyzed for significant differences using one-tailed unpaired student's t-test with unequal variance. All displayed values are means ± SEM. All p-values below or equal 0.05 were considered significant (★ $p \leq 0.05$; ★★ $p \leq 0.01$; ★★★ $p \leq 0.001$).

3 Results

3.1 Energy and glucose homeostasis in murine models with total *Cadm1* deletion

In order to investigate effects of *Cadm1* deficiency on energy and glucose homeostasis, total *Cadm1* knock-out *(Cadm1*KO) mice, as previously described (van der Weyden, Arends et al. 2006), were obtained. *Cadm1*KO mice were backcrossed to C57BL/6N mice for four generations. Unless otherwise described, *Cadm1*KO mice were compared to gender-matched, littermate controls, which were heterozygous or wild-type for the *Cadm1* null allele.

3.1.1 Reduced postnatal growth and decreased fat mass in *Cadm1*KO male mice

The physiological function of CADM1 in energy homeostasis was addressed first by measuring body weight of *Cadm1*KO animals in comparison to control mice. One day after birth, neither male nor female *Cadm1*KO mice showed significant differences in body weight compared to control animals **(Figure 9A, B).** However, between age of 4 and 21 postnatal days both male and female *Cadm1*KO mice developed significantly lower body weight compared to littermate control mice. After weaning at 4 weeks of age, significant lower body weight in male **(Figure 9C)** and female *Cadm1*KO mice **(Figure 9D)** was observed at all measured time points. Between 4 and 12 weeks of age, average body weight gain per week was not different between the genotypes of both genders **(Figure 9E)**. Furthermore, adult male *Cadm1*KO mice showed significantly reduced body length **(Figure 9F),** while body weight to body length ratio was significantly reduced in adult male and female *Cadm1*KO mice **(Figure 9G)**.

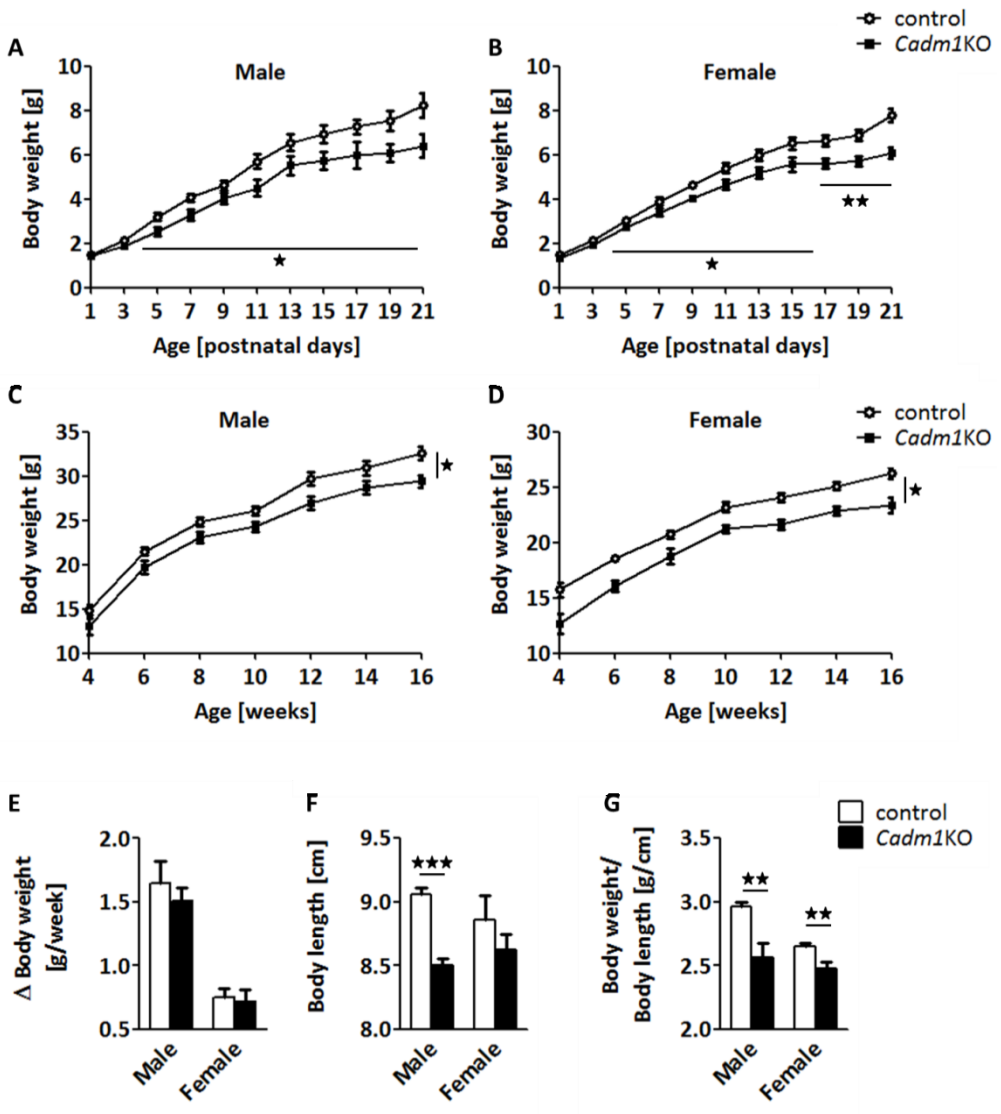

Figure 9: Body weight and body length of *Cadm1*KO mice

[A] Body weight of male control (N = 8 - 13) and *Cadm1*KO (N = 5 - 10) mice between 1 and 21 days of age **[B]** Body weight of female control (N = 11 - 16) and *Cadm1*KO (N = 7 - 9) mice between 1 and 21 days of age **[C]** Body weight of male control (N = 12 - 29) and *Cadm1*KO (N = 15 - 21) mice between 4 and 16 weeks of age **[D]** Body weight of female control (N = 15 - 33) and *Cadm1*KO (N = 6 - 18) mice between 4 and 16 weeks of age **[E]** Average body weight gain per week of male control (N = 12) and *Cadm1*KO (N = 7) mice and female control (N = 19) and *Cadm1*KO (N = 10) mice between 4 and 12 weeks of age **[F]** Body length and **[G]** Body weight to body length ratio of male control (N = 9) and *Cadm1*KO (N = 7) mice and female control (N = 9) and *Cadm1*KO (N = 10) mice between 12 and 16 weeks of age. Displayed values are means ± S.E.M. ★ $p \leq 0.05$; ★★ $p \leq 0.01$; ★★★ $p \leq 0.001$

To investigate if body weight differences are only caused by different body lengths of *Cadm1*KO mice, body composition of *Cadm1*KO and control animals was measured by nuclear magnetic resonance (NMR). In *Cadm1*KO males, absolute fat mass as well as absolute lean body mass were significantly reduced **(Figure 10A,B)**, confirming the reduced body weight of these animals. Fat mass relative to body weight was significantly reduced in male *Cadm1*KO mice, whereas lean body mass relative to body weight was significantly increased in these animals **(Figure 10C,D).** *Cadm1*KO females did not show differences in absolute fat mass but exhibited reduced absolute lean body mass **(Figure 10A,B)**. Furthermore, fat mass and lean body mass relative to body weight were not significantly changed in *Cadm1*KO females **(Figure 10C,D).**

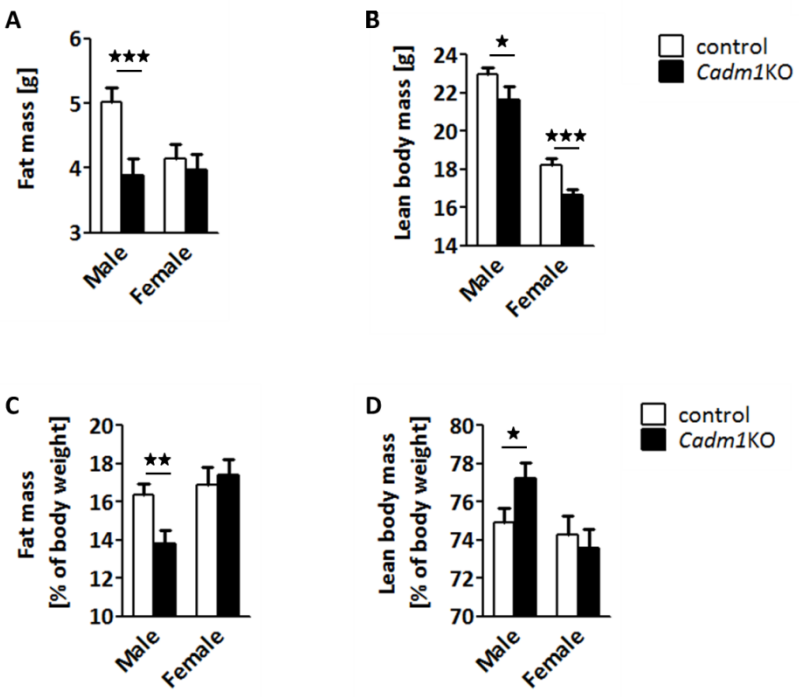

Figure 10: Body composition of *Cadm1*KO mice
[A] Absolute body fat mass and **[B]** Absolute lean body mass and **[C]** Relative body fat mass normalized to body weight and **[D]** Relative lean body mass normalized to body weight of male control (N = 11) and *Cadm1*KO (N = 9) mice and female control (N = 19) and *Cadm1*KO (N = 23) mice between 12 and 20 weeks of age. Displayed values are means ± S.E.M. ★ $p \leq 0.05$; ★★ $p \leq 0.01$; ★★★ $p \leq 0.001$

3.1.2 Decreased leptin levels, unchanged food intake and increased locomotor activity in *Cadm1*KO male mice

Reduced body fat content correlates with reduced circulating levels of leptin and increased sensitivity to leptin (1.2.1). Since *Cadm1*KO male mice showed reduced body fat content (Figure 10), it was questioned whether circulating leptin is altered in *Cadm1*KO mice. Circulating leptin levels of male *Cadm1*KO mice were reduced in comparison to littermate controls, corresponding to reduced body fat content **(Figure 11)**.

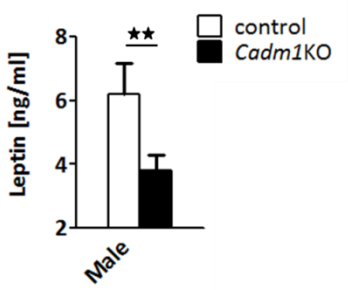

Figure 11: Blood leptin levels in male *Cadm1*KO mice
Random circulating leptin levels of male control (N = 16) and *Cadm1*KO (N = 7) mice between 12 and 16 weeks of age. Displayed values are means ± S.E.M. ★★ $p \leq 0.01$

To investigate the cause of the leaner phenotype, it was examined if *Cadm1*KO mice show changes in food intake. Compared to control animals, absolute basal food intake was similar in male and female *Cadm1*KO mice **(Figure 12A)**. Since body weight and absolute lean body mass are significantly decreased in *Cadm1*KO male mice (Figure 10), absolute food intake has to be adjusted for comparison. As discussed by Kaiyala et al. and Tschöp et al. (Kaiyala, Morton et al. 2010; Tschop, Speakman et al. 2011), normalization by division by body weight or lean body mass can yield confounding results, since the intercept of the relation between lean or body mass and food intake is not zero. Therefore, analysis of covariance (ANCOVA) was used to adjust food intake for lean body mass (Meyer, Neubronner et al. 2007; Butler and Kozak 2010; Choi, Yablonka-Reuveni et al. 2011; Tschop, Speakman et al. 2011). After adjustment of food intake for

lean body mass using ANCOVA, male and female *Cadm1*KO mice showed no significant differences in food intake compared to littermate control mice **(Figure 12B,C,D)**. These data suggest that basal food intake of control and *Cadm1*KO mice would not be significantly different, if animals from both genotypes had the same lean body mass. Besides basal food intake, we also questioned whether food intake after food deprivation for 24 h (rebound feeding) might be changed. *Cadm1*KO mice ate significantly more during the first three hours after refeeding, suggesting that food desire is enhanced in *Cadm1*KO mice **(Figure 12E)**. Body weight loss during the 24 h starvation time was not significantly altered in *Cadm1*KO mice, indicating that increased weight loss was not the cause of the increased starvation-induced food intake **(Figure 12F)**.

Furthermore, gene expression of *Pomc* and *Npy*, important genes in the regulation of food intake (1.1.4, 1.1.6), were investigated in hypothalami of random fed control and *Cadm1*KO mice. Compared to control mice, *Pomc* expression was significantly decreased and *Npy* expression not significantly altered in the hypothalami of random fed *Cadm1*KO mice **(Figure 12G).**

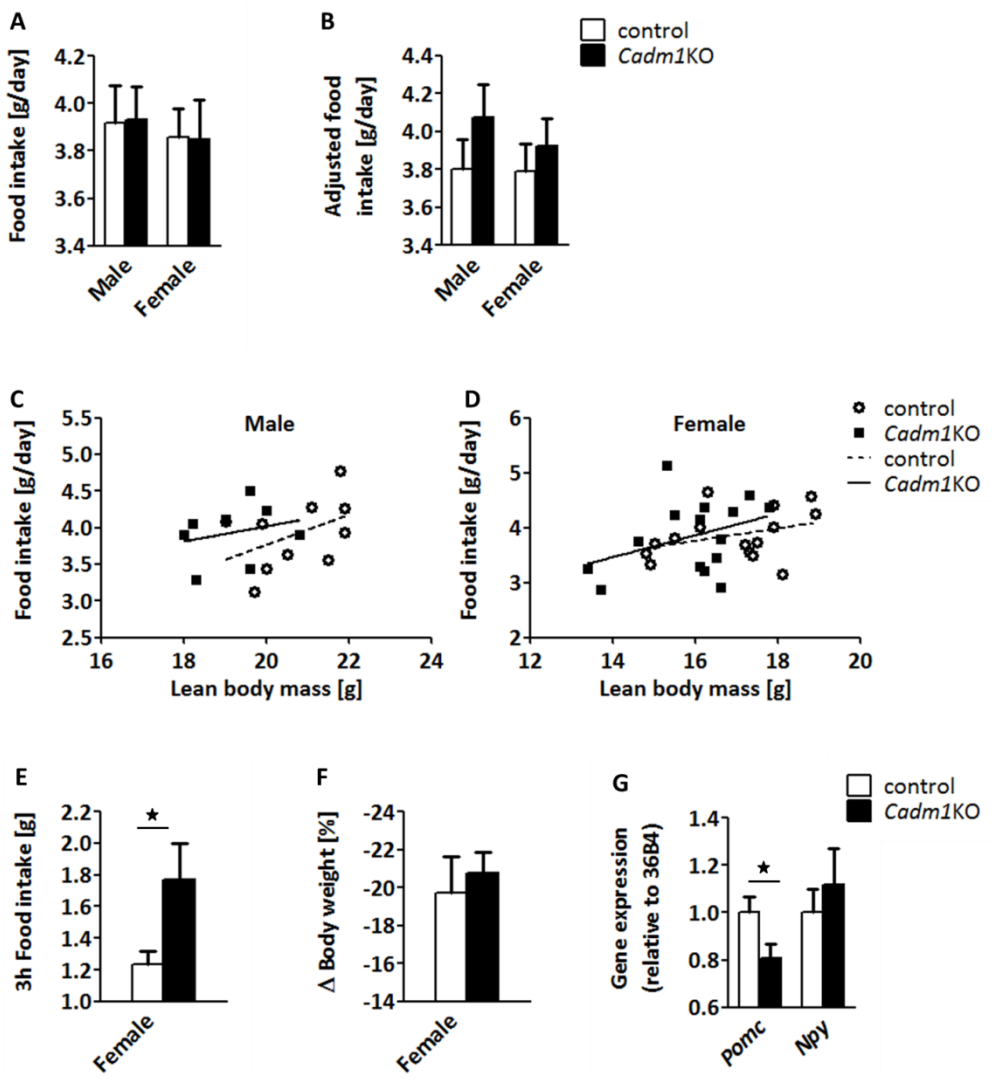

Figure 12: Basal and post-starvation food intake of *Cadm1*KO mice

[A] Absolute food intake and **[B]** For lean body mass at 20.0444 g adjusted food intake using ANCOVA for male control (N = 10) and *Cadm1*KO mice (N = 8) and for lean body mass at 16.4133 g adjusted food intake for female control (N = 15) and *Cadm1*KO mice (N = 16) **[C]** Scatterplot showing linear regression for food intake as a function of group and lean body mass for male control (N = 10) and *Cadm1*KO mice (N = 8) (control: $y = 0.2055 \times x - 0.3447; r^2 = 0.1985;$ *Cadm1*KO: $y = 0.1037 \times x + 1.942; r^2 = 0.0646$) between 12 and 20 weeks of age **[D]** Scatterplot showing linear regression for food intake as a function of group and lean body mass for female control (N = 15) and *Cadm1*KO mice (N = 16) (control: $y = 0.1132 \times x + 1.951; r^2 = 0.1207;$ *Cadm1*KO: $y = 0.1983 \times x + 0.6892; r^2 = 0.1360$) between 12 and 20 weeks of age **[E]** 3 h food intake and **[F]** relative body weight difference after 24 h starvation of female control (N = 3) and *Cadm1*KO (N = 3) mice between 12 and 16 weeks of age **[G]** *Pomc* and *Npy* gene

expression measured by qRT-PCR in hypothalami of random fed control (N = 4) and *Cadm1*KO (N = 4) mice between 12 and 16 weeks of age. Displayed values are means ± S.E.M. ★ $p \leq 0.05$. Gene expression analysis was conducted by Sudhir Gopal Tattikota, AG Poy, MDC Berlin-Buch.

To further investigate changes on food intake in *Cadm1*KO mice, gene expression, protein expression and protein activity of 5' adenosine monophosphate-activated protein kinase (AMPK) were investigated in hypothalami of *Cadm1*KO and control mice. AMPK activity in the hypothalamus directly correlates with food intake and body weight (Minokoshi, Alquier et al. 2004). First, deletion of CADM1 was confirmed by Western blotting. Western blotting of hypothalami revealed a protein band for CADM1 at around 100 kDa in control mice, which was only weakly present in *Cadm1*KO mice **(Figure 13A)**. CADM1 was detected at around 100 kDa instead of 75 kDa as expected from the molecular weight since the protein is highly glycosylated, as shown previously (Robbins, Krupp et al. 2010). However, other bands at lower sizes were detected in both *Cadm1*KO and control mice. This is likely due to cross-reactivity of the CADM1 antibody to CADM2, CADM3 and CADM4, since these proteins show strong homology at the c-terminus, the part that is detected by the antibody against CADM1 (Biederer, Sara et al. 2002).

AMPK is activated by phosphorylation at threonine 172 (p-AMPKα (Thr172)) (Woods, Dickerson et al. 2005). Abundance of p-AMPKα (Thr172) **(Figure 13B)** was normalized to tubulin and divided by abundance of total-AMPKα (T-AMPKα) **(Figure 13A)** normalized to tubulin in order to estimate AMPK activity. Compared to control mice, AMPK activity was significantly increased in *Cadm1*KO mice after starvation **(Figure 13C).** Furthermore, *Prkaa1* and *Prkaa2* expression, genes coding for the catalytic subunits AMPKα1 and AMPK*a*2 of AMPK (Lage, Dieguez et al. 2008), were significantly enhanced in hypothalami of random fed *Cadm1*KO mice **(Figure 13D).** Taken together, these data indicate that AMPK activity and expression is increased in hypothalami of *Cadm1*KO mice.

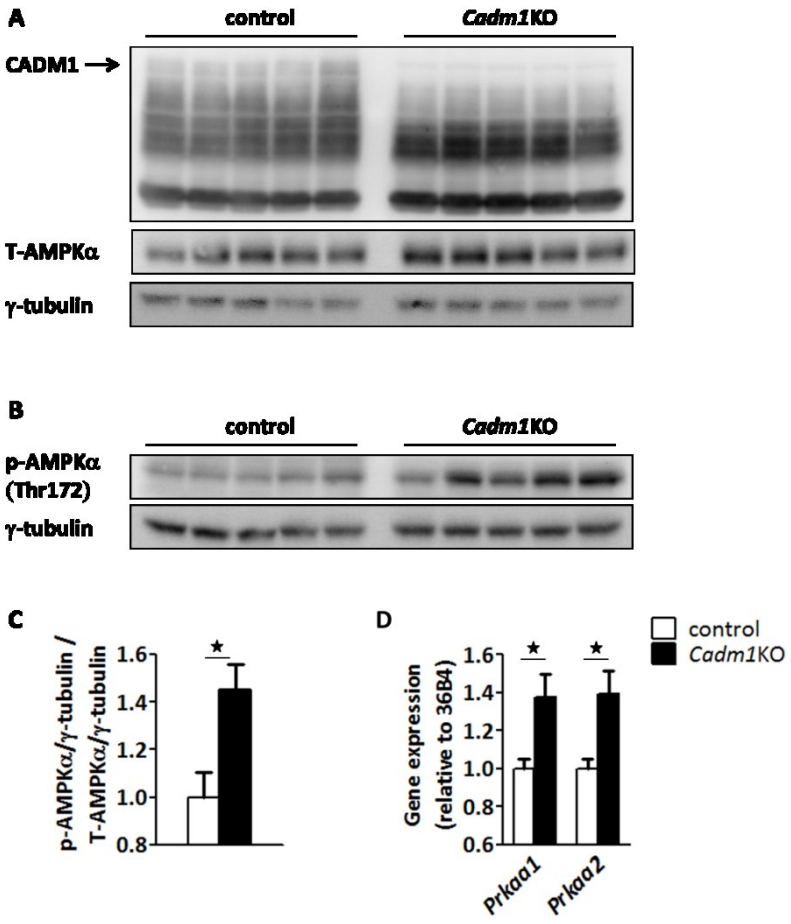

Figure 13: *In vivo* AMPK protein and gene expression of *Cadm1*KO mice
[A] Western blot analysis for protein abundance of CADM1 and total-AMPKα (T-AMPKα) in hypothalami of 24 h fasted control (N = 5) and *Cadm1*KO (N = 5) mice **[B]** Western blot analysis for protein abundance of AMPKα phosphorylated at Thr172 (p-AMPKα (Thr172)) in hypothalami of 24 h fasted control (N = 5) and *Cadm1*KO (N = 5) mice **[C]** Quantification of p-AMPKα (Thr172) protein abundance divided by γ-tubulin from [B] and normalized to T-AMPKα divided by γ-tubulin from [A] **[D]** qRT-PCR for gene expression of *Prkaa1* and *Prkaa2* coding for AMPKα1 and AMPKα2, respectively, in random fed control (N = 5) and *Cadm1*KO (N = 4) mice. Displayed values are means ± S.E.M. ★ $p \leq 0.05$. Gene expression analysis was conducted by Sudhir Gopal Tattikota, AG Poy, MDC Berlin-Buch.

To further address whether energy homeostasis of *Cadm1*KO mice is altered, energy expenditure of *Cadm1*KO mice and control mice was investigated. Energy expenditure is the sum of basal metabolic rate, thermogenesis and locomotor activity (1.1.5) and can be measured by indirect calorimetry. Therefore, oxygen (O_2) and carbon dioxide (CO_2) respiration was measured by using indirect calorimetry and locomotor activity was measured by infrared-light beams during indirect calorimetry measurements. In male *Cadm1*KO mice, absolute O_2 consumption was significantly increased compared to littermate control mice, while absolute CO_2 expiration was unchanged **(Table 5)**. The calculated absolute energy expenditure was significantly increased in male *Cadm1*KO mice compared to control mice. The respiratory rate (RER), calculated by CO_2 expiration divided by O_2 consumption, was not significantly different in male *Cadm1*KO mice in comparison to control mice. Locomotor activity was significantly increased in male *Cadm1*KO mice.

In female *Cadm1*KO animals, indirect calorimetry yielded no significant differences for absolute O_2 and CO_2 respiration, energy expenditure or respiratory rate **(Table 5)**. Also locomotor activity was unchanged *Cadm1*KO females when comparing to control animals.

	Male		Female	
	Control	***Cadm1*KO**	**Control**	***Cadm1*KO**
VO_2 [l/h]	88.0 ± 1.1	91.3 ± 1.1 ★	83.6 ± 1.2	81.6 ± 2.0
VCO_2 [l/h]	82.2 ± 1.4	83.9 ± 1.2	80.7 ± 1.4	80.0 ± 2.1
EE [kcal/h]	0.44 ± 0.01	0.45 ± 0.01 ★	0.42 ± 0.01	0.41 ± 0.01
RER	0.93 ± 0.01	0.91 ± 0.01	0.96 ± 0.01	0.97 ± 0.01
Locomotor activity [counts/h]	2094.0 ± 65.7	2459.0 ± 64.6★★★	2485.1 ± 128.7	2448.4 ± 121.3

Table 5: Energy expenditure, RER and locomotor activity of *Cadm1*KO mice
Average oxygen (VO_2) and carbon dioxide (VCO_2) respiration, calculated energy expenditure (EE) and respiratory rate (RER) as well as locomotor activity of male control (N = 12) and *Cadm1*KO (N = 9) mice and female control (N = 15) and *Cadm1*KO (N = 16) mice between 12 and 20 weeks of age of 3 consecutive days. Displayed values are means ± S.E.M. ★ $p \leq 0.05$; ★★★ $p \leq 0.001$

Since male *Cadm1*KO mice showed differences in lean body mass and body weight compared to control mice (Figure 9, Figure 10), O_2 and CO_2 respiration as well as energy expenditure have to be adjusted. ANCOVA was used to adjust energy expenditure for lean body mass as described above (Figure 12). After adjustment of energy expenditure for lean body mass using ANCOVA, male *Cadm1*KO mice showed significantly increased energy expenditure compared to littermate control mice **(Figure 14A,B).** In order to

evaluate whether the increase in energy expenditure might be explained by increased activity, ANCOVA was further used to adjust energy expenditure for locomotor activity**.** Energy expenditure adjusted for locomotor activity was unchanged between male *Cadm1*KO and control mice **(Figure 14C,D).** These results indicate that energy expenditure of control and *Cadm1*KO mice would not be significantly different, if animals from both genotypes had the same locomotor activity. Therefore, it can be suggested that increased locomotor activity is the main, if not the only factor leading to increased energy expenditure in *Cadm1*KO male mice.

In female *Cadm1*KO mice, adjustment of energy expenditure for lean body mass did not show significant differences compared to control female mice **(Figure 15A,B).** In addition, energy expenditure adjusted for locomotor activity did not show significant differences between female control and *Cadm1*KO mice **(Figure 15C,D)**.

Taken together, *Cadm1*KO mice display reduced body weight gain between postnatal day four and postnatal day 21, while body weight gain after four weeks of age is not significantly different in comparison to control mice. Body length of adult *Cadm1*KO animals is decreased, while food intake is unchanged. Furthermore, *Cadm1*KO males exhibit reduced fat mass and increased lean body mass relative to body weight. Locomotor activity is increased in *Cadm1*KO males, causing increased energy expenditure. *Cadm1*KO female mice do not show differences on body composition, energy expenditure or locomotor activity.

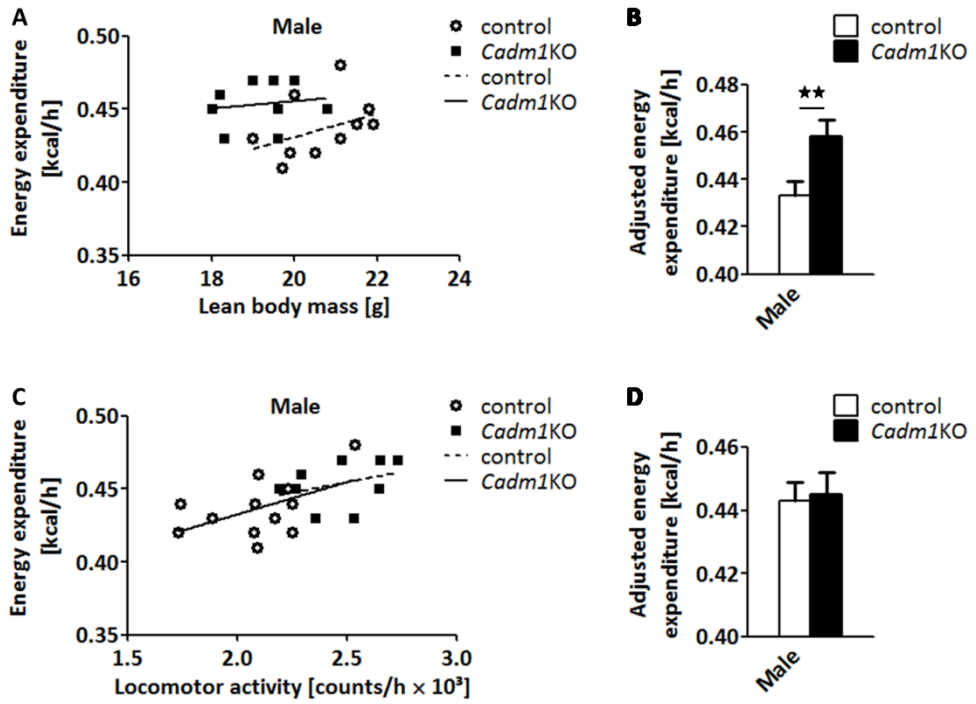

Figure 14: Analysis of covariance (ANCOVA) of energy expenditure and locomotor activity in male *Cadm1*KO mice

[A] Scatterplot showing linear regression for energy expenditure as a function of group and lean body mass (control: $y = 0.008 \times x + 0.2694; r^2 = 0.1543$; *Cadm1*KO: $y = 0.0025 \times x + 0.4050; r^2 = 0.02179$) and **[B]** Energy expenditure adjusted for lean body mass at 20.0905 g using ANCOVA and **[C]** Scatterplot showing linear regression for energy expenditure as a function of group and locomotor activity (control: $y = 0.04426 \times x + 0.3440; r^2 = 0.2615$; *Cadm1*KO: $y = 0.02853 \times x + 0.3832; r^2 = 0.1222$) and **[D]** Energy expenditure adjusted for locomotor activity at 2.25 counts/h × 10^3 using ANCOVA for male control (N = 12) and *Cadm1*KO (N = 9) mice between 12 and 20 weeks of age. Displayed values are means ± S.E.M. ★★ $p \leq 0.01$

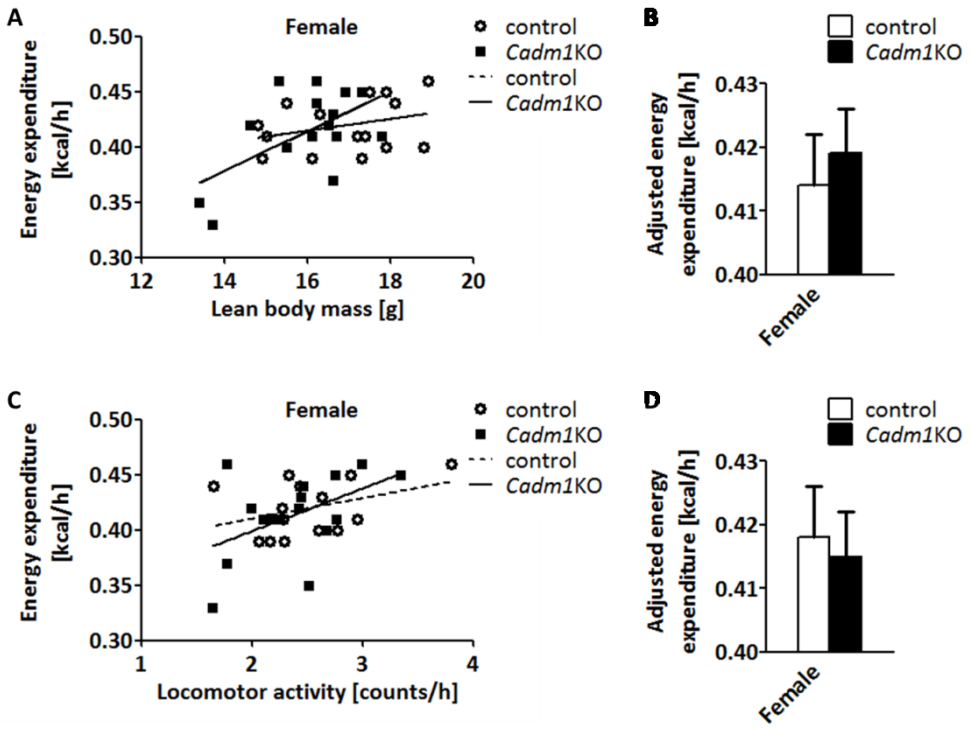

Figure 15: Analysis of covariance (ANCOVA) of energy expenditure and locomotor activity in female *Cadm1*KO mice

[A] Scatterplot showing linear regression for energy expenditure as a function of group and lean body mass (control: $y = 0.0053 \times x + 0.3294; r^2 = 0.09405$; *Cadm1*KO: $y = 0.01792 \times x + 0.1276; r^2 = 0.3342$) and **[B]** Energy expenditure adjusted for lean body mass at 16.4226 g using ANCOVA and **[C]** Scatterplot showing linear regression for energy expenditure as a function of group and locomotor activity (control: $y = 0.0186 \times x + 0.3732; r^2 = 0.1483$; *Cadm1*KO: $y = 0.0386 \times x + 0.3220; r^2 = 0.2299$) and **[D]** Energy expenditure adjusted for locomotor activity at 2.429 counts/h × 10^3 using ANCOVA for female control (N = 15) and *Cadm1*KO (N = 16) mice between 12 and 20 weeks of age. Displayed values are means ± S.E.M.

3.1.3 Increased insulin sensitivity and insulin secretion in *Cadm1*KO mice

To validate the physiological function of CADM1 in glucose homeostasis, random and 16 h starved blood glucose levels of *Cadm1*KO mice were measured. Compared to littermate controls, *Cadm1*KO mice did not show significant differences in blood glucose levels at either random or fasted state **(Figure 16A,B).** To further investigate the ability of *Cadm1*KO mice to control blood glucose levels, these mice were challenged by intraperitoneal injections of glucose (glucose tolerance test, GTT). Blood glucose levels were measured before (0 min) and at 15, 30, 60 and 120 min after injections. In male *Cadm1*KO mice, glucose levels at 0 and 15 min were not significantly changed compared to control animals **(Figure 16C)**. However, the blood glucose levels of male *Cadm1*KO mice were significantly lower at 30, 60 and 120 min after glucose injections. Female *Cadm1*KO mice had significantly decreased glucose levels at 15 min and strongly decreased levels at 30 min after glucose injections compared to control mice ($p = 0.058$) **(Figure 16D).** These data suggest improved glucose tolerance in *Cadm1*KO mice**.**

Lower blood glucose levels after glucose challenge can be caused by increased release of insulin or increased sensitivity to insulin. To establish whether insulin sensitivity was changed in *Cadm1*KO mice, an insulin tolerance test (ITT) was performed by measuring blood glucose levels before and after intraperitoneal insulin injections**.** Due to insulin stimulated glucose uptake by peripheral tissues, all animals showed decreasing blood glucose levels up to 60 min after insulin injections, followed by increasing glucose levels due to hepatic gluconeogenesis. Male *Cadm1*KO mice showed unchanged glucose levels after insulin injections compared to control mice **(Figure 16E)**. However, *Cadm1*KO females had significantly decreased glucose levels at 30 and 120 min after insulin injections, suggesting improved insulin sensitivity in female *Cadm1*KO mice **(Figure 16F)**.

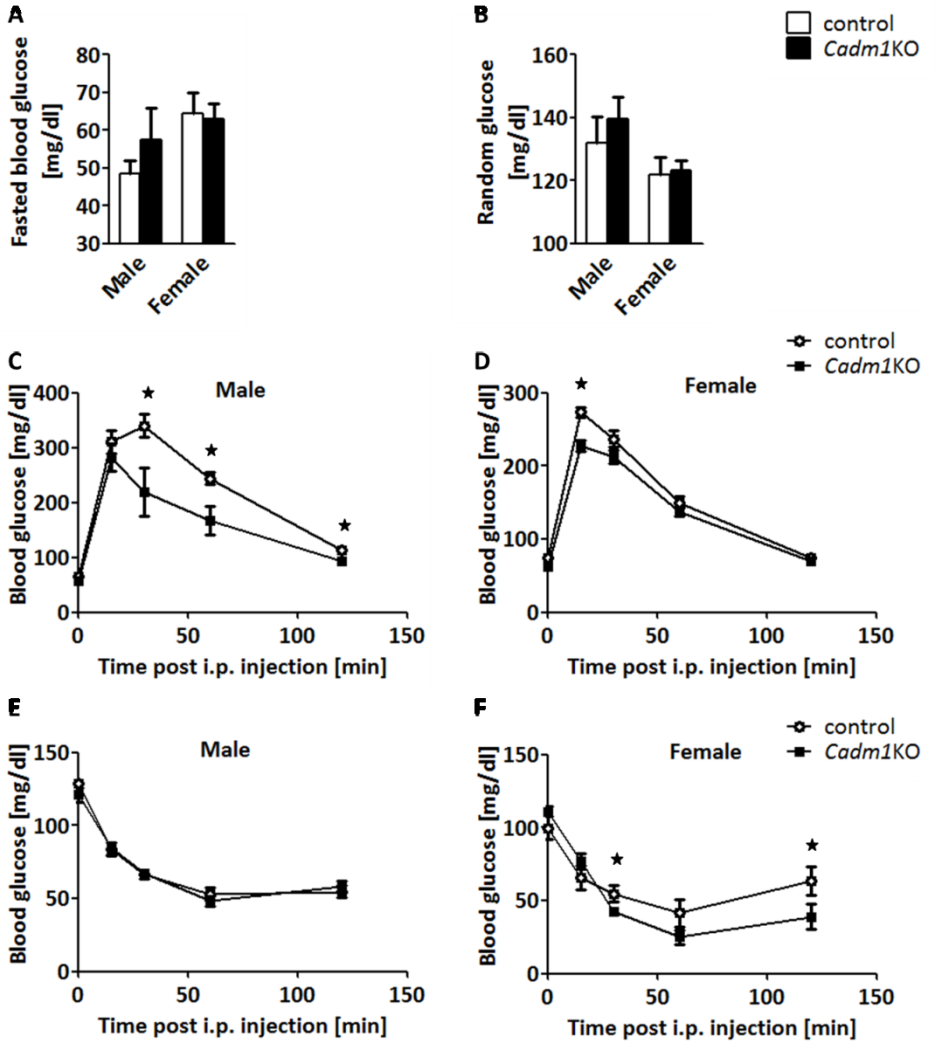

Figure 16: Glucose and insulin sensitivity of *Cadm1*KO mice
[A] 16 h fasted blood glucose levels of male control (N = 9) and *Cadm1*KO (N = 7) mice and female control (N = 5) and *Cadm1*KO (N = 5) mice **[B]** Random glucose of male control (N = 7) and *Cadm1*KO (N = 11) mice and female control (N = 18) and *Cadm1*KO (N = 9) mice **[C]** Glucose tolerance test of male control (N = 6) and *Cadm1*KO (N = 4) mice **[D]** Glucose tolerance test of female control (N = 15) and *Cadm1*KO (N = 10) mice **[E]** Insulin tolerance test of male control (N = 17) and *Cadm1*KO (N = 16) mice **[F]** Insulin tolerance test of female control (N = 5) and *Cadm1*KO (N = 5) mice. All animals were between 12 and 16 weeks of age. Displayed values are means ± S.E.M. ★ $p \leq 0.05$

To investigate whether the release of insulin upon glucose challenge was changed in *Cadm1*KO animals, an *in vivo* insulin release test was performed by measuring blood

insulin levels before and after intraperitoneal glucose injections. At 5 min after glucose injection, male *Cadm1*KO mice showed significantly higher blood insulin levels than control mice, suggesting an improved pancreatic insulin release **(Figure 17A).** Female *Cadm1*KO mice showed a strong trend for increased blood insulin levels 2.5 min after i.p. glucose injections (p = 0.066) **(Figure 17B)**. Pancreatic insulin content of *Cadm1*KO mice was unaltered in male and female mice **(Figure 17C,D),** suggesting that release rather than production of insulin was affected in *Cadm1*KO mice.

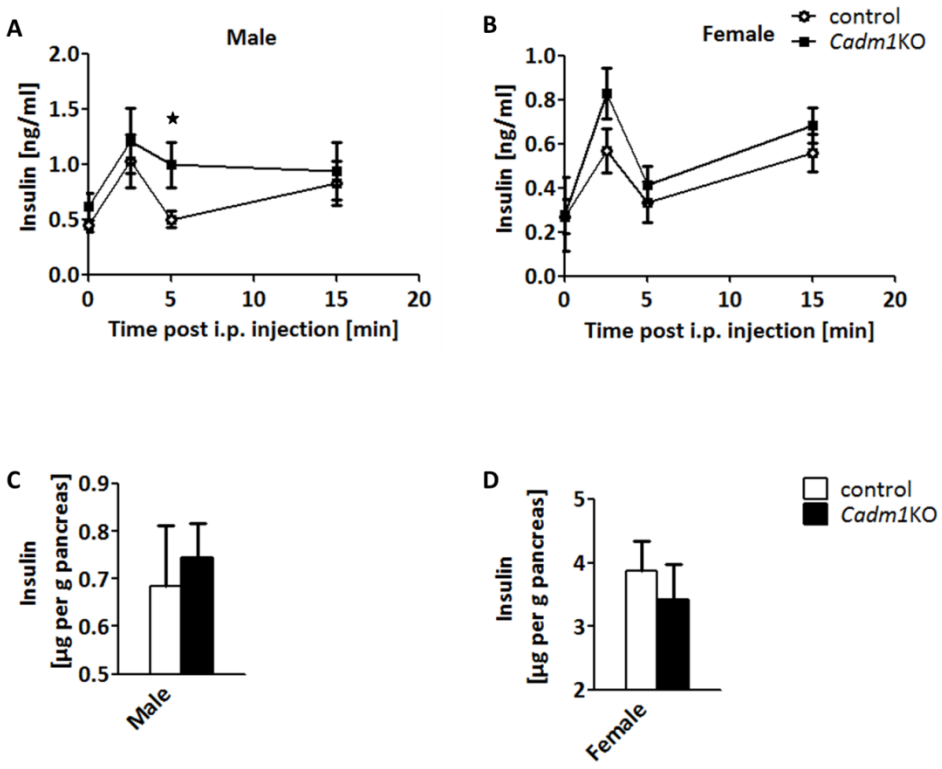

Figure 17: Insulin release and pancreatic insulin content of *Cadm1*KO mice
[A] *In vivo* insulin release of male control (N = 6) and *Cadm1*KO (N = 4) mice **[B]** *In vivo* insulin release of female control (N = 5) and *Cadm1*KO (N = 5) mice **[C]** Pancreatic insulin content of male control (N = 6) and *Cadm1*KO (N = 5) mice **[D]** Pancreatic insulin content of female control (N = 7) and *Cadm1*KO (N = 5) mice. All animals were between 12 and 16 weeks of age. Displayed values are means ± S.E.M. ★ $p \leq 0.05$

3.1.4 **Increased insulin release in *Cadm1*-depleted MIN6 cells**

To further prove that insulin release was enhanced by depletion of CADM1, *Cadm1* was knocked-down *in vitro* in MIN6 cells, a cell line derived from pancreatic murine β-cells (Miyazaki, Araki et al. 1990). Knock-down was achieved by using a siRNA against *Cadm1* and the knock-down efficiency was confirmed by Western Blotting **(Figure 18A)** and immunofluorescence microscopy **(Figure 18B)**. Secreted insulin was significantly higher in *Cadm1*-depleted MIN6 cells compared to control cells after treatment with high and low glucose concentrations, representing basal and postprandial glucose concentration respectively **(Figure 18C)**. These *in vitro* data confirmed the *in vivo* findings that *Cadm1* deficiency increases pancreatic insulin release.

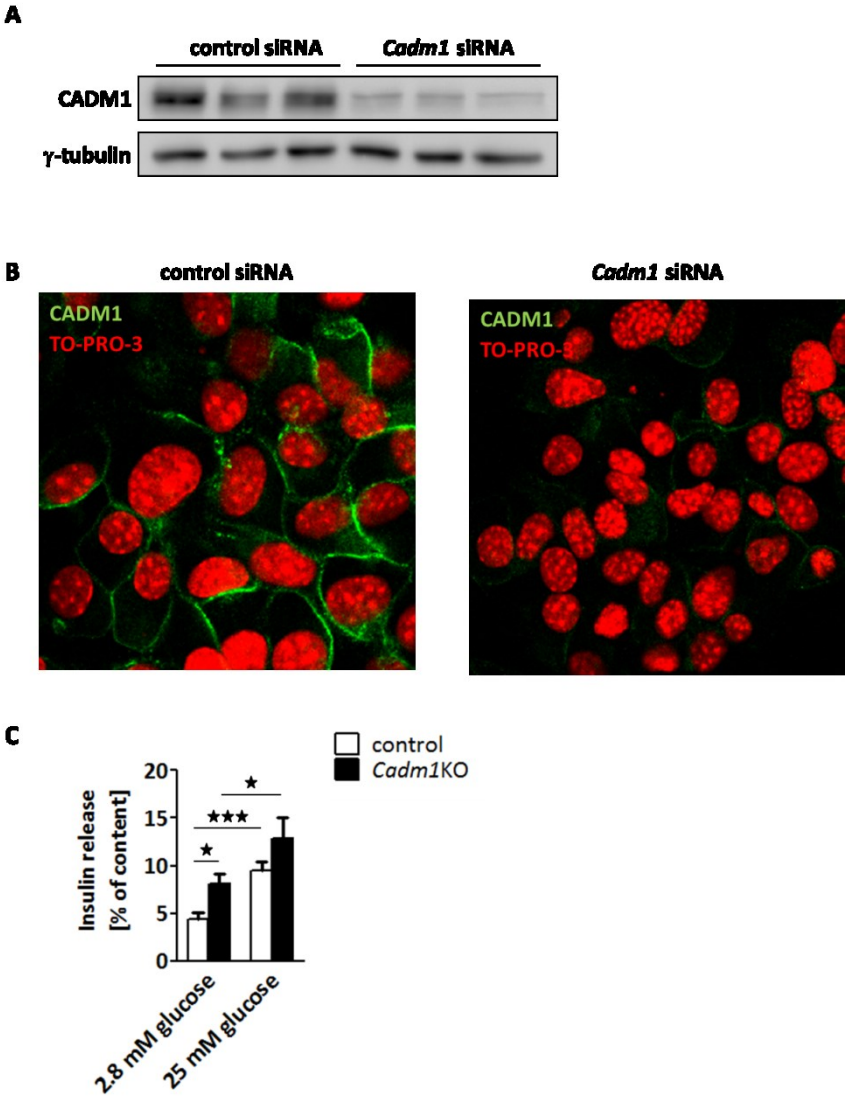

Figure 18: Insulin secretion of *Cadm1*-depleted MIN6 cells
[A] Confirming knock-down of CADM1 by Western blot analysis of MIN6 cells transfected with control siRNA and siRNA against *Cadm1*; upper panel: CADM1 expression; lower panel: γ-tubulin used as loading **[B]** Confirming knock-down of CADM1 by immunocytochemistry of MIN6 cells transfected with control siRNA (left) and siRNA against *Cadm1* (right); CADM1 is stained in green; nuclei are stained in red **[C]** *In vitro* insulin secretion of MIN6 cells transfected with control siRNA and siRNA against *Cadm1* and treated with low glucose medium (2.8 mM glucose) or high glucose medium (25 mM glucose). Displayed values are means ± S.E.M. ★ $p \leq 0.05$; ★★★ $p \leq 0.001$

3.1.5 *Cadm1*KO mice have decreased IPSC frequency onto POMC-eGFP neurons

Recent investigations showed that CADM1 influences synaptic plasticity, a process altering synaptic strength and efficacy in response to synaptic activity (1.3.1). Synaptic plasticity is also known to be influenced by peripheral hormones, such as leptin, ghrelin and estrogens (Pinto, Roseberry et al. 2004; Gao, Mezei et al. 2007) as well as high fat diet (HFD) feeding in the hypothalamus (Horvath, Sarman et al. 2010). In order to investigate whether changes in synaptic connections in the hypothalamus of *Cadm1* deficient mice might explain the metabolic phenotype of these mice, measurements of postsynaptic currents were conducted from the hypothalamus of young *Cadm1*KO mice. Young mice between postnatal day 14 and 21 were chosen to avoid disturbing effects by myelination. Postsynaptic currents were measured from POMC-Enhanced green fluorescent protein (eGFP) neurons (Cowley, Smart et al. 2001) in the ARC, since these neurons play an important role in the regulation of energy and glucose homeostasis (1.1.4, 1.1.6).

Inhibitory postsynaptic potential (IPSC) firing frequency onto POMC-eGFP neurons from *Cadm1*KO mice (*Cadm1*KO POMC-eGFP) was significantly reduced compared to control mice (control POMC-eGFP) (**Figure 19 A, B**), while excitatory postsynaptic potential (EPSC) frequency was not significantly different between mice of the two genotypes (**Figure 19 C, D**). In accordance to previous reports, amplitudes of IPSCs and EPSCs were not significantly different between *Cadm1*KO and control mice (**Figure 19 B, D**) (Robbins, Krupp et al. 2010). These data suggest that synaptic connectivity of hypothalamic *Pomc*-expressing neurons is influenced by *Cadm1* expression in the brain and might explain altered energy and glucose homeostasis in *Cadm1*KO mice.

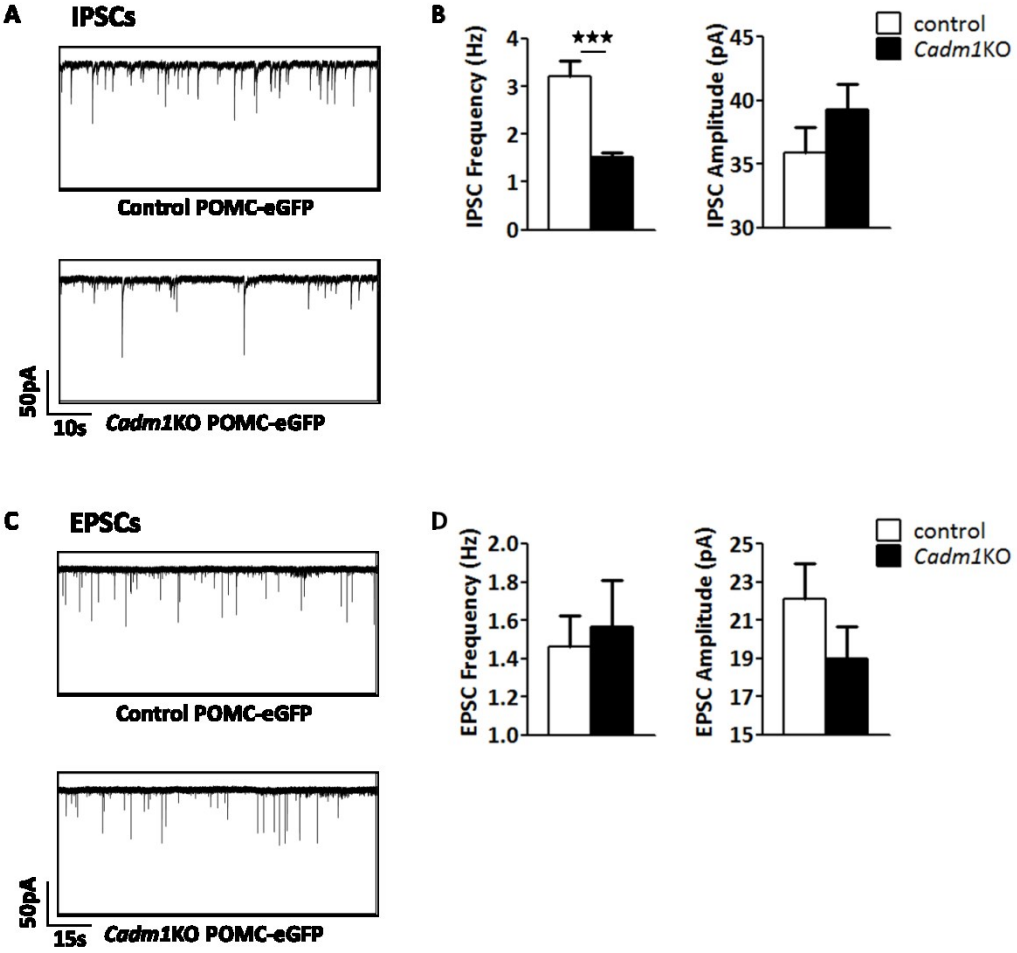

Figure 19: IPSCs and EPSCs onto POMC-eGFP neurons from control and *Cadm1*KO mice
[A] Recording samples showing spontaneous inhibitory postsynaptic potentials (IPSC)s onto pro-opiomelanocortin (POMC)-enhanced green fluorescent protein (eGFP) neurons and **[B]** Pooled data of frequency or amplitude of IPSCs recorded from control POMC-eGFP neurons (N = 12 cells from 4 mice) and *Cadm1*KO POMC-eGFP neurons (N = 15 cells from 4 mice) **[C]** Recording samples showing spontaneous excitatory postsynaptic potentials (EPSC)s onto POMC-eGFP neurons and **[D]** Pooled data of frequency or amplitude of EPSCs recorded from control POMC-eGFP neurons (N = 11 cells from 4 mice) and *Cadm1*KO POMC-eGFP neurons (N = 7 cells from 4 mice). Displayed values are means ± S.E.M. ★ $p \leq 0.05$. Electrophysiological analyses were conducted by Dr. Mirko Moroni, AG Siemens, MDC Berlin-Buch.

3.1.6 *Cadm1* deletion does not disturb GH production or release

Growth hormone (GH) is produced in the anterior pituitary and is a major positive regulator of longitudinal growth (List, Sackmann-Sala et al. 2011). Furthermore, GH is responsible for maintenance of glucose homeostasis in caloric-restricted situations (Zhao, Liang et al. 2010). GH exerts its effects on glucose homeostasis through induction of hyperinsulinemia and subsequent insulin resistance (Dominici and Turyn 2002). Conversely, GH deficient mice exhibit decreased β-cell mass and increased insulin sensitivity (Liu, Coschigano et al. 2004).

*Cadm1*KO mice show reduced longitudinal length (Figure 9) and increased insulin sensitivity (Figure 16). A potential role of CADM1 in GH release or signaling has not been investigated yet. However, CADM1 was shown to be expressed in hypothalamic neurons producing gonadotropin-releasing hormone (GnRH) (Sandau, Mungenast et al. 2011). Disruption of CADM1 in mice diminishes GnRH release from these neurons, reducing fertility in female mice. It was therefore questioned whether CADM1 might also be necessary for the proper production or release of the hypothalamic growth hormone-releasing hormone (GHRH). GHRH is responsible for releasing GH from the pituitary gland (Löffler and Petrides 2003).

First, it was questioned whether circulating GH levels might be different in *Cadm1*KO mice compared to control mice. Since GH levels alter in a circadian pattern over the day and might not be comparable between mice, circulating IGF-1 levels were measured instead of GH levels (Shuto, Shibasaki et al. 2002). IGF-1 is produced in the liver and correlates with GH levels independent of circadian rhythms (Shuto, Shibasaki et al. 2002). As shown before, IGF-1 levels were lower in female control mice than in male control mice (Mao, Yang et al. 2009) **(Figure 20A)**. In addition, IGF-1 levels were significantly reduced in both male and female *Cadm1*KO mice compared to littermate controls.

In order to investigate whether production of *Ghrh, Gh* or *growth hormone receptor* (*Ghr*) might be changed in *Cadm1*KO mice, qRT-PCR was performed on hypothalami,

pituitary glands and livers from adult *Cadm1*KO and littermate control mice. Hypothalamic *Ghrh* gene expression was not significantly different between *Cadm1*KO and littermate control mice **(Figure 20B)**. Likewise, *Gh* gene expression in the pituitary gland and *Ghr* gene expression in the liver were unchanged in *Cadm1*KO mice**.**

Next, it was investigated whether CADM1 might influence the secretion capacity of GHRH or GH by challenging the release of these hormones. Intraperitoneal ghrelin injections were used to challenge release of GHRH in neurons of the ARC, which triggers GH release from the pituitary gland (Tennese and Wevrick 2011). Circulating GH levels showed no significant difference in *Cadm1*KO mice compared to control mice after ghrelin challenge **(Figure 20C)**. These data suggest that secretion of GHRH and GH is not diminished in *Cadm1*KO mice.

Taken together, circulating IGF1 levels were decreased in *Cadm1*KO mice compared to control mice, reflecting reduced body length in *Cadm1*KO mice. However, these changes were not caused by alterations in production or release of hypothalamic or pituitary gland hormones of the GH-GHRH axis in *Cadm1*KO mice. Although GH signaling was not investigated, the unchanged expression of *Ghr might* indicate a normal response to GH in *Cadm1*KO mice.

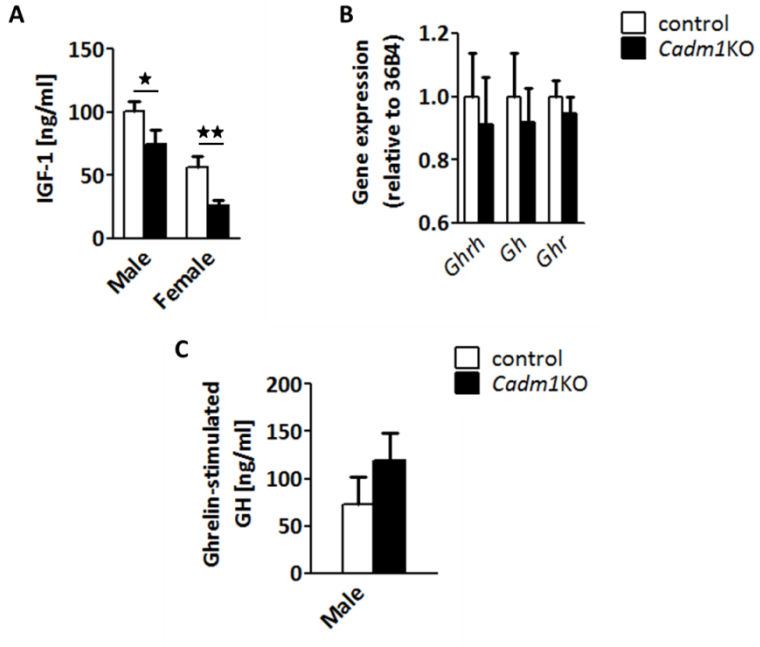

Figure 20: Basal IGF-1 levels, *Ghrh*, *Gh* and *Ghr* gene expression and ghrelin-challenged GH levels in *Cadm1*KO mice

[A] Circulating IGF-1 concentrations in random fed male control (N = 7) and *Cadm1*KO (N = 6) mice and female control (N = 6) and *Cadm1*KO (N = 5) mice between 12 and 16 weeks of age **[B]** Gene expression assessed by qRT-PCR of hypothalamic *growth hormone-releasing hormone (Ghrh)* in control (N = 7) and *Cadm1*KO mice (N = 8), pituitary gland *growth hormone* (*Gh*) in control (N = 9) and *Cadm1*KO mice (N = 9) and hepatic *growth hormone receptor (Ghr)* in control (N = 4) and *Cadm1*KO mice (N = 5) at random fed state between 12 and 16 weeks of age **[C]** GH concentrations after i.p. ghrelin injections in random fed male control (N = 7) and *Cadm1*KO (N = 7) mice between 12 and 16 weeks of age. Displayed values are means ± S.E.M. ★ $p \leq 0.05$; ★★ $p \leq 0.01$. Gene expression analysis was conducted by Sudhir Gopal Tattikota, AG Poy, MDC Berlin-Buch.

3.2 *Cadm1* deletion in pathophysiologic models of insulin resistance and obesity

Since *Cadm1* deletion improves glucose homeostasis and decreases body fat content in CHOW fed mice (3.1), it was questioned whether CADM1 also effects susceptibility to obesity and insulin resistance. Two models of obesity were chosen: a genetic-induced model of obesity and insulin resistance that is caused by leptin deficiency (*ob/ob* mouse) and a diet-induced model of obesity and insulin resistance (diet-induced obesity, DIO) caused by 10 weeks on HFD.

3.2.1 *Cadm1* deletion does not protect from weight gain but improves insulin sensitivity in genetic-induced obesity

In order to address the effects of *Cadm1* deficiency on genetic-induced obesity, *Cadm1*KO mice were crossed to *ob/ob* mice (The Jackson Laboratory, Bar Harbor, USA). The resulting leptin deficient *Cadm1*KO mice (*Cadm1*/*ob*) were compared to littermate *ob/ob* animals.

To elucidate whether *Cadm1* deletion might rescue genetic-induced obesity, energy homeostasis of *Cadm1/ob* compared to *ob/ob* was investigated. At weaning, male and female *Cadm1/ob* animals showed reduced body weight compared to *ob/ob* animals, which was consistent over the time of observation **(Figure 21A,B)**. However, average body weight gain per week was not significantly different between *Cadm1/ob* and *ob/ob* animals in both genders **(Figure 21C).** Similar to *Cadm1*KO mice, body length was significantly reduced in adult *Cadm1/ob* males and strongly reduced in *Cadm1/ob* females ($p = 0.07$) **(Figure 21D)**.

In order to investigate whether the differences in body weight in *Cadm1/ob* mice might be due to changes in body composition, body fat mass and lean body mass were measured in adult *Cadm1/ob* and *ob/ob* mice by NMR. Absolute fat mass was strongly reduced in *Cadm1/ob* mice of both genders, while absolute lean body mass was unchanged in these mice compared to *ob/ob* mice **(Figure 22A,B)**. Body fat content

relative to body weight was reduced, whereas lean body mass relative to body weight was increased in male and female *Cadm1*/*ob* mice **(Figure 22C,D)**.

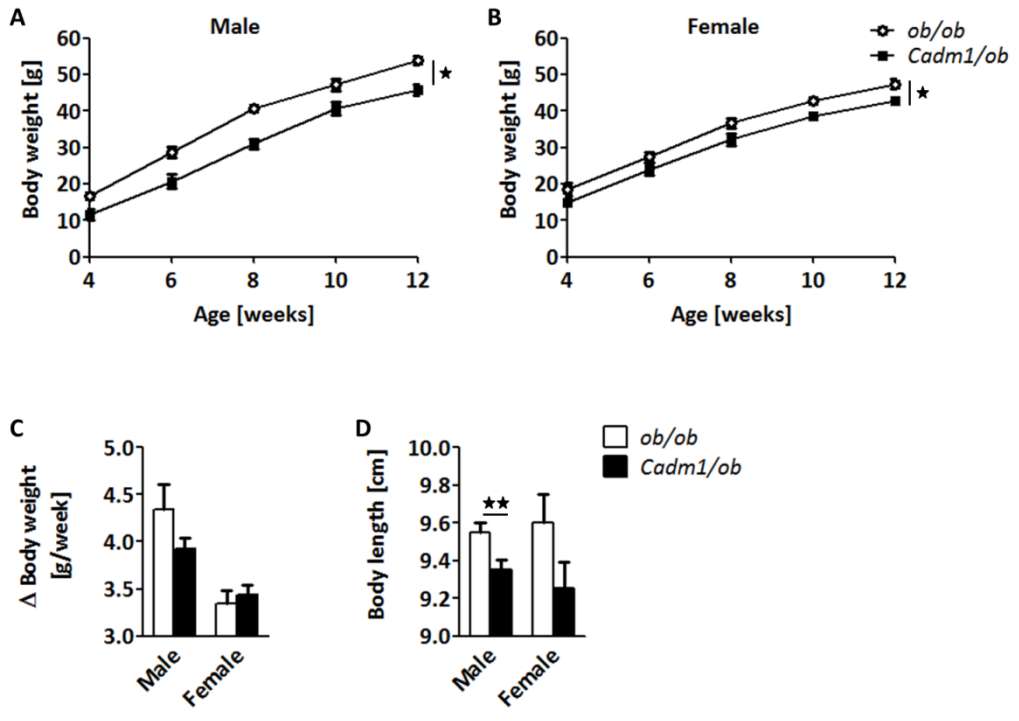

Figure 21: Body weight and body length of *Cadm1/ob* mice
[A] Body weight of male *ob/ob* (N = 5 - 7) and *Cadm1/ob* (N = 5 - 7) mice between 4 and 12 weeks of age **[B]** Body weight of female *ob/ob* (N = 8 - 13) and *Cadm1/ob* (N = 4 - 8) mice between 4 and 12 weeks of age **[C]** Average body weight gain per week of male *ob/ob* (N = 4) and *Cadm1/ob* (N = 5) mice and female *ob/ob* (N = 8) and *Cadm1/ob* (N = 6) mice between 6 and 12 weeks of age **[D]** Body length of male *ob/ob* (N = 5) and *Cadm1/ob* (N = 6) mice and female *ob/ob* (N = 5) and *Cadm1/ob* (N = 3) mice between 12 and 16 weeks of age. Displayed values are means ± S.E.M. ★ $p \leq 0.05$; ★★ $p \leq 0.01$

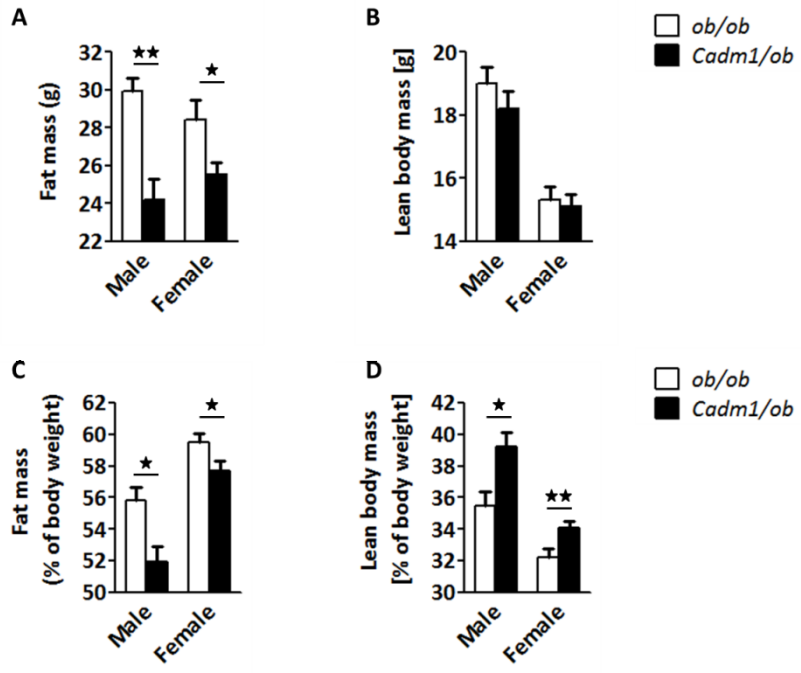

Figure 22: Body composition of *Cadm1/ob* mice
[A] Absolute body fat content and **[B]** Absolute lean body mass content and **[C]** Relative body fat content normalized to body weight and **[D]** Relative lean body mass content normalized to body weight of male *ob/ob* (N = 5) and *Cadm1/ob* (N = 7) mice and female *ob/ob* (N = 10) and *Cadm1/ob* (N = 7) mice at 13 weeks of age. Displayed values are means ± S.E.M. ★ $p \leq 0.05$; ★★ $p \leq 0.01$

To address whether changes in food intake might have caused the decrease in body weight and body fat content of *Cadm1/ob* mice, food intake of male *Cadm1/ob* and *ob/ob* mice was measured. Absolute food intake **(Figure 23A)** and food intake adjusted for lean body mass by using ANCOVA **(Figure 23B,C)** showed no significant differences between *Cadm1/ob* mice and *ob/ob* males. Unchanged food intake adjusted for lean body mass is in line with the results that neither absolute food intake nor lean body mass is changed in *Cadm1/ob* mice in comparison to *ob/ob* males.

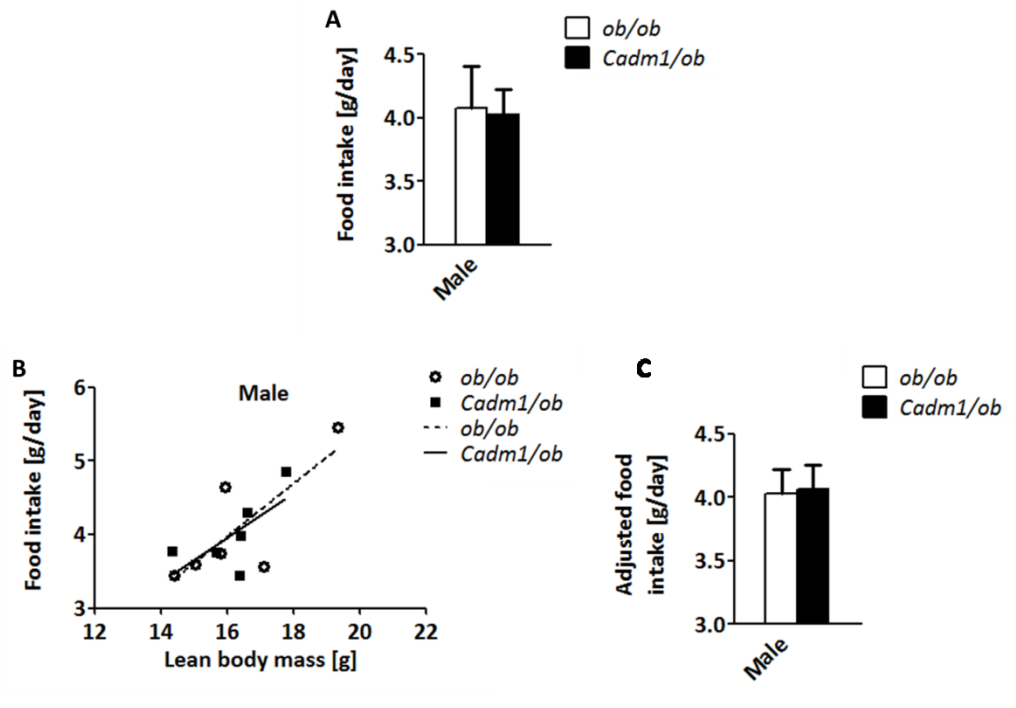

Figure 23: Food intake of *Cadm1/ob* mice
[A] Absolute food intake and **[B]** Scatterplot showing linear regression for food intake as a function of group and lean body mass (*ob/ob*: $y = 0.3588 \times x - 1.761; r^2 = 0.6137$; *Cadm1/ob*: $y = 0.2993 \times x - 0.8279; r^2 = 0.4648$) and **[C]** Food intake adjusted for lean body mass at 16.2276 g using ANCOVA of 3 consecutive days of *ob/ob* (N = 6) and *Cadm1/ob* (N = 6) males between 12 and 16 weeks of age. Displayed values are means ± S.E.M.

We further investigated the energy homeostasis of *Cadm1*/*ob* mice, by evaluating energy expenditure through indirect calorimetry and locomotor activity of *ob/ob* and *Cadm1*/*ob* males. Absolute O_2 and CO_2 respiration, calculated energy expenditure and respiratory rate were not significantly different between the genotypes **(Table 6)**. However, locomotor activity was significantly increased in male *Cadm1*/*ob* mice compared to *ob/ob* mice. Energy expenditure adjusted for locomotor activity using ANCOVA was significantly reduced in *Cadm1/ob* compared to *ob/ob* mice **(Figure 24A,B)**. These data suggest that *Cadm1/ob* mice would have lower energy expenditure if these animals had the same locomotor activity like *ob/ob* mice. The reason might be

that lower body weight of *Cadm1/ob* mice decreases energy costs for locomotor activity and therefore reduces energy expenditure in these mice.

	ob/ob	***Cadm1/ob***
VO_2 [l/h]	88.57 ± 5.77	93.74 ± 6.44
VCO_2 [l/h]	83.34 ± 4.87	87.2 ± 5.28
EE [kcal/h]	0.44 ± 0.03	0.47 ± 0.04
RER	0.94 ± 0.01	0.93 ± 0.01
Locomotor activity [counts/h]	1382.7 ± 161.1	2024.1 ± 237.8 ★

Table 6: Energy expenditure, RER and locomotor activity of *Cadm1/ob* mice
Average oxygen (VO_2) and carbon dioxide (VCO_2) respiration, calculated energy expenditure (EE) and respiratory rate (RER) as well as locomotor activity of male *ob/ob* (N = 6) and *Cadm1/ob* (N = 6) mice of 3 consecutive days between 12 and 16 weeks of age. Displayed values are means ± S.E.M. ★ $p \leq 0.05$

Furthermore, changes on glucose homoeostasis of *Cadm1/ob* compared to *ob/ob* mice were investigated. At 12 weeks of age, when hyperglycemia and insulin resistance of *ob/ob* mice is highly developed (Tomita, Doull et al. 1992), *Cadm1*/*ob* animals of both genders showed reduced blood glucose at random fed statues compared to *ob/ob* mice **(Figure 25A)**. Insulin sensitivity of *Cadm1*/*ob* mice was tested by performing an ITT. *Cadm1*/*ob* animals showed significantly reduced blood glucose levels at all time-points after insulin injections compared to *ob/ob* animals, suggesting an improved insulin tolerance in *Cadm1*/*ob* mice **(Figure 25B)**. Likewise, pancreatic insulin content, which is highly elevated in *ob/ob* mice due to insulin resistance (Tomita, Doull et al. 1992), was decreased in *Cadm1*/*ob* mice compared to *ob/ob* mice **(Figure 25C)**. These data suggest

that deletion of *Cadm1* partially rescues insulin resistance that is caused by genetic-induced obesity.

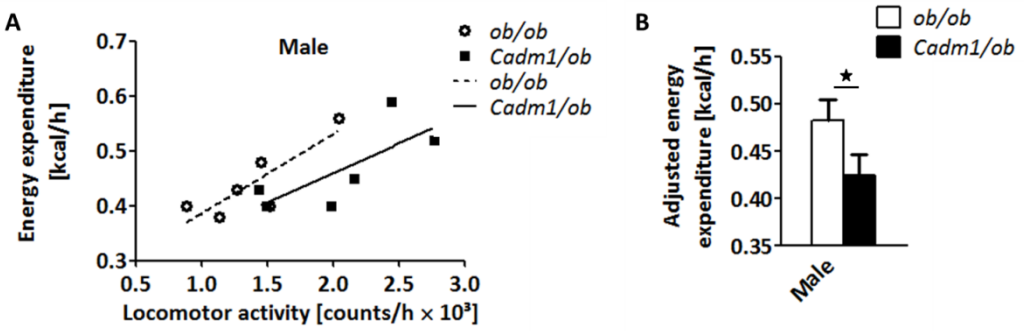

Figure 24: Analysis of covariance (ANCOVA) of energy expenditure and locomotor activity in male *Cadm1*/ob mice
[A] Scatterplot showing linear regression for energy expenditure as a function of group and locomotor activity (*ob/ob*: $y = 0.1443 \times x + 0.2422; r^2 = 0.7088$; *Cadm1/ob*: $y = 0.1081 \times x + 0.2437; r^2 = 0.5618$) and **[B]** Energy expenditure adjusted for locomotor activity at 1.714 counts/h × 10^3 using ANCOVA for male control (N = 6) and *Cadm1*KO (N = 6) mice between 12 and 16 weeks of age. Displayed values are means ± S.E.M. ★ $p \leq 0.05$.

Taken together, deletion of *Cadm1* in a genetic-induced model of obesity does not affect body weight gain but increases locomotor activity without affecting energy expenditure or food intake. Furthermore, *Cadm1* deletion in genetically obese animals rescues the obesity-related insulin resistance partially.

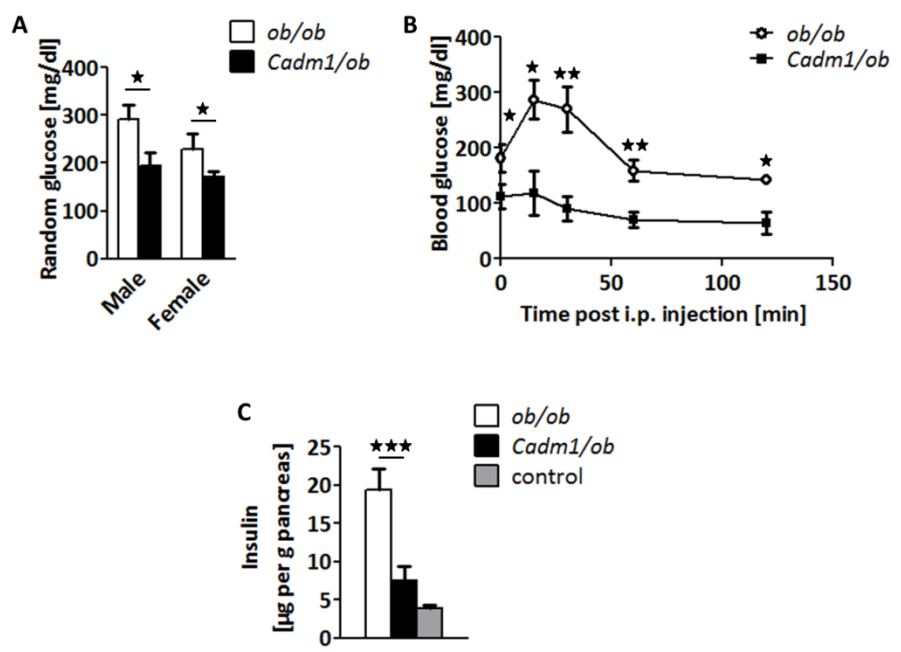

Figure 25: Glucose homoeostasis of *Cadm1/ob* mice
[A] Random glucose of male *ob/ob* (N = 7) and *Cadm1/ob* (N = 9) mice and female *ob/ob* (N = 13) and *Cadm1/ob* (N = 10) mice at 12 weeks of age **[B]** Insulin tolerance test of male and female *ob/ob* (N = 6) and *Cadm1/*ob (N = 3) mice between 12 and 16 weeks of age **[C]** Pancreatic insulin content of male and female *ob/ob* (N = 6), *Cadm1/ob* (N = 6) and *Cadm1*KO (N = 7) mice between 12 and 16 weeks of age. Displayed values are means ± S.E.M. ★ $p \leq 0.05$; ★★ $p \leq 0.01$; ★★★ $p \leq 0.001$

3.2.2 *Cadm1* deletion does not protect from weight gain but improves insulin sensitivity in diet-induced obesity

To further address effects of *Cadm1* deletion on the pathophysiology of obesity, obesity induced by HFD feeding (56 % of calories from fat) for 10 weeks was chosen as a second obesity model. *Cadm1*KO mice together with littermate control mice were changed to HFD between 4 and 7 weeks of age. Control mice fed HFD for 10 weeks showed significantly increased body weight compared to age-matched control mice on CHOW diet **(Figure 26)**, confirming that obesity was induced by HFD after this period.

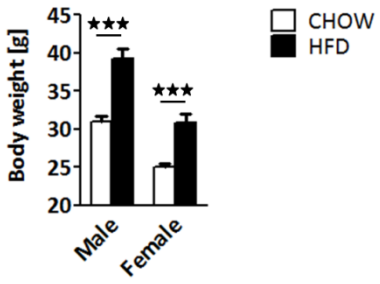

Figure 26: Body weight of control mice fed with CHOW or HFD
Body weight of male control mice after 10 weeks on CHOW diet (N = 20) or high fat diet (HFD) (N = 7) and female control mice on CHOW diet (N = 24) or high fat diet (HFD) (N = 9). Displayed values are means ± S.E.M. ★★★ $p \leq 0.001$

Before starting the HFD period, body weight measurements of multiple litters showed significant lower body weight for male and female *Cadm1*KO mice compared to control animals **(Figure 27A,B)**, confirming the results above (Figure 9). During the following 10 weeks on HFD, *Cadm1*KO males displayed a significantly reduced body weight in comparison to control mice **(Figure 27A)**. *Cadm1*KO females had significantly reduced body weight at 1, 4, 6 and 8 weeks after starting HFD feeding **(Figure 27B)**. Overall, average body weight gain per week between 0 and 10 weeks after the start of HFD feeding was not significantly different between control and *Cadm1*KO mice **(Figure 27C)**.

Measurements of body composition by NMR showed that male *Cadm1*KO mice did not display significant differences in absolute fat mass, fat mass relative to body weight and lean body mass relative to body weight **(Figure 28A, C, D).** Absolute lean body mass was significantly lower in male *Cadm1*KO mice compared to control mice **(Figure 28B)**. These data showed that decreased body weight in HFD fed *Cadm1*KO males is mainly caused by decreased lean body mass. Female *Cadm1*KO mice did not show significant differences in absolute fat mass, lean body mass, fat mass relative to body weight or lean mass relative to body weight **(Figure 28A, B, C, D).** These data suggest that *Cadm1*KO mice are not protected from weight gain and elevated fat mass induced by HFD feeding.

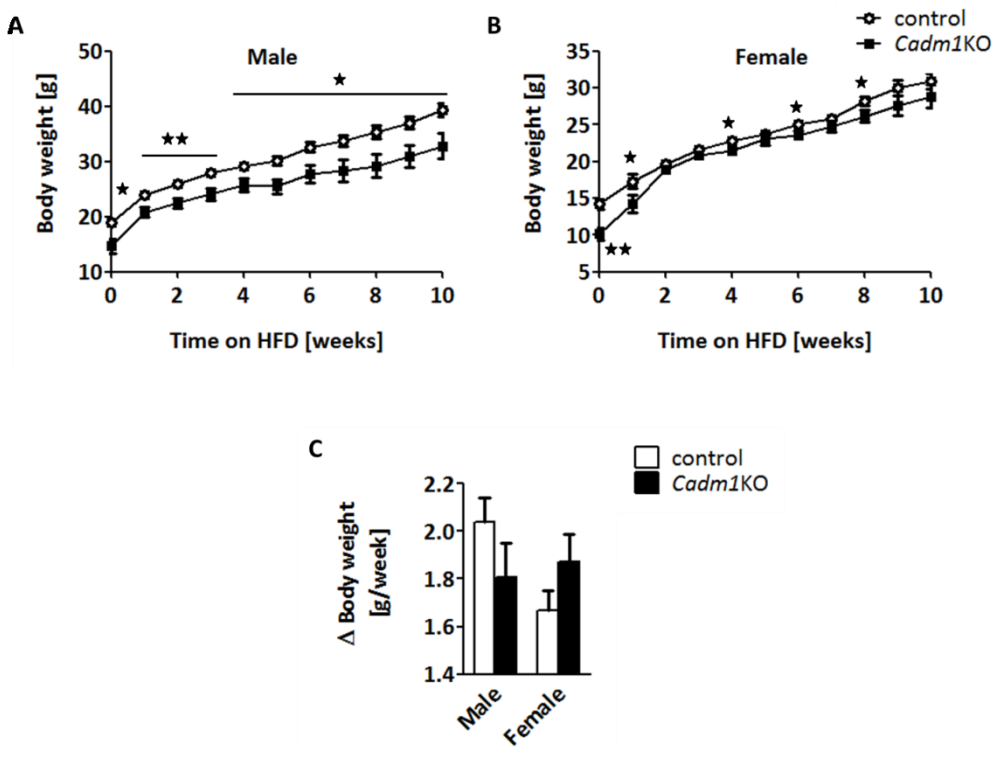

Figure 27: Body weight of *Cadm1*KO mice during 10 weeks of HFD feeding
[A] Body weight of male control (N = 7) and *Cadm1*KO (N = 6) mice and **[B]** Body weight of female control (N = 9) and *Cadm1*KO (N = 7) mice on high fat diet (HFD) **[C]** Average body weight gain per week of male control (N = 7) and *Cadm1*KO (N = 6) mice and female control (N = 9) and *Cadm1*KO (N = 7) mice between 0 and 10 weeks after start of HFD. Mice were changed to HFD between 4 and 7 weeks of age. Displayed values are means ± S.E.M. ★ $p \leq 0.05$; ★★ $p \leq 0.01$

To investigate whether changes on energy expenditure occur in *Cadm1*KO mice after HFD feeding, indirect calorimetry was conducted with control and *Cadm1*KO mice after 10 weeks of HFD feeding. For male HFD *Cadm1*KO mice, indirect calorimetry showed that absolute O_2 consumption, CO_2 expiration and calculated energy expenditure were decreased compared to control mice **(Table 7)**. Locomotor activity was significantly increased, while RER was unchanged in male *Cadm1*KO mice. Female HFD mice did not show significant differences between the genotypes **(Table 7).** Linear regression showed that energy expenditure and body weight are positively correlated in HFD male mice of both genotypes **(Figure 29A)**. These data explain why male *Cadm1*KO mice on HFD,

which have lower body weight than control mice on HFD (Figure 27), also show lower energy expenditure compared to control mice on HFD (Table 7). Nevertheless, energy expenditure adjusted for locomotor activity did not show significant differences between control and *Cadm1*KO mice on HFD **(Figure 29B,C)**. These experiments suggest that energy expenditure of control and *Cadm1*KO mice on HFD would not be significantly different, if animals from both genotypes had the same locomotor activity. Food intake measurements were not conducted with HFD fed mice, since HFD is crumbly and spills into the cage bedding.

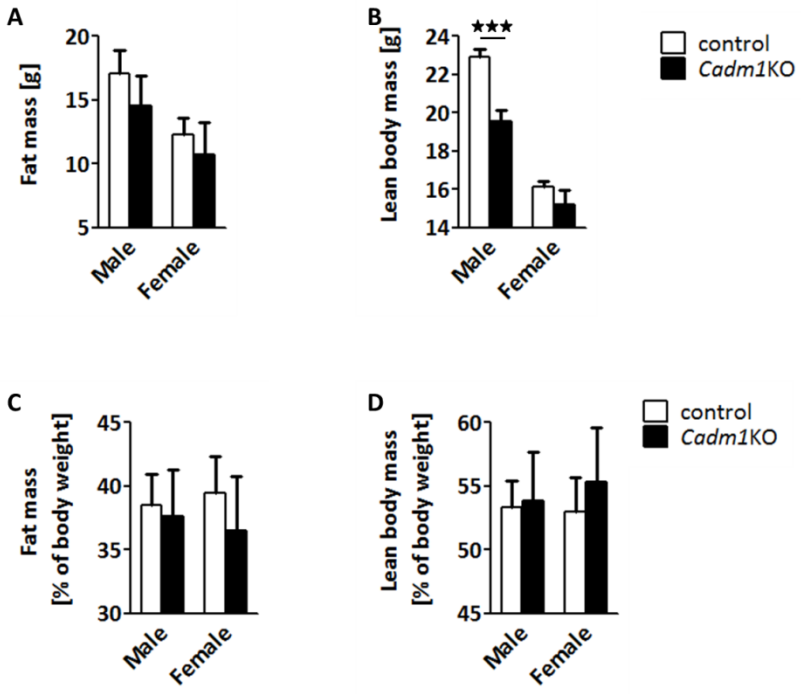

Figure 28: Body composition of *Cadm1*KO mice after 10 weeks of HFD feeding
[A] Absolute body fat mass and **[B]** Absolute lean body mass and **[C]** Relative body fat mass normalized to body weight and **[D]** Relative lean body mass normalized to body weight of male control (N = 7) and *Cadm1*KO (N = 6) mice and female control (N = 5) and *Cadm1*KO (N = 4) mice after 10 weeks of high fat diet (HFD). Mice were changed to HFD between 4 and 7 weeks of age. Displayed values are means ± S.E.M. ★★★ $p \leq 0.001$

	Male		Female	
	Control	***Cadm1*KO**	**Control**	***Cadm1*KO**
VO_2 [l/h]	102.3 ± 2.6	95.3 ± 2.2 ★	87.9 ± 4.4	86.6 ± 6.7
VCO_2 [l/h]	81.2 ± 2.0	74.4 ± 1.8 ★	69.7 ± 3.9	67.9 ± 4.3
EE [kcal/h]	0.49 ± 0.01	0.46 ± 0.01 ★	0.42 ± 0.02	0.44 ± 0.03
RER	0.79 ± 0.01	0.78 ± 0.01	0.79 ± 0.01	0.78 ± 0.01
Locomotor activity [counts/h]	1721.9 ± 68.5	2046.6 ± 133.7★	2546.4 ± 379.2	2138.1 ± 123.5

Table 7: Energy expenditure, RER and locomotor activity of *Cadm1*KO mice after 10 weeks of HFD feeding

Average oxygen (VO_2) and carbon dioxide (VCO_2) respiration, calculated energy expenditure (EE) and respiratory rate (RER) as well as locomotor activity of male control (N = 7) and *Cadm1*KO (N = 6) mice and female control (N = 5) and *Cadm1*KO (N = 4) mice after 10 weeks on HFD of 3 consecutive days. Mice were changed to HFD between 4 and 7 weeks of age. Displayed values are means ± S.E.M. ★ $p \leq 0.05$

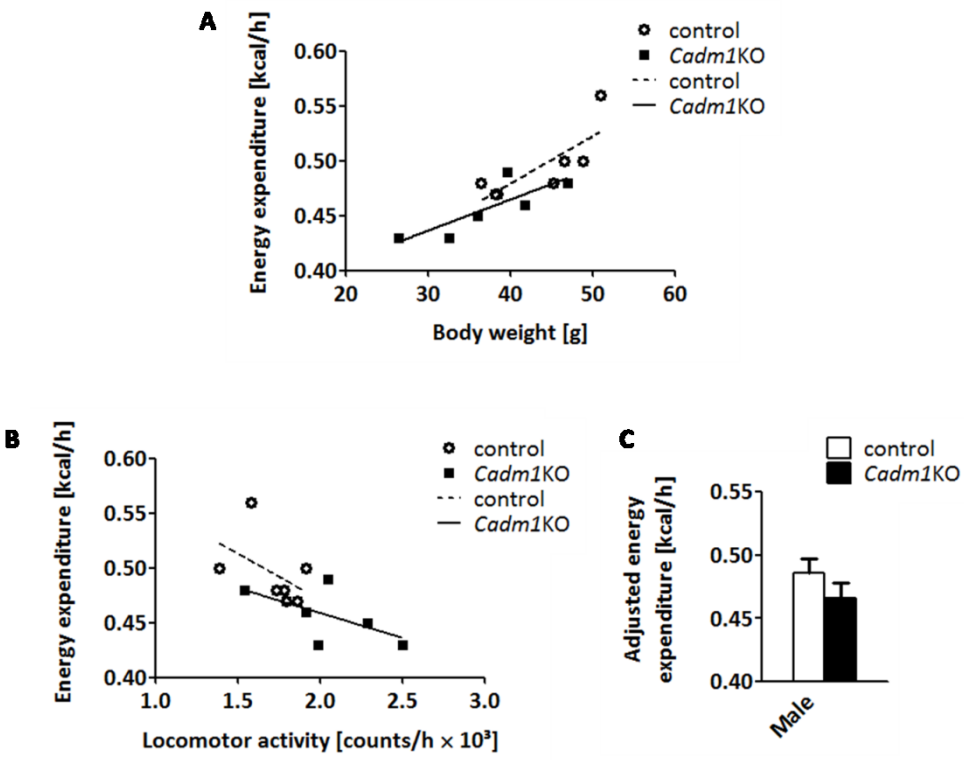

Figure 29: Analysis of covariance (ANCOVA) of energy expenditure and locomotor activity in male *Cadm1*KO mice after 10 weeks of HFD feeding
[A] Scatterplot showing linear regression for energy expenditure as a function of group and body weight (control: $y = 0.004318 \times x + 0.3065; r^2 = 0.6285$; *Cadm1*KO: $y = 0.002831 \times x + 0.3514; r^2 = 0.6714$) and **[B]** Scatterplot showing linear regression for energy expenditure as a function of group and locomotor activity (control: $y = -0.0845 \times x + 0.6398; r^2 = 0.2354$; *Cadm1*KO: $y = -0.04542 \times x + 0.5496; r^2 = 0.3531$) **[C]** Energy expenditure adjusted for locomotor activity at 1.87 counts/h × 10³ using ANCOVA for male control (N = 7) and *Cadm1*KO (N = 6) mice after 10 weeks of HFD feeding. Displayed values are means ± S.E.M.

Furthermore, it was questioned whether insulin resistance, which is induced by DIO (1.1.4), can be improved by *Cadm1* deletion. Male mice of both genders were challenged with an ITT after 10 weeks on HFD. As previously shown (Mori, Hanada et al. 2004), control mice showed an attenuated response to insulin 15 min after insulin injections, further confirming that insulin resistance was induced by 10 weeks on HFD **(Figure 30)**. However, *Cadm1*KO male mice showed significantly lower blood glucose

levels compared to control mice at 60 and 120 min after insulin injections, suggesting improved insulin sensitivity in *Cadm1*KO mice after HFD feeding.

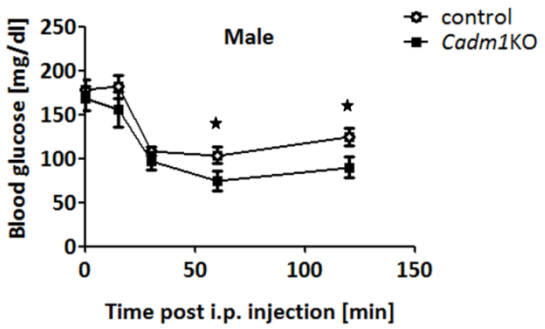

Figure 30: Insulin sensitivity of *Cadm1*KO mice after 10 weeks of HFD feeding
Insulin tolerance test of male control (N = 7) and *Cadm1*KO (N = 7) mice after 10 weeks on high fat diet (HFD). Mice were changed to HFD between 4 and 7 weeks of age. Displayed values are means ± S.E.M. ★ $p \leq 0.05$

In summary, deletion of *Cadm1* in diet- and genetic-induced models of obesity increases locomotor activity without increasing energy expenditure. Body weight gain is unaffected by *Cadm1* deletion in models of obesity, while obesity-induced insulin resistance is rescued partially.

3.3 Energy and glucose homeostasis in mice with tissue-specific *Cadm1* deletion

In order to assess in which tissues CADM1 exerts its effects on energy and glucose homeostasis, conditional *Cadm1*KO mice were bred by crossing *Cadm1* floxed mice (van der Weyden, Arends et al. 2006) with mouse lines expressing cre-recombinase under the control of gene promoters that are specifically expressed in neuronal- and glia cells or in cells expressing the *Lepr* (The Jackson Laboratory, Bar Harbor, USA). The resulting animals with tissue-specific *Cadm1* deletion were examined for the phenotype similar to *Cadm1*KO mice.

3.3.1 Increased lean body mass and increased insulin sensitivity in mice with neuron and glia cell-specific *Cadm1* deletion

The brain is a major regulator of homeostasis and can regulate both energy and glucose homeostasis (1.1.1; 1.1.5). CADM1 is highly expressed in different areas of the brain (1.3.1). In order to address CADM1's role in central regulation of energy and glucose homeostasis, mice with a specific deletion of *Cadm1* in neuronal and glia cell were bred by crossing mice carrying a floxed *Cadm1* allele ($Cadm1^{lox/lox}$) with mice expressing cre recombinase under the control of the rat *nestin* (*Nes*) promoter (*Cadm1NesCre*KO). The *Nes* promoter is active in glia- and neuronal precursors only (Tronche, Kellendonk et al. 1999). Tissue-specific recombination was confirmed by Western Blotting in brain and lung, organs with the highest CADM1 protein expression **(Figure 31)** (Fogel, Akins et al. 2007). While CADM1 could not be detected in the hypothalamus of *Cadm1NesCre*KO animals, lung tissue of these mice showed CADM1 protein expression. In addition, high CADM1 protein expression was detected in pituitary gland of *Cadm1NesCre*KO mice, which is in accordance to the previously described expression pattern of the *Nes* promoter (Tronche, Kellendonk et al. 1999). Unlike *Cadm1NesCre*KO mice, *Cadm1*KO mice showed no CADM1 protein expression in any of the tested tissues **(Figure 31)**.

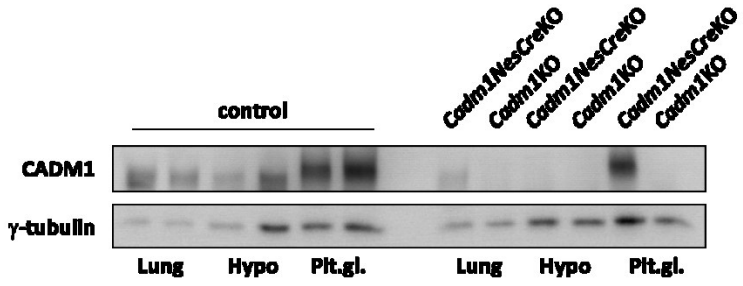

Figure 31: CADM1 protein abundance in *Cadm1NesCre*KO and *Cadm1*KO mice
Western blot analysis of CADM1 in lung, hypothalamus (hypo) and pituitary gland (pit.gl.) of control, *Cadm1NesCre*KO and *Cadm1*KO mice. γ-tubulin abundance was used as loading control.

To address the contribution of the brain in the phenotype of *Cadm1*KO mice, energy homeostasis of *Cadm1NesCre*KO mice was investigated. *Cadm1NesCre*KO mice of both genders between 10 and 13 weeks showed significantly lower body weight compared to control animals **(Figure 32A)**. In addition, body length was decreased in *Cadm1NesCre*KO males **(Figure 32B)**. To further address whether the reduced body weight of *Cadm1NesCre*KO mice is also caused by changes in body composition, fat mass and lean body mass of *Cadm1NesCre*KO and control mice were measured by NMR. Male *Cadm1NesCre*KO mice exhibited strongly decreased absolute body fat content (p=0.087) and significantly reduced absolute lean body mass **(Figure 32C,D)**, while body fat content relative to body weight and body lean mass relative to body weight were unchanged **(Figure 32E,F)**. Female *Cadm1NesCre*KO mice showed a significant reduction in absolute fat mass but an unchanged absolute lean body mass **(Figure 32C,D)**. When normalized to body weight, relative fat mass was significantly reduced, whereas relative lean body mass was significantly increased in female *Cadm1NesCre*KO mice compared to control mice **(Figure 32E,F).**

Furthermore, food intake of *Cadm1NesCre*KO mice was measured to evaluate whether changes in food intake might cause the decrease in body weight and body fat of these mice. Similar to *Cadm1*KO mice (Figure 11), absolute basal food of *Cadm1NesCre*KO male mice was unchanged compared to control mice **(Figure 33)**.

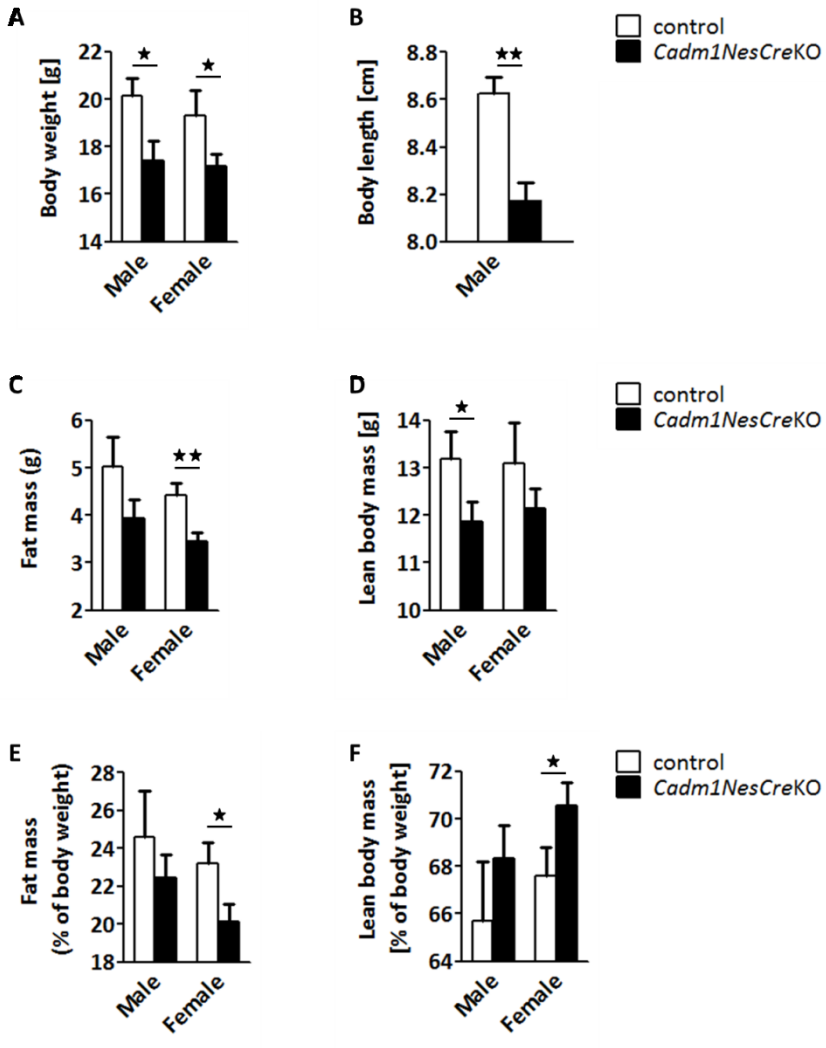

Figure 32: Body weight and body composition of *Cadm1NesCre*KO mice
[A] Body weight of male control (N = 8) and *Cadm1NesCre*KO (N = 4) mice and female control (N = 9) and *Cadm1NesCre*KO (N = 8) mice between 12 and 16 weeks of age **[B]** Body length of male control (N = 4) and *Cadm1NesCre*KO (N = 3) mice between 12 and 16 weeks of age **[C]** Absolute body fat content and **[D]** Absolute lean body mass content and **[E]** Relative body fat content normalized to body weight and **[F]** Relative lean body mass normalized to body weight of male control (N = 8) and *Cadm1NesCre*KO (N = 4) mice and female control (N = 9) and *Cadm1NesCre*KO (N = 8) mice between 12 and 16 weeks of age. Displayed values are means ± S.E.M. ★ $p \leq 0.05$; ★★ $p \leq 0.01$

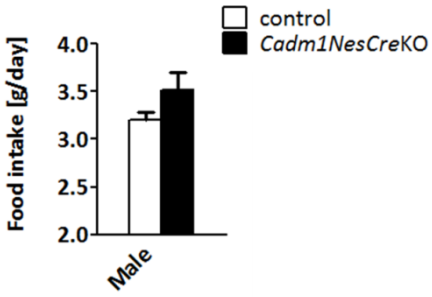

Figure 33: Food intake of *Cadm1NesCre*KO mice
Absolute food intake of 5 consecutive days of male control (N = 4) and *Cadm1NesCre*KO (N = 3) mice between 12 and 16 weeks of age. Displayed values are means ± S.E.M.

Next, glucose and insulin sensitivity of *Cadm1NesCre*KO mice were assessed to evaluate the influence of *Cadm1* deletion in neuronal and glia cells on glucose homeostasis. Similar to *Cadm1*KO mice (Figure 16), *Cadm1NesCre*KO male mice showed lower glucose levels compared to control mice at 30, 60 and 120 min after intraperitoneal injections of glucose **(Figure 34A)**. Blood glucose levels of *Cadm1NesCre*KO males were also significantly lower 15 min after intraperitoneal injections of insulin **(Figure 34B)**. Furthermore, 30 min after intraperitoneal injections blood glucose levels showed a strong trend for being lower in *Cadm1NesCre*KO mice ($p = 0.06$) compared to control mice**.**

Taken together, deletion of *Cadm1* specifically in neuronal and glia cells decreases body weight, body length and fat mass, which is not caused by decreased food intake. Furthermore, sensitivity to glucose and insulin is improved by deletion of *Cadm1* specifically in neuronal and glia cells. These results are consistent with the phenotype observed in *Cadm1*KO mice with the exception that female but not male *Cadm1NesCre*KO mice showed changes in body composition.

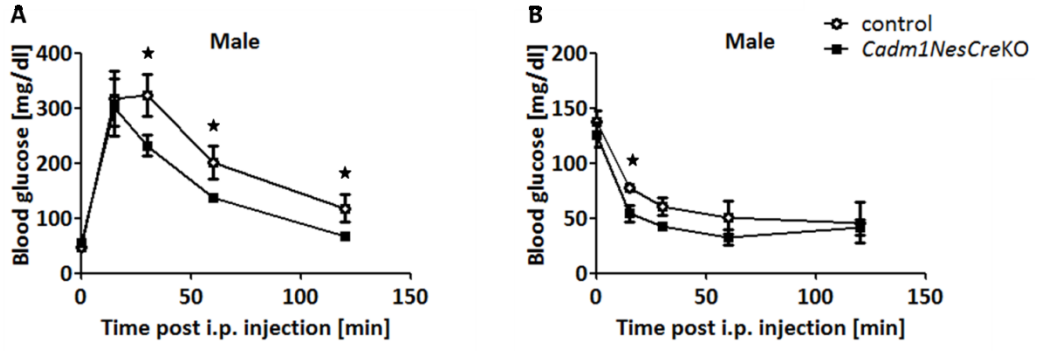

Figure 34: Glucose and insulin sensitivity of *Cadm1NesCre*KO mice
[A] Glucose tolerance test of male control (N = 6) and *Cadm1NesCre*KO (N = 5) mice between 12 and 16 weeks of age **[B]** Insulin tolerance test of male control (N = 3) and *Cadm1NesCre*KO (N = 3) mice between 12 and 16 weeks of age. Displayed values are means ± S.E.M. ★ $p \leq 0.05$

3.3.2 Unaltered lean body mass and slightly increased insulin sensitivity in mice with *Cadm1* deletion in *Lepr*-expressing cells

In order to address in which subpopulation of neuronal cells CADM1 might influence energy and glucose homeostasis, *Cadm1* was deleted in specific cell types expressing *Lepr*. These cell types were chosen since leptin plays an essential role in regulating glucose and energy homeostasis in the brain (1.1.6). Therefore, mice carrying a floxed *Cadm1* allele (*Cadm1*$^{lox/lox}$) were crossed with mice carrying cre recombinase under the control of the promoter of the *Lepr* gene (*LepRCre*) (Balthasar, Coppari et al. 2004). *Cadm1* deletion in the resulting *Cadm1LepRCre*KO mice was expected to be restricted to cells expressing *Lepr*, such as hypothalamic arcuate nucleus neurons. In order to visualize specific recombination in *Lepr*-expressing cells, reporter mice expressing *LepRCre* and *yellow fluorescent protein* (*YFP*) under the control of the ubiquitously expressed *Rosa26* promoter were used (*Rosa26-YFP*). By using immunohistochemistry, YFP immunofluorescence could be detected in a subpopulation of neurons in the ARC and median eminence **(Figure 35)**, confirming recombination in a subpopulation of cells as shown before (Louis, Leinninger et al. 2010). This suggests that recombination of

LepRCre and *Cadm1*$^{lox/lox}$ might yield a similar cell specific deletion of *Cadm1* in the hypothalamus and in other *Lepr*-expressing cells.

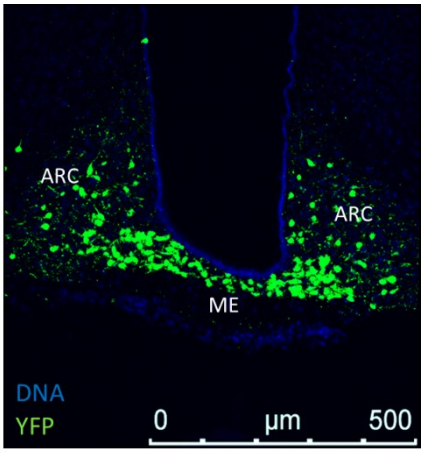

Figure 35: Recombination of *LepRCre* and *Rosa26-YFP* in the arcuate nucleus and median eminence
Immunohistochemistry of the hypothalamic arcuate nucleus (ARC) and median eminence (ME) of mice expressing *LepRCre* and *Rosa26-YFP* (YFP: green) between 12 and 16 weeks of age. Blue shows DAPI staining for nuclei. Immunohistochemistry and visualization was conducted by Kun Song, AG Siemens, MDC Berlin-Buch.

To test whether CADM1 might affect energy and glucose homeostasis in *Lepr*-expressing cells, the phenotype of *Cadm1LepRCre*KO mice was analyzed in a similar manner as *Cadm1*KO mice. *Cadm1LepRCre*KO mice of both genders did not show significant differences in body weight at 13 weeks of age compared to control mice **(Figure 36A)**. Since body weight was unchanged in *Cadm1LepRCre*KO mice, it was questioned whether body composition was also unchanged in these mice. Indeed, absolute body fat and lean body mass **(Figure 36B,C)** as well as body fat and lean body mass normalized to body weight **(Figure 36D,E)** did not show differences between the genotypes in both genders at 13 weeks of age.

In addition, absolute food intake was not significantly different between female *Cadm1LepRCre*KO and control mice **(Figure 37A)**. Similarly, food intake and body weight loss after 24 h food deprivation were unchanged in *Cadm1LepRCre*KO females **(Figure 37B,C)**.

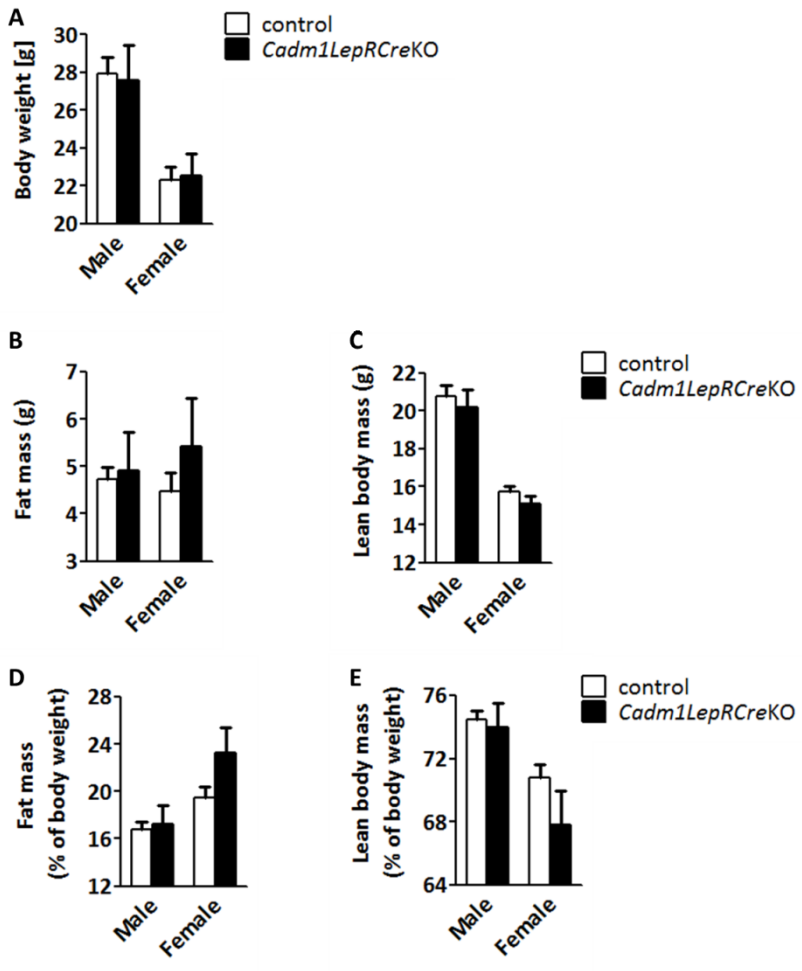

Figure 36: Body weight and body composition of *Cadm1LepRCre*KO mice
[A] Body weight and **[B]** Absolute body fat content and **[C]** Absolute lean body mass and **[D]** Relative body fat content normalized to body weight and **[D]** Relative lean body mass normalized to body weight of male control (N = 12) and *Cadm1LepRCre*KO (N = 7) mice and female control (N = 15) and *Cadm1LepRCre*KO (N = 8) mice between 13 - 16 weeks of age. Displayed values are means ± S.E.M.

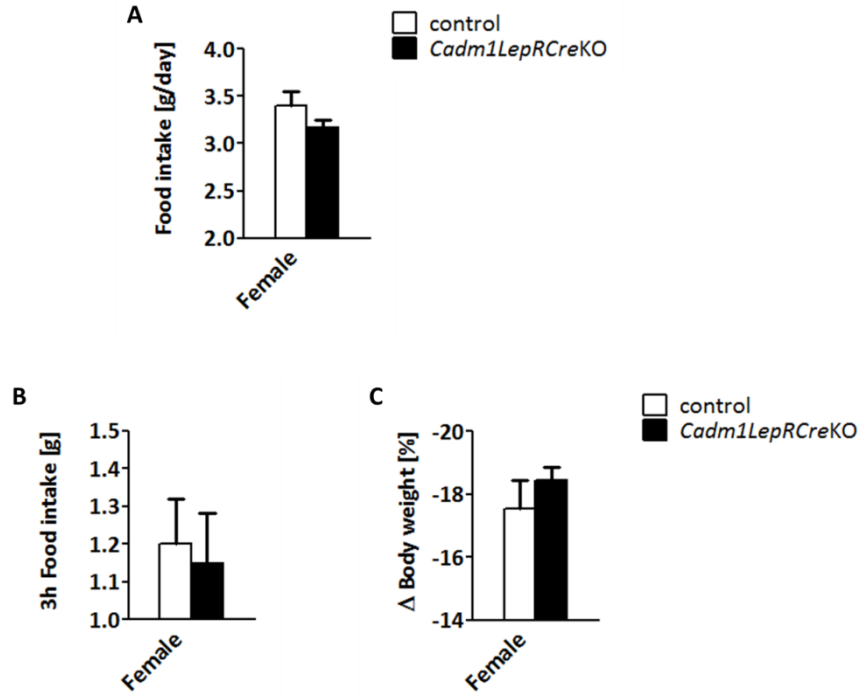

Figure 37: Food intake of *Cadm1LepRCre*KO mice
[B] Absolute food intake of 5 consecutive days and **[B]** 3 h food intake after 24 h starvation and **[D]** Relative body weight change after 24 h starvation of female control (N = 7) and *Cadm1LepRCre*KO (N = 4) mice between 12 and 16 weeks of age after 24 h starvation. Displayed values are means ± S.E.M

Furthermore, it was addressed whether glucose homeostasis is affected by deletion of *Cadm1* in *Lepr*-expressing cells. Sensitivity tests for insulin and glucose did not show significant differences in female *Cadm1LepRCre*KO mice at 15, 30 or 60 min after intraperitoneal injections of either insulin or glucose compared to their littermate controls **(Figure 38 A,B)**. Only 120 min after intraperitoneal insulin injections, female *Cadm1LepRCre*KO mice showed a slight but significant increase in insulin sensitivity **(Figure 38 B)**.

In summary, mice which presumably carry a *Cadm1* deletion in cells expressing *Lepr* do not exhibit changes in body weight, body composition or glucose sensitivity as opposed to *Cadm1*KO mice, while insulin sensitivity is slightly improved by *Cadm1* deletion in *Lepr*-expressing cells.

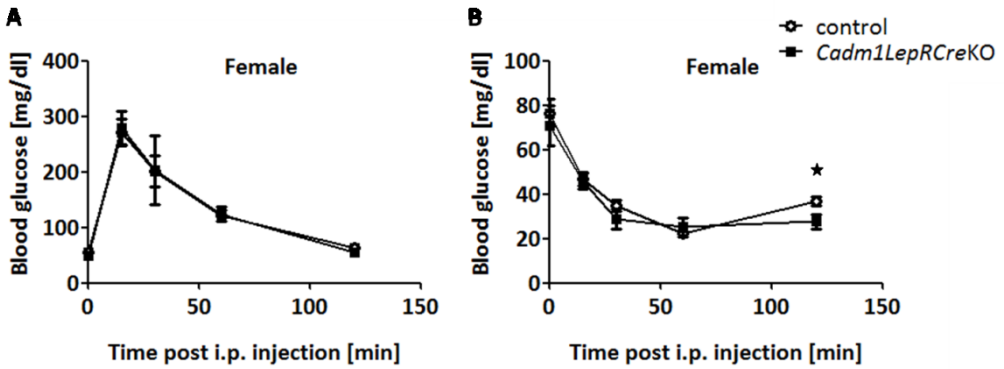

Figure 38: Glucose and insulin sensitivity of *Cadm1LepRCre*KO mice
[A] Glucose tolerance test of female control (N = 6) and *Cadm1LepRCre*KO (N = 4) mice between 12 and 16 weeks of age **[B]** Insulin tolerance test of female control (N = 17) and *Cadm1LepRCre*KO (N = 9) mice between 12 and 16 weeks of age. Displayed values are means ± S.E.M. ★ $p \leq 0.05$

4 Discussion

CADM1 has been described as a mediator of synapse formation and functioning with implications in spatial memory and learning behavior (Robbins, Krupp et al. 2010; Stagi, Fogel et al. 2010). In the past, several studies provided basic descriptions of CADM1 in pancreatic islets (Koma, Furuno et al. 2008; Suckow, Comoletti et al. 2008; Poy, Hausser et al. 2009). However, a role of CADM1 in controlling energy and glucose homeostasis in pancreatic islets, the brain or other tissues has not been investigated yet.

The aim of our work was to evaluate the influence of CADM1 in peripheral and central tissues on glucose and energy homeostasis of the body. Our data suggest that CADM1 influences both energy and glucose homeostasis in mice. Analyses of energy homeostasis showed that male *Cadm1*KO mice have increased energy expenditure through enhanced locomotor activity. Furthermore, *Cadm1*KO males displayed decreased relative fat mass and increased relative lean body mass and thus showed changed body composition. Blood leptin levels were also decreased in *Cadm1*KO males. Glucose-stimulated insulin secretion was enhanced in male *Cadm1*KO animals. In addition, insulin sensitivity of *Cadm1*KO males was enhanced after HFD feeding. In *Cadm1*KO female mice, insulin sensitivity was increased and glucose-stimulated insulin secretion was strongly, but not significantly enhanced. Female *Cadm1*KO mice did not show changes in energy expenditure or body composition. *Cadm1*KO mice of both genders showed reduced postnatal growth and unchanged body weight gain after four weeks of age as well as reduced body length as adult mice. Food intake was unchanged in both genders of *Cadm1*KO mice compared to control mice.

Cadm1 deletion in models of genetic and diet-induced obesity improved sensitivity to insulin but did not prevent weight gain, suggesting that CADM1 improves obesity-induced insulin resistance but does not influence susceptibility to obesity. Mice with neuronal and glia cell specific *Cadm1* deletion showed similar changes in body composition, body length, food intake and insulin sensitivity like *Cadm1*KO mice. As *Cadm1* deletion in neuronal and glia cells results in a similar phenotype like *Cadm1*

deletion in the whole body, an important role of CADM1 in these tissues for energy and glucose homeostasis can be suggested.

4.1 Validation of *Cadm1* deletion models

While mouse models with *Cadm1* deletion in different tissues are available and relatively easily to study, human patients with *CADM1* missense mutations have not been investigated for their metabolic phenotype (Murakami 2005). However, CADM1 is highly conserved in vertebrates with highest homology between human and mouse reaching 98 % sequence homology (Biederer 2006). Mice are therefore a useful model organism for the prediction of CADM1 functions in other vertebrate species, including humans.

4.1.1 Mice completely deficient for *Cadm1* and deficient for *Cadm1* in neuronal and glia cells

In order to address whether CADM1 might play a role in energy and glucose homeostasis, we assessed mice with total *Cadm1* deletion and tissue specific *Cadm1* deletion for changes in energy and glucose homeostasis. Deletion of *Cadm1* in hypothalamus, lung and pituitary gland of total *Cadm1*KO mice was confirmed by Western blotting (Figure 31). Mice with a specific *Cadm1* deletion in neuronal and glia cells (*Cadm1NesCre*KO) exhibited deletion in the hypothalamus but not in lung and pituitary gland (Figure 31). These data confirm the previously described expression pattern of *NesCre* in neuronal tissue (Tronche, Kellendonk et al. 1999). *Cadm1*KO and *Cadm1NesCre*KO mice are therefore expected to carry deletion in *Cadm1* in the whole body or in neuronal and glia cells only, respectively.

4.1.2 Mice deficient for *Cadm1* in *Lepr*-expressing cells

In addition, we used a previously described mouse model expressing cre recombinase under the control of the *Lepr* promoter (*LepRCre)* to generate *Cadm1LepRCre*KO mice (DeFalco, Tomishima et al. 2001) in order to study the contribution of CADM1 in leptin sensitive cell types. However, deletion of genes and their corresponding proteins in a defined subpopulation of cells in the hypothalamus is usually difficult to detect by gene

or protein expression analysis, since the cells affected by gene deletion reflect a very small portion in the whole hypothalamus (Konner, Janoschek et al. 2007). Using immunohistochemistry to visualize *Cadm1* deletion in hypothalamic *Lepr*-expressing cells is also not possible, since available antibodies for immunohistochemistry also detect CADM2, CADM3 and CADM4 (Sandau, Mungenast et al. 2011) (Figure 13). Therefore, mice carrying *LepRCre* were crossed with reporter mice expressing *YFP* under the control of the *Rosa26* promoter (*Rosa26-YFP*). Immunofluorescent detection of YFP could be detected in a subpopulation of cells in the ARC and ME (Figure 35), similar to what was shown before (Louis, Leinninger et al. 2010). It is therefore expected, that crossing mice carrying *LepRCre* with *Cadm1*$^{lox/lox}$ mice would yield animals with a similar deletion of *Cadm1* specifically in cells expressing *Lepr*. However, a clear prove for correct recombination of the *LepRCre* and *Cadm1*$^{lox/lox}$ alleles is missing and results of the *Cadm1LepRCre*KO mice have to be interpreted with caution. Furthermore, *Lepr* expression was found in several peripheral tissues of the body (Fruhbeck 2001), including pancreas. Endocrine cells of the pancreas also express *Cadm1* (1.3.2) and conditional deletion of *Cadm1* in these cells might influence glucose homeostasis in *Cadm1LepRCre*KO mice.

4.2 Role of CADM1 in energy homeostasis

4.2.1 CADM1 influences locomotor activity and body composition

Male *Cadm1* deficient mice showed increased locomotor activity (Table 5, Figure 14). These findings could be confirmed in diet and genetic-induced obese *Cadm1* deficient mice (Figure 24,

Figure 29). Furthermore, relative and absolute body fat content was decreased in *Cadm1*KO males and in genetic-induced obese *Cadm1* deficient mice (Figure 10, Figure 22). Enhanced physical activity influences body composition in humans and rodents mainly by reducing body fat content (Yki-Jarvinen and Koivisto 1983; Davies, Gregory et al. 1995; Saltzman and Roberts 1995; Swallow, Koteja et al. 2001). These data suggest that increased locomotor activity caused by deletion of *Cadm1* might lead to changes in body composition in *Cadm1* deficient mice.

The brain has a fundamental role in the control of locomotor activity and genetic variations which induce hyperactivity, e.g. through altering GABA signaling in the brain, have been described (Viggiano 2008; Mignogna and Viggiano 2010). CADM1 is also highly expressed in the brain and can influence GABA signaling there (1.3.1; 1.3.3). Direct measurements of locomotor activity in *Cadm1NesCre*KO mice have not been conducted in our studies for technical reasons. However, *Cadm1NesCre*KO males showed strongly reduced body fat content (Figure 32), suggesting that locomotor activity might be increased in these mice. We therefore postulate that CADM1 controls locomotor activity through its action in neuronal tissues.

Unlike genetic-induced obese *Cadm1*KO males, diet-induced obese *Cadm1*KO mice lack significant changes in body fat content (Figure 22, Figure 28). This might be explained by the previously shown high variations in susceptibility to diet-induced obesity in the C57BL/6N strain that we used as background strain for our *Cadm1*KO mice (de Leeuw van Weenen, Parlevliet et al. 2011). These high variations in susceptibility to obesity could hide the differences between *Cadm1*KO and control mice. The reason why

genetic-induced obese *Cadm1*KO and *Cadm1NesCre*KO females showed significantly changed body composition but *Cadm1*KO females did not is currently not clear (Figure 22, Figure 32, Figure 10).

Taken together, we suggest that *Cadm1* deletion increase locomotor activity through its action in the brain and subsequently changes body composition by reducing body fat content.

4.2.2 CADM1 effects on locomotor influence insulin sensitivity

Locomotor activity was increased in male *Cadm1*KO mice (Figure 14, Table 7), while body fat content of male *Cadm1*KO mice was reduced (Figure 10). Insulin sensitivity was increased in male *Cadm1*KO mice under HFD feeding (Figure 28). Similar, *Cadm1/ob* showed increased locomotor activity, reduced body fat content and increased insulin sensitivity (Figure 24, Figure 22, Figure 25). Also *Cadm1NesCre*KO mice showed increased insulin sensitivity and reduced body fat content (Figure 34, Figure 32). Enhancement of energy expenditure can increase insulin sensitivity in humans and mice (Hu, Sigal et al. 1999; Kriska, Saremi et al. 2003; Birkenfeld, Lee et al. 2011; Choi, Yablonka-Reuveni et al. 2011). The improving effect of physical activity on insulin sensitivity can be explained by two independent mechanisms. On one hand, physical activity can increase glucose uptake in skeletal muscle through mechanisms such as increased GLUT4 expression (Nesher, Karl et al. 1985; Wallberg-Henriksson and Holloszy 1985; Kraniou, Cameron-Smith et al. 2006). On the other hand, physical activity reduces body fat content, which is associated with increased insulin sensitivity (Yki-Jarvinen and Koivisto 1983; Banerji, Faridi et al. 1999). These results implicate that increased locomotor activity might improve insulin sensitivity in *Cadm1*KO mice directly or through reducing body fat content.

*Cadm1*KO male mice did not show significant changes in body fat content after HFD feeding (Figure 28). This might be caused by high variations in susceptibility to diet-induced obesity as explained above (4.2.1). Alternatively, increased locomotor activity

might directly increase insulin sensitivity in these mice, through increasing glucose uptake as discussed above.

In summary, we suggest that reduced body fat content or increased locomotor activity or both are at least partially responsible for improved insulin sensitivity in *Cadm1* deficient mice.

4.2.3 Influence of CADM1 on food intake and body weight

In our work, we demonstrated that male *Cadm1*KO mice showed increased locomotor activity compared to control mice (Figure 14). Furthermore, average body weight gain in *Cadm1*KO mice was not significantly different between 4 and 12 weeks of age (Figure 9). Decreased *Pomc* expression (Figure 12) and increased AMPK activity and expression (Figure 13) were measured in *Cadm1*KO mice. Both changes are expected to induce food intake in the brain (Minokoshi, Alquier et al. 2004) (1.1.4, 1.1.6). Starvation-induced food intake was enhanced in *Cadm1*KO mice (Figure 12). These results indicate that basal food intake in *Cadm1*KO mice is increased compared to control mice. We therefore suggest that enhanced locomotor activity in adult *Cadm1*KO mice together with enhanced food intake results in unchanged body weight gain for these animals.

Due to technical limitations, energy expenditure and food intake have to be measured in single-housed animals, while body weight was measured in group-housed mice. In order to investigate energy expenditure and food intake in *Cadm1* deficient mice, we allowed newly isolated mice to acclimatize for 24 hours in the measurement cages followed by three days of measurements. Acute isolation between one and 24 h induces anxiety-related behavior in rats (Maisonnette, Morato et al. 1993). *Cadm1* deficient mice were reported to display increased anxiety-related behavior, even under normal conditions (Takayanagi, Fujita et al. 2010). Therefore, *Cadm1*KO mice might be prone to anxiety-related behavior under single housing conditions more than control mice, possibly influencing measurements of energy expenditure and food intake. Therefore data from single housing, such as the unchanged basal food intake from *Cadm1*KO mice (Figure

12), should be treated with caution. Nevertheless, the increased locomotor activity measured under single housing conditions is likely to occur also under group housing conditions, since changes in body composition, which were measured in group-housed animals, are thought to be caused by increased locomotor activity as discussed above (4.2.1). However, these results need further confirmation. Future studies should therefore include adaptation times to single housing of several weeks before measuring energy homeostasis in *Cadm1* deficient mice. Alternatively, all animals used for experiments on energy and glucose homeostasis should be housed individually to avoid differences in behavior to influence experimental results.

For young *Cadm1*KO mice between postnatal day 14 and 21, IPSC frequency onto hypothalamic *Pomc*-expressing neurons was decreased compared to control mice (Figure 19). A decreased IPSC frequency onto *Pomc*-expressing neurons is expected to enhance α-MSH release, one anorexic product of the *Pomc* gene (Tung, Piper et al. 2006). At this age, also body weight gain was impaired in *Cadm1*KO mice compared to control mice (Figure 9). It is therefore likely, that the decreased IPSC frequency onto *Pomc*-expressing neurons reflects reduced food intake in young *Cadm1*KO mice, which might explain the impaired body weight gain at that age.

4.2.4 CADM1 and its role in controlling leptin signaling

Cadm1/ob mice showed changes like *Cadm1*KO mice in locomotor activity, body weight, body weight gain and food intake (Figure 21, Figure 24). Since *Cadm1/ob* mice lack leptin signaling but show a similar phenotype like *Cadm1*KO mice, it is likely that leptin is dispensable for the effects of CADM1 on energy homeostasis signaling. *Cadm1LepRCre*KO mice showed no differences in body composition or body weight (Figure 36), indicating that deletion of CADM1 in leptin sensitive cells is unlikely to be responsible for the effects of CADM1 on energy homeostasis. Together, these data suggest that CADM1 does not mediate effects on energy homeostasis through regulating leptin signaling.

Leptin is an anabolic hormone enhancing energy expenditure and decreasing food intake (Balthasar, Dalgaard et al. 2005). Changes in leptin signaling should therefore lead to changes in body weight gain in adult mice (Satoh, Ogawa et al. 1997; Mori, Hanada et al. 2004). However, body weight gain was not different in adult *Cadm1*KO mice and in diet and genetic-induced obese *Cadm1* deficient mice (Figure 9, Figure 21, Figure 27). Instead, body weight differences in adult *Cadm1*KO animals were probably caused by differences in body weight gain during postnatal development (Figure 9). Recent literature suggests that leptin influences GABA signaling on postsynaptic *Pomc*-expressing neurons (Cowley, Smart et al. 2001; Vong, Ye et al. 2011). Body weight gain is regulated by these leptin-mediated effects on postsynaptic *Pomc*-expressing neurons. Since body weight gain was not changed in *Cadm1* deficient mice (Figure 9, Figure 21, Figure 27), also an effect of CADM1 on postsynaptic *Pomc*-expressing neurons through its influence on GABA signaling is unlikely to be the mechanism of CADM1-mediated changes on energy homeostasis. These data further implicate that CADM1 does not affect energy homeostasis through regulation of leptin signaling.

Circulating leptin levels correlate with body fat content (1.1.6). Our results showed that male *Cadm1*KO mice have reduced leptin blood concentrations and reduced body fat content (Figure 11, Figure 10). *Cadm1NesCre*KO mice showed strongly reduced body fat content (Figure 32) and a similar phenotype in regards to body weight and food intake like *Cadm1*KO mice (Figure 32, Figure 33), suggesting that *Cadm1NesCre*KO might also show changes in leptin levels. *Nestin* expression is restricted to neuronal and glia cells (Tronche, Kellendonk et al. 1999) and *Cadm1NesCre*KO mice are expected to express *Cadm1* in adipose tissue, the tissue responsible for leptin secretion (1.2.1). Therefore, it is unlikely that CADM1 regulates the release of leptin in adipose tissue. Instead, *Cadm1* deletion is likely to reduce body fat mass in *Cadm1* deficient mice, which then causes secondary changes in leptin levels. It can therefore be suggested that CADM1-mediated effects on energy homeostasis are not caused by CADM1 acting on leptin signaling or leptin release.

In conclusion, we propose that *Cadm1* deletion in male mice increases locomotor activity through its action in neuronal tissues, while food intake is compensatory increased or vice versa. Increased locomotor activity subsequently decreases body fat content. Reduced body fat content contributes to increased insulin sensitivity and causes decreased circulating leptin levels.

4.3 Role of CADM1 in neuronal insulin signaling

We suggested that CADM1 influences insulin sensitivity by changing locomotor activity and subsequent body composition (4.2.2). In *Cadm1*KO females, insulin sensitivity was improved (Figure 16) but locomotor activity and body composition were unchanged (Figure 10, Figure 15). Therefore, insulin sensitivity seems to be improved in *Cadm1* deficient animals also by other mechanisms than body composition or locomotor activity alterations.

4.3.1 CADM1 might influence insulin sensitivity through regulating neuronal insulin signaling

As discussed above, CADM1 does not seem to exert its effects on energy homeostasis through influencing leptin signaling (4.2.4). Enhanced insulin sensitivity also occurred in leptin deficient *Cadm1/ob* mice (Figure 25), indicating that leptin signaling is dispensable for CADM1-mediated effects on insulin sensitivity. Another important regulator of insulin sensitivity in neuronal tissues is insulin itself (1.1.4). Könner *et al.* showed that neuronal insulin signaling enhances insulin sensitivity, the inulin-mediated decrease of blood glucose levels, through suppression of HGP (Konner, Janoschek et al. 2007). Insulin-mediated regulation of HGP involves reduced firing frequency of *Agrp*-expressing neurons and reduced release of AGRP and other neurotransmitters from these neurons. Due to technical limitations, insulin-stimulated firing frequency of *Agrp*-expressing neurons from *Cadm1*KO mice could not be measured. However, we showed that IPSC frequency onto *Pomc*-expressing neurons from *Cadm1*KO mice was reduced (Figure 19). It is known that *Pomc*-expressing neurons are inhibited by innervation from *Agrp*-expressing neurons (Cowley, Smart et al. 2001; Tong, Ye et al. 2008) (1.1.4). It is therefore possible, that the reduced IPSC frequency onto *Pomc*-expressing neurons in *Cadm1*KO mice is caused by reduced firing frequency of *Agrp*-expressing neurons. Reduced firing frequency of *Agrp*-expressing neurons results in reduced HGP (Konner, Janoschek et al. 2007). Thus, reduced firing frequency of *Agrp*-expressing neurons and

subsequent reduced HGP might be the cause of the lower blood glucose levels after insulin injections in *Cadm1*KO mice (**Figure 39**).

Basal and fasted blood glucose levels were unchanged in *Cadm1*KO mice compared to control mice (Figure 16). The study by Könner *et al.* also reported that basal and fasted blood glucose levels of mice with deficient insulin signaling in *Agrp*-expressing neurons were unchanged, suggesting that altered insulin signaling in *Agrp*-expressing neurons does not induce major disturbances in glucose homeostasis (Konner, Janoschek et al. 2007). Our results confirm that CADM1 might influence HGP through neuronal insulin signaling without inducing major disturbance in glucose homeostasis. Furthermore, we measured enhanced glucose tolerance In *Cadm1*KO mice (Figure 16), which can partially be explained by increased glucose-stimulated insulin release (Figure 17). The study by Könner *et al.* showed that the decreased suppression of HGP in mice with deficient insulin signaling in *Agrp*-expressing neurons is balanced by increased glucose uptake in white adipose tissue (Konner, Janoschek et al. 2007), resulting in unchanged glucose tolerance. Other studies by Lin et al. showed that overexpression of *insulin receptor* in *Agrp*-expressing neurons does not lead to significant changes in peripheral glucose uptake, suggesting that a balancing glucose uptake in peripheral tissue does not exist in models with enhanced neuronal insulin sensitivity (Lin, Plum et al. 2010). We therefore suggest that *Cadm1* deletion might increase neuronal insulin signaling through reducing firing frequency from *Agrp*-expressing neurons. Subsequent reduced HGP reduces blood glucose levels in *Cadm1*KO mice, which is not compensated by glucose uptake from peripheral tissues. This might contribute to enhanced glucose tolerance and results in increased insulin sensitivity.

Our results showed that EPSC frequency was unchanged, while IPSC firing frequency was significantly reduced in the hypothalamus of *Cadm1*KO mice (Figure 19). Studies by Robbins *et al.* reported that EPSC frequency was significantly reduced in the hippocampus of *Cadm1* deficient mice, while IPSC firing frequency was not affected in these mice (Robbins, Krupp et al. 2010). These differences can be explained by the predominant number of inhibitory GABAergic neurons in the ARC (Vong, Ye et al. 2011),

while excitatory glutamatergic neurons dominate in the hippocampus (Robbins, Krupp et al. 2010). While *Cadm1* deletion reduces firing frequency in inhibitory and excitatory neurons, the neuron type affected by CADM1 seems to be dependent on the local abundance of each neuron type.

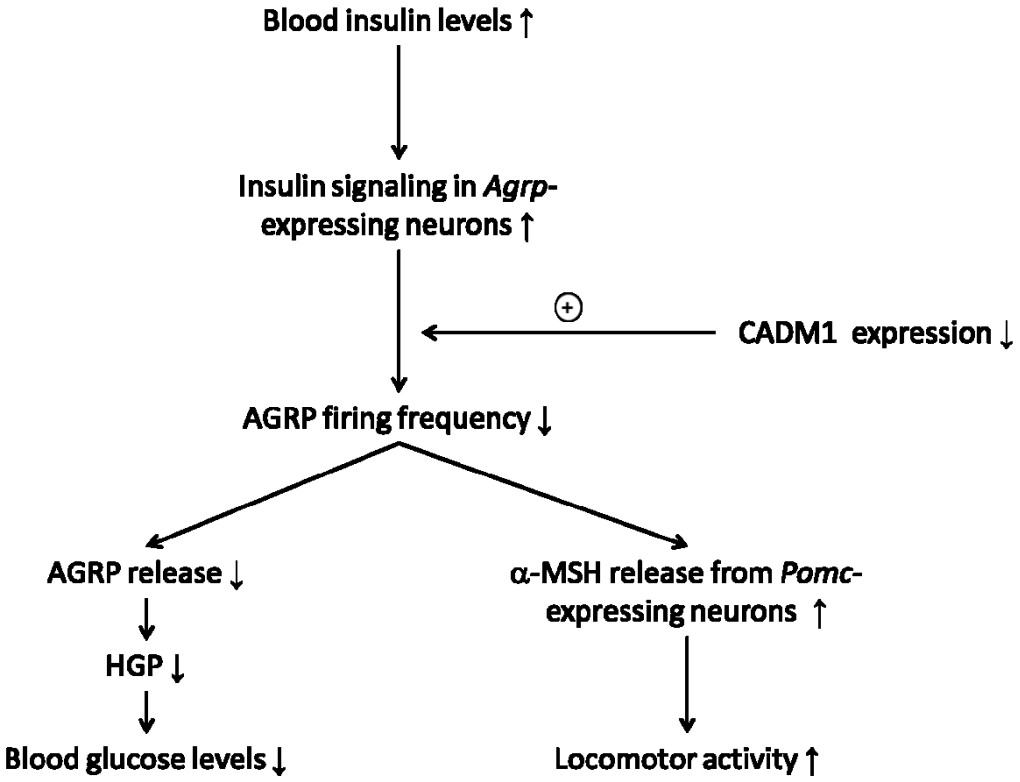

Figure 39: *Cadm1* deficiency might enhance neuronal insulin signaling
Increased insulin levels in the blood enhance insulin signaling in *Agrp*-expressing neurons, which subsequently reduces firing frequency and AGRP release from these neurons. Reduced AGRP release reduces HGP and subsequent blood glucose levels. In addition, *Agrp*-expressing neurons innervate *Pomc*-expressing neurons. Reduced insulin-mediated firing frequency from *Agrp*-expressing neurons increases α-MSH release, the most important protein product of the *Pomc* gene, and subsequent locomotor activity. *Cadm1* deficiency is postulated to further decrease insulin-mediated firing frequency from *Agrp*-expressing neurons or AGRP signaling or both, leading to decreased insulin-mediated blood glucose levels and increased locomotor activity.
Abbreviations: Agouti-related protein (AGRP); Hepatic glucose production (HGP); α-Melanocyte-stimulating hormone (α-MSH)

4.3.2 CADM1 might influence locomotor activity through regulating neuronal insulin signaling

Our results showed that IPSC frequency onto *Pomc*-expressing neurons was reduced in *Cadm1*KO mice (Figure 19). Locomotor activity was increased in *Cadm1*KO male mice (Table 5, Figure 14). Strikingly, CADM1 effects on locomotor activity do not alter body weight gain (4.2.2). Recent literature reports that changes in neuronal insulin signaling can alter locomotor activity without changing body weight gain (Konner, Janoschek et al. 2007; Lin, Plum et al. 2010). Insulin-mediated effects on locomotor activity involve increased insulin signaling in *Pomc*-expressing neurons and subsequent enhanced α-MSH release (Lin, Plum et al. 2010). Since we measured decreased IPSC frequency onto *Pomc*-expressing neurons in *Cadm1*KO mice, it can be assumed that these neurons also release increased α-MSH amounts. This increased α-MSH release might be responsible for increased locomotor activity in *Cadm1*KO mice. We therefore hypothesize that CADM1 regulates locomotor activity through regulation of excitation of *Pomc*-expressing neurons **(Figure 39)**. This might involve regulation of AGRP release, as discussed above (4.3.1), or GABA signaling between *Agrp*-expressing neurons and *Pomc*-expressing neurons, since CADM1 was implicated to be involved in GABA-mediated inhibitory signaling (Fujita, Tanabe et al. 2012) (1.3.1) and GABA is coexpressed in *Npy/Agrp*-expressing neurons (Cowley, Smart et al. 2001; Tong, Ye et al. 2008) (1.1.4).

The study by Könner *et al.* showed that inhibition of insulin signaling in *Agrp*-expressing neurons or *Pomc*-expressing does not change circulating leptin levels. The data from Könner *et al.* further suggested that body composition and possibly locomotor activity is not changed in mice with deletion of *insulin receptor* in *Agrp*-expressing or *Pomc*-expressing neurons (Konner, Janoschek et al. 2007), since leptin levels directly correlate with body fat content and body fat content is negatively regulated by physical activity (1.1.6, 4.2.1). In contrast, overexpression of *insulin receptor* in *Pomc*-expressing neurons reduces circulating leptin levels and increases locomotor activity (Lin, Plum et al. 2010). It can therefore be concluded that inhibition of neuronal insulin signaling does not change locomotor activity and leptin levels, whereas induction of neuronal insulin

signaling increases locomotor activity and reduces leptin levels. Our data showed that male *Cadm1*KO mice also exhibit reduced circulating leptin levels besides increased locomotor activity (Figure 11, Figure 14). These data further support our hypothesis that deletion of *Cadm1* might increase locomotor activity through enhancing neuronal insulin signaling. Changes in locomotor activity likely decrease leptin levels as disused before (4.2.4).

Male *Cadm1*KO mice exhibited increased locomotor activity (Figure 14). Hypothalamic *Pomc* expression was decreased in *Cadm1*KO mice (Figure 12). Recent literature suggests that increased locomotor activity can be induced by increased signaling from *Pomc*-expressing neurons (Lin, Plum et al. 2010). Increased signaling from *Pomc*-expressing neurons correlates with increased *Pomc* expression (Birnberg, Lissitzky et al. 1983; Loeffler, Demeneix et al. 1986). These findings seem to contradict our findings of increased locomotor activity besides decreased *Pomc* expression. It has been shown that different subpopulations of *Pomc*-expressing neurons exist in the hypothalamus with differing functions (Balthasar, Dalgaard et al. 2005; Williams, Margatho et al. 2010; Sohn, Xu et al. 2011). It is therefore possible that locomotor activity and food intake might be regulated by distinct *Pomc*-expressing neuron populations. The majority of *Pomc*-expressing neurons might regulate food intake and decrease overall *Pomc* expression in hypothalami of *Cadm1*KO mice in order to increase food intake (Figure 12) (4.2.3). A minority of *Pomc*-expressing neurons might regulate locomotor activity and lie in a distinct region compared to food intake regulating *Pomc*-expressing neurons. Enhanced α-MSH release from these neurons might increase locomotor activity in *Cadm1*KO mice.

In summary, we suggest that *Cadm1* deletion might increase locomotor activity through decreasing insulin-mediated signaling between *Agrp*-expressing and *Pomc*-expressing neurons. Activity of *Pomc*-expressing neurons is subsequently increased, resulting in increased locomotor activity in *Cadm1*KO mice. Regulation of food intake and locomotor activity seems to be mediated through different subpopulations of *Pomc*-expressing neurons.

4.3.3 CADM1 might influence signaling from *insulin receptor*-expressing neurons but not from *Lepr*-expressing neurons

Recent publications suggested that *insulin receptor* and *Lepr* might be expressed on different subpopulations of *Pomc*-expressing and *Agrp*-expressing neurons and cross-talk between these different subpopulations connect both signaling cascades (Williams, Margatho et al. 2010). We hypothesized that CADM1 influences signaling from *Agrp*-expressing neurons or between *Pomc*- and *Agrp*-expressing neurons (4.3.1, 4.3.2). Our experiments revealed that leptin signaling is dispensable for the effects of CADM1 on energy homeostasis (4.2.4). We therefore suggest that CADM1 might be expressed in *Agrp*-expressing neurons which express *insulin receptor*, but not in *Agrp*-expressing neurons expressing *Lepr*. This way, CADM1 would influence insulin signaling, but not leptin signaling from *Agrp*-expressing neurons.

Our experiments showed that mice with specific *Cadm1* deletion in neurons expressing *Lepr* (*Cadm1LepRCre*KO) displayed only slight improvements of insulin sensitivity (Figure 38). These data indicate that CADM1 does not influence insulin sensitivity mainly through influencing leptin signaling in *Lepr*-expressing cells. Slight changes on insulin sensitivity in *Cadm1LepRCre*KO mice might be a result of deletion of *Cadm1* in a few cells expressing *insulin receptor* and *Lepr.* However, we expect the majority of *Cadm1*-deleted neurons to express only *Lepr*, which does not affect insulin signaling. Alternatively, slight changes on insulin sensitivity in *Cadm1LepRCre*KO mice might be a result of *Cadm1* deletion in *Lepr*-expressing cells affecting neighboring cell types, such as *insulin receptor*-expressing cells, since cross-talk between *Lepr*- and *insulin receptor*-expressing cells has been described (Williams, Margatho et al. 2010).

4.3.4 CADM1 influences neuronal insulin signaling in male mice differently than in female mice

Our experiments showed that male *Cadm1*KO mice have increased locomotor activity after CHOW and HFD feeding (Figure 14, Table 7) and improved insulin sensitivity after

HFD feeding (Figure 30). Female *Cadm1*KO mice exhibited improved insulin sensitivity but did not show changes in locomotor activity or energy expenditure (Figure 16, Figure 15). These data point to a gender-specific effect of CADM1 on the regulation of energy and glucose homeostasis. Gender-specific effects have also been reported for NIRKO mice (Bruning, Gautam et al. 2000). Under CHOW diet, female NIKRO mice showed a 10 to 15 % increase in body weight accompanied by an increase in food intake, fat mass, leptin levels and insulin resistance. Male NIRKO mice also showed increased fat mass and leptin levels but without effects on food intake and body weight. However, when NIRKO mice were fed a HFD, both genders developed DIO. In addition to these defects in energy and glucose homeostasis, NIRKO mice suffer from hypogonadism, with reduced luteinizing hormone (LH) concentrations in both genders. The reason for the gender-specific effects in energy and glucose metabolism in NIRKO mice has not been identified but it was speculated that the hypogonadism might be associated with the observed differences (Konner, Janoschek et al. 2007). Gonadotropins, such as LH and follicle-stimulating hormone (FSH), are produced in the anterior pituitary, also called adenohypophysis, and are responsible for reproduction in both genders (Schmidt, Thews et al. 2000; Löffler and Petrides 2003). In female humans and rodents, insulin resistance was shown to be associated with hypergonadism (Mauras, Welch et al. 1998; Niklasson, Daneryd et al. 2000). In male humans, obesity and type 2 diabetes is associated with hypogonadism (Dhindsa, Miller et al. 2010). From these results we conclude that disturbance of the hypothalamic-pituitary axis might affect glucose and energy homeostasis of females and males differently. CADM1 was shown to affect gonadotropin-releasing hormone (GnRH) release by controlling cell adhesion between hypothalamic astrocytes and GnRH neurons (Sandau, Mungenast et al. 2011; Sandau, Mungenast et al. 2011). GnRH is produced in the hypothalamus and responsible for the release of FSH and LH (Schmidt, Thews et al. 2000; Löffler and Petrides 2003). Therefore, *Cadm1* deficiency might induce changes in the hypothalamic-pituitary axis, affecting insulin sensitivity and locomotor activity differently in each gender.

Alternatively, deletion of the *insulin receptor* might affect different areas with different effects on energy and glucose homeostasis. Indeed, gender-specific differences in

regional expression of insulin receptors have been reported before (Xu, Huber et al. 2007; Hami, Sadr-Nabavi et al. 2012). The gender-specific effects of *Cadm1* deletion on energy and glucose homeostasis observed in our experiments might be caused by gender-specific expression of the *insulin receptor* or *Cadm1.* These differences might result in different regional interactions between CADM1 and insulin signaling in male and female mice and different effects on insulin sensitivity and locomotor activity in both genders.

4.3.5 Possible molecular mechanisms of CADM1 influencing neuronal insulin signaling

The recently identified function of CADM1 in localizing to postsynaptic receptor complexes might be a mechanism how CADM1 influences neuronal insulin signaling (Fujita, Tanabe et al. 2012). CADM1 might regulate neurotransmitter receptor signaling by stabilizing inhibitory GABA or AGRP receptor complexes at postsynaptic membranes. Binding to postsynaptic GABA and glutamate receptor complexes have been shown recently for CADM1 (1.3.1) (Fujita, Tanabe et al. 2012). Postsynaptic receptor complexes influenced by CADM1 might exist in *Pomc*-expressing neurons, which we measured in our studies (Figure 19), or other second-order **(Figure 40 (1))**. *Cadm1* deletion might lead to destabilizing of these complexes and subsequent reduced AGRP signaling, decreasing HGP and enhancing locomotor activity, as discussed above (4.3.1, 4.3.2).

Alternatively, CADM1 might influence presynaptic neurotransmitter release of *Npy*-expressing neurons **(Figure 40 (2))**. Potential binding partners of CADM1 at the presynaptic membrane include N-type Ca^{2+} channels, which are known to bind to the VELI-CASK-MINT1 complex (Maximov, Sudhof et al. 1999) (1.3.1). Blockage of N-type Ca^{2+} channels inhibits potassium-stimulated NPY release (King, Widdowson et al. 1999). *Cadm1* deficiency might destabilize and similarly block presynaptic N-type Ca^{2+} channels. This blockage would reduce AGRP release from *Agrp*-expressing neurons. Since GABA is co-expressed with NPY from *Npy*-expressing neurons (Cowley, Smart et al. 2001), GABA-mediated IPSC frequency on *Pomc*-expressing neurons would be decreased in *Cadm1*KO

mice (Figure 19). In conclusion, CADM1 might stabilize presynaptic N-type Ca^{2+} channels in *Npy*-expressing neurons, which prevents insulin-mediated inhibition of NPY release.

Last, CADM1 might influence glucose and energy homeostasis by regulating synaptogenesis between insulin sensitive neurons and other neurons during postnatal development. CADM1 is an important regulator of synaptogenesis (1.3.1). Alterations in neurotransmitter trafficking between insulin sensitive neurons and other neurons could be consequences of loss of CADM1. Since CADM1 is proposed to be necessary to maintain synaptic numbers (Robbins, Krupp et al. 2010), these alterations cannot be compensated in adult mice and might cause increased locomotor activity and insulin sensitivity in adult *Cadm1*KO mice.

In summary, we hypothesize that *Cadm1* deletion reduces insulin-mediated suppression of AGRP or GABA signaling between *Agrp*-expressing neurons and *Pomc*-expressing neurons and between *Agrp*-expressing neurons and second-order neurons. These effects are likely to include CADM1 action at the postsynaptic or presynaptic membranes or CADM1 regulating synaptogenesis. Decreased AGRP and GABA signaling increases α-MSH release and subsequent locomotor activity and reduces HGP and blood glucose levels, increasing insulin sensitivity. Enhanced locomotor activity reduces body fat content and circulating leptin levels, which further increases insulin sensitivity.

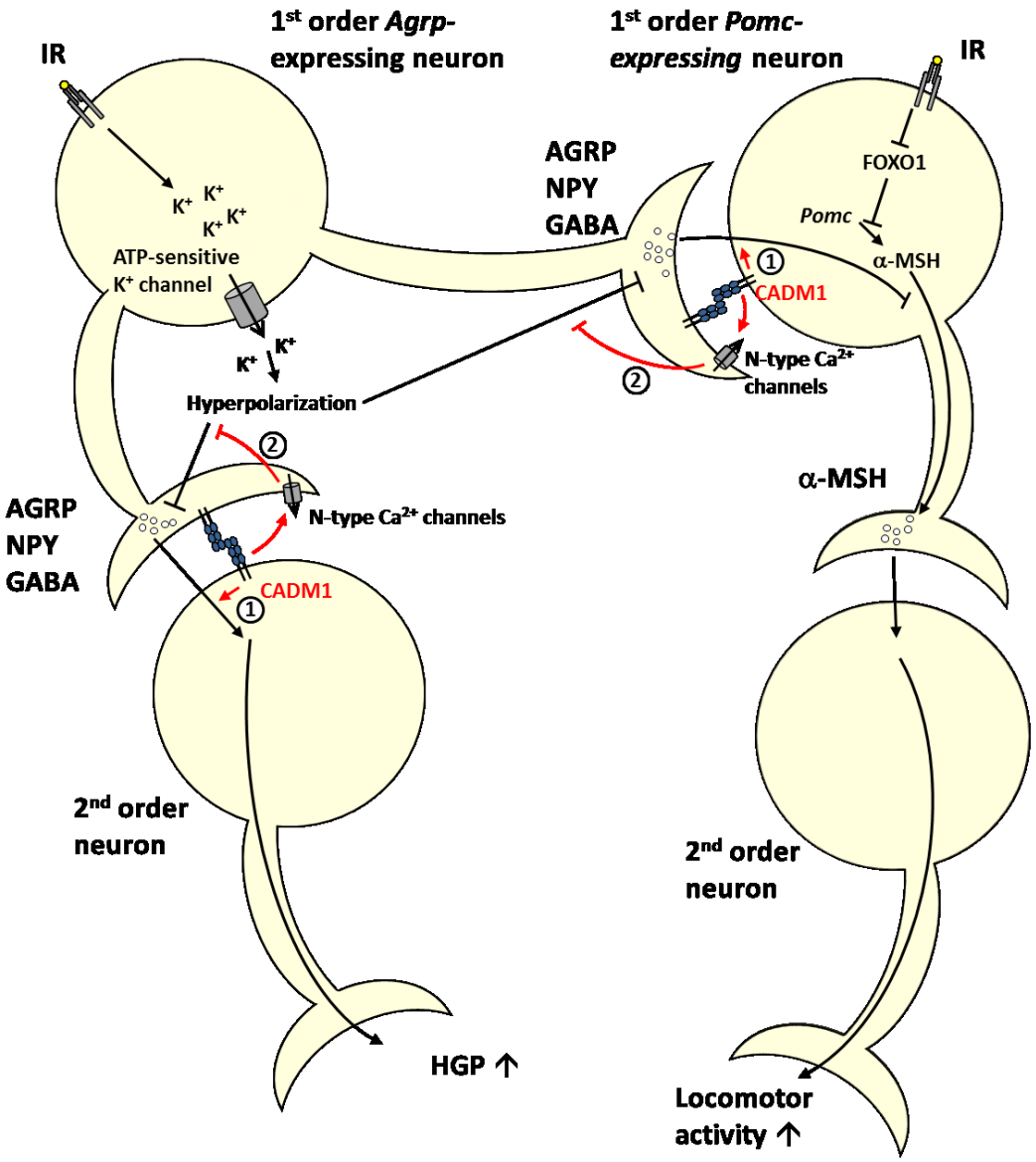

Figure 40: Postulated mechanisms of CADM1 inhibiting insulin-mediated suppression of neurotransmitter release

Insulin signaling in 1st order neurons expressing *insulin receptor* and *Agrp* (left) leads to opening of ATP-sensitive K^+-channels and subsequent hyperpolarization. Insulin-mediated hyperpolarization of *Agrp*-expressing neurons represses release of neurotransmitters, such as NPY, AGRP and GABA. Reduced neurotransmitter release signals through 2nd order neurons and hepatic innervation and results in decreased HGP. In *Pomc*-expressing neurons (right), insulin signaling causes release of α-MSH, a transcribed protein of the *Pomc* gene, directly through inhibition of FOXO1 and

indirectly through inhibited release of NPY, AGRP and GABA. Insulin-mediated α-MSH release promotes locomotor activity.
CADM1 is postulated to be a positive regulator of postsynaptic NPY, AGRP and GABA signaling by stabilizing their neurotransmitter receptor complexes **(1)**. Alternatively, CADM1 might be a suppressor of presynaptic insulin-mediated inhibition of NPY, AGRP and GABA release **(2)**. *Cadm1* deficiency therefore decreases insulin-mediated NPY, AGRP and GABA release and subsequently inhibits HGP and increases locomotor activity.
Abbreviations: Agouti-related protein (AGRP); γ-aminobutyric acid (GABA); Hepatic glucose production (HGP); Insulin receptor (IR); α-Melanocyte-stimulating hormone (α-MSH); Neuropeptide Y (NPY); *Pro-opiomelanocortin* (*Pomc*)

4.4 Role of CADM1 in insulin secretion

Our data showed that glucose-stimulated insulin release was enhanced in *Cadm1*KO mice compared to control mice (Figure 17). We also observed increased glucose-stimulated insulin secretion in *Cadm1*-depleted MIN6 cells (Figure 18). Basal glucose levels were unchanged in *Cadm1*KO mice (Figure 16). In addition, pancreatic insulin content was unchanged in *Cadm1*KO mice (Figure 17). Based on these data, we suggest that CADM1 negatively regulates glucose-stimulated insulin release in pancreatic β-cells but does not affect basal insulin levels or pancreatic insulin content.

CADM1 has been described as a target of miR-375 (Poy, Hausser et al. 2009) (1.2.3). *MiR-375*KO mice showed enhanced CADM1 expression as well increased glucose-stimulated insulin secretion (Poy, Eliasson et al. 2004; Poy, Hausser et al. 2009). Overexpression of *Cadm1* has not been conducted in our studies but we observed increased glucose-stimulated insulin secretion after reduced CADM1 expression. Enhanced CADM1 expression, like in *miR-375*KO mice, is therefore unlikely to also result in increased glucose-stimulated insulin secretion. MiR-375 seems to target other genes than CADM1 to effect insulin secretion.

Our data showed that *Cadm1*-depleted MIN6 cells, a cell line derived from pancreatic β-cells, have increased insulin secretion in response to glucose compared to control MIN6 cells (Figure 18). While indirect effects on *in vivo* insulin secretion, such as sympathic innervation, cannot be excluded in mice, cell culture *in vitro* experiments provide a model with only one cell type involved. Our data of *Cadm1* depletion enhancing insulin secretion in MIN6 cells therefore emphasizes that CADM1 might regulate insulin secretion in an autocrine manner. Nevertheless, MIN6 cells have been reported to express genes which resemble a mixed pancreatic endocrine cell line rather than a pure insulin-secreting cell line (Nakashima, Kanda et al. 2009). These results might question the validity of MIN6 cells as model for pancreatic β-cells. Therefore, results of a function of CADM1 in MIN6 cells should be confirmed by *in vivo* models. Currently, all available models to investigate genes in pancreatic β-cells *in vivo* have severe limitations. The

mouse lines express cre recombinase driven by the rat *insulin* promoter (*RIP*) in β-cells, but also show cre recombinase activity in the brain, e.g. in the hypothalamus (Wicksteed, Brissova et al. 2010). This region influences glucose homeostasis and might therefore confound β-cell specific knock-down effects, as shown previously (Nguyen, Tajmir et al. 2006; Kong, Tong et al. 2012). However, the unpublished mouse line expressing cre recombinase under the control of the mouse *insulin 1* promoter (*MIP-Cre*) expresses cre activity only in β-cells and might be useful in future studies to investigate the role of CADM1 in β-cells only (Wicksteed, Brissova et al. 2010).

Cadm1 deficient mice were shown to have enhanced glucagon release from pancreatic α-cells (Ito, Ichiyanagi et al. 2012). These data are similar to our observations that *Cadm1* deficient mice have enhanced insulin release from pancreatic β-cells. It is therefore possible that CADM1 influences hormone release from α- and β-cells through similar mechanisms. Early studies suggested that CADM1 influences hormone release similarly in α- and β-cell (Koma, Furuno et al. 2008). Insulin-mediated GABA signaling inhibits insulin secretion in an autocrine manner (1.1.1) as well as glucagon release from α-cells (Wendt, Birnir et al. 2004). In light of the function of CADM1 in binding to postsynaptic receptor signaling complexes (Hoy, Constable et al. 2009; Fujita, Tanabe et al. 2012) (1.3.1), CADM1 might stabilize GABAR complexes of pancreatic α- and β-cells **(Figure 41 (1))**. *Cadm1* deficiency would therefore decrease glucose-induced GABA signaling and subsequently increase insulin release from pancreatic β-cells and glucagon release from pancreatic α-cells.

Alternatively to a role of CADM1 in GABA signaling in β-cells, CADM1 might influence communication between autonomic nerves and β-cells in order to regulate insulin secretion. CADM1 is known to regulate neurotransmitter trafficking (1.3.1) and to be expressed in neuronal crest cells of pancreatic islets (Shimada, Tachibana et al. 2012) (1.3.2). Recent literature showed that neuronal crest cells differentiate into neuronal cells, such as autonomic nerves (Shimada, Tachibana et al. 2012). Therefore, CADM1 might positively regulate sympathic innervation **(Figure 41 (2))** or negatively regulate parasympathic innervation **(Figure 41 (3))** of pancreatic β-cells. In both cases, loss of

CADM1 would increase glucose-stimulated insulin secretion as observed in *Cadm1*KO mice. Likewise, a role of CADM1 in regulating autonomic innervation in the brain might be possible. Autonomic innervation of pancreatic β-cells is regulated by neurons of the ventromedial hypothalamus (VMH) (Tokunaga, Fukushima et al. 1986; Evans, McCrimmon et al. 2004; Osundiji, Lam et al. 2012). These neurons are sensitive to glucose and downstream signaling cascades of these neurons are dependent on GABA receptor signaling (Jetton, Liang et al. 1994; Chan, Lawson et al. 2007; Zhu, Czyzyk et al. 2010). In addition, reduced insulin signaling in the VMH impairs pancreatic insulin secretion (Paranjape, Chan et al. 2011). CADM1 is highly expressed in the brain (Biederer, Sara et al. 2002; Fujita, Urase et al. 2005) and influences GABA signaling (Fujita, Tanabe et al. 2012). Therefore, CADM1 might regulate GABA signaling from glucose sensitive neurons or neuronal insulin signaling in the VMH, as discussed above (4.3.1). Molecular mechanisms of CADM1 action in autonomic innervation or pancreatic islets might include presynaptic or postsynaptic mechanisms or regulation of synaptogenesis as explained above (4.3.5).

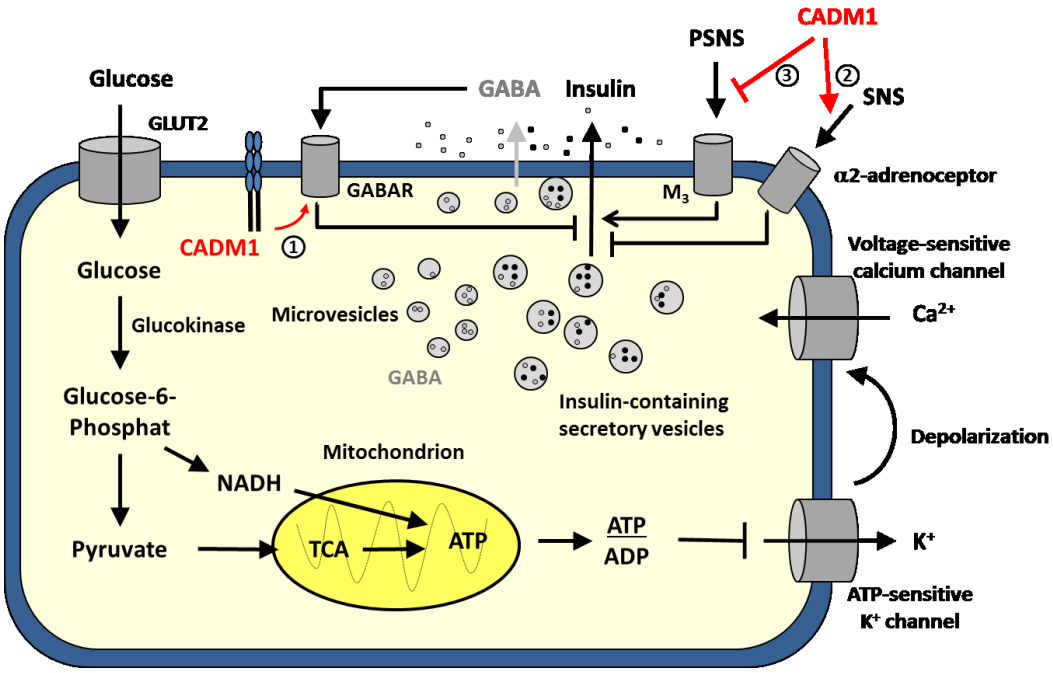

Figure 41: Postulated mechanisms of CADM1 inhibiting glucose-stimulated insulin secretion

Glucose is taken up by insulin-independent GLUT2 and metabolized to NADH and pyruvate through glycolysis. Pyruvate is fueled into the TCA cycle, generating $FADH_2$ and NADH. The electron transport chain in mitochondria converts NADH and $FADH_2$ to ATP, increasing cytosolic ATP/ADP ratio. Enhanced ATP/ADP ratio closes ATP sensitive K^+ channels, which depolarizes the membrane and opens voltage-gated Ca^{2+} channels. Increased cytosolic Ca^{2+} concentrations trigger docking of insulin-containing secretory vesicles and insulin release. Furthermore, GABA contained in secretory vesicles and synaptic like microvesicles is secreted similarly to insulin. Autocrine GABA signaling and sympathic innervation negatively regulate insulin secretion. Parasympathic innervation positively regulates insulin secretion. CADM1 might stabilize GABAR complexes **(1)**. Alternatively, CADM1 might positively influence sympathic innervation **(2)** or negatively influence parasympathic innervation **(3)**. In all cases, *Cadm1* deficiency would increase glucose-stimulated insulin secretion.

Abbreviations: Adenosine diphosphate (ADP); Adenosine-5'-triphosphate (ATP); γ-aminobutyric acid (GABA); γ-aminobutyric acid receptor (GABAR); Glucose transporter (GLUT2); Muscarinic cholinergic receptor 3 (M3); Nicotinamide adenine dinucleotide (NADH); Sympathetic nervous system (SNS); Parasympathetic nervous system (PSNS); Tricarboxylic acid cycle (TCA)

4.5 Alternative models of CADM1 influencing insulin sensitivity and energy homeostasis

4.5.1 CADM1 might regulate postnatal growth, energy homeostasis and insulin sensitivity by influencing autistic-like behavior

*Cadm1*KO mice showed reduced postnatal growth (Figure 9). It has been shown that increased insulin levels in the body increase postnatal body weight (Catlin, Cha et al. 1985), while lack of insulin signaling in the brain results in unchanged body weight of male mice (Bruning, Gautam et al. 2000). Increased neuronal insulin signaling, which likely contributes to increased locomotor activity and insulin sensitivity in *Cadm1*KO mice (4.3), is therefore most likely not responsible for postnatal growth deficiency. It can therefore be suggested that another mechanism causes postnatal growth deficiency in *Cadm1*KO mice.

The basis of the hypothesized role of CADM1 in neuronal insulin signaling was built on our data showing that IPSC frequency onto hypothalamic *Pomc*-expressing neurons is decreased in *Cadm1*KO mice (Figure 19). However, alterations of postsynaptic potentials do not have to be caused by signaling from presynaptic neurons but might be caused by neurons in other areas of the brain. Recent studies showed that electrical stimulation of the hippocampus directly induces synaptic changes in the thalamus (Tsanov, Vann et al. 2011). Other studies emphasized that changes in certain brain areas can induce synaptic alterations through alterations of the phenotype: Rodents that were sleep-deprived through lesions of the ventrolateral preoptic nucleus showed synaptic changes in the hippocampus (Arrigoni, Lu et al. 2009). Furthermore, rats, which were obesity-induced through insulin receptor reduction in the hypothalamus, developed synaptic alterations in the hippocampus (Grillo, Piroli et al. 2011). These studies indicate that synaptic changes in certain areas might be caused in other areas of the brain through direct neuronal connections or indirect phenotypical changes. It is therefore possible that alterations in IPSC frequency onto hypothalamic *Pomc*-expressing neurons in *Cadm1*KO mice are caused by CADM1 deficiency effects in other brain areas.

A function of CADM1 has been described in Purkinje cells of the cerebellum (Fujita, Tanabe et al. 2012; Fujita, Tanabe et al. 2012) (1.3.3). The loss of these cells is associated with ASD in humans (Ritvo, Freeman et al. 1986; Fatemi, Halt et al. 2002; Martin, Goldowitz et al. 2010; Tsai, Hull et al. 2012). The loss of Purkinje cells in ASD patients occurs during the final weeks of gestation in humans, a time corresponding to the second and third postnatal week in rodents (Whitney, Kemper et al. 2009). Therefore, *Cadm1* deficiency might reduce postnatal growth through inducing autistic-like behavior in the cerebellum. These alterations might further affect other regions of the brain.

In particular, loss of CADM1 in rodents or humans might destabilize postsynaptic GABBR2 complexes (Fujita, Tanabe et al. 2012) **(Figure 42)**. The destabilization of the GABBR2 complex might lead to loss of cerebellar Purkinje cells. Alternatively, CADM1 might attach cerebellar Purkinje cells to other surrounding cell types, such as astrocytes. CADM1 expression in astrocytes has been confirmed before (Sandau, Mungenast et al. 2011; Sandau, Mungenast et al. 2011). Loss of CADM1 expression might destabilize Purkinje cells number and result in decreased cell number and alterations in GABA signaling. Lastly, loss of Purkinje cells and altered cerebellar GABA signaling might be independent consequences of loss of CADM1 expression and one or both events contribute to the occurrence of autism-like behavior.

4.5.1.1 Role of repetitive behavior in insulin sensitivity of *Cadm1* deficient mice

Our experiments showed increased locomotor activity in male *Cadm1*KO mice (Figure 14) and increased food-seeking behavior in female *Cadm1*KO mice (Figure 12). One clinical criterion for the diagnostic auf autism in humans is restricted, repetitive behavior (American Psychiatric Association 2011). Murine models of autism show increased repetitive behaviors, hyperactivity and increased food-seeking behavior (Martin, Goldowitz et al. 2010; Tsai, Hull et al. 2012). Increased locomotor activity is known to induce increased insulin sensitivity directly through induction of glucose uptake in

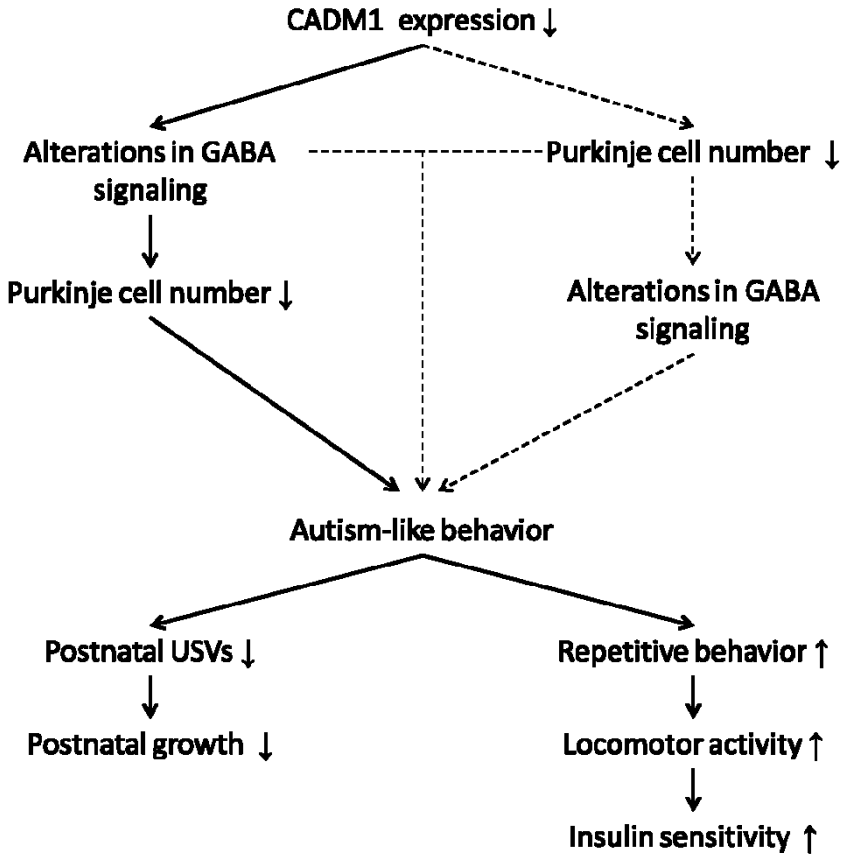

Figure 42: Postulated mechanism of loss of CADM1 expression influencing insulin sensitivity and postnatal growth through induction of autistic-like behavior

Loss of CADM1 protein expression destabilizes Mupp1–GABBR2 complex and might lead to altered GABA signaling (left). Altered GABA signaling might decrease Purkinje cell number in the cerebellum, which is associated with autistic-like behavior. Alternatively, loss of CADM1 as cell adhesion molecule between Purkinje cells and other cell types might decrease Purkinje cell number and lead to alterations in GABA signaling and subsequent induction of autism-like behavior (right). Also loss of Purkinje cell number or alterations in GABA or both as consequence of loss of CADM1 might directly induce autistic-like behavior (middle). Autism-like behavior, such as decreased USVs, reduces caretaking behavior from the mother, leading to malnutrition and impaired postnatal growth in *Cadm1*KO pups (lower left). Autism-like behavior, such as repetitive behavior, increases locomotor activity and subsequent insulin sensitivity (lower right). Dashed lines show alternative mechanisms.

Abbreviations: Ultrasonic vocalizations (USVs); γ-aminobutyric acid (GABA)

Figure based on data from (Fujita, Tanabe et al. 2012; Fujita, Tanabe et al. 2012).

skeletal muscle and indirectly through reduction of body fat content (4.2.2). Loss of *Cadm1* expression in *Cadm1*KO mice might therefore induce autistic-like behavior and subsequently increased locomotor activity **(Figure 42)**. Increased locomotor activity might increase insulin sensitivity through enhanced glucose uptake or changes in body composition or both.

Of note, female *Cadm1*KO mice did not show changes in locomotor activity despite increased insulin sensitivity (Figure 15, Figure 16). A higher prevalence for autistic-like behavior was reported in male humans and mice (Yeargin-Allsopp, Rice et al. 2003; Stack, Lim et al. 2008; Guariglia, Jenkins et al. 2011; 2012). In humans, a higher occurrence of repetitive behavior was reported in males compared to females with ASD (May, Cornish et al. 2012). It is therefore possible that female *Cadm1*KO mice show less autistic-like behavior, such as repetitive behavior, compared to male *Cadm1*KO mice. The increased insulin sensitivity of female *Cadm1*KO mice might be a consequence of the above discussed hypothesized mechanism of CADM1 influencing neuronal insulin signaling (4.3).

4.5.1.2 Postnatal growth deficiency might be caused by reduced ultrasonic vocalizations in *Cadm1* deficient mice

Our data showed that *Cadm1*KO mice exhibit impairments of body weight gain during postnatal development (Figure 9). Adult *Cadm1*KO mice showed decreased body length (Figure 9). This was also observed in other *Cadm1* deficient mice in recent studies (Fujita, Tanabe et al. 2012), confirming our findings. In these studies, *Cadm1* deficient mice were identified to have severely decreased postnatal USVs, which was suggested to be similar to impairment of language in autistic human patients (Fujita, Tanabe et al. 2012). USVs are important for the communication between pup and mother during the first two weeks of life and evokes caretaking behavior (Branchi, Santucci et al. 2001). An impairment of postnatal USVs might reduce caretaking behavior from the mother and lead to undernourishment and decreased growth of *Cadm1*KO pups. Reduced postnatal

growth due to reduced USVs might be the first manifesting phenotype of autistic-like behavior in *Cadm1*KO mice **(Figure 42)**. Since USVs decrease naturally two weeks after birth in mice (Branchi, Santucci et al. 2001), the deficiency to produce USVs might not affect the feeding of *Cadm1*KO mice later on.

4.5.2 Effects of CADM1 on growth hormone signaling

The reduced postnatal growth and increased insulin sensitivity of *Cadm1*KO mice might imply that *Cadm1* deletion impairs GH signaling. This is however unlikely as we discuss in the following. Growth retardation and altered glucose homeostasis can be found in mouse models with defective GH signaling due to mutations in *Gh* or *growth hormone receptor* (*Ghr*). Mice with defective GH signaling exhibit a smaller increase in body weight during their first four weeks of life and similar growth speed compared to control mice after 6 weeks of life (Meyer, Korthaus et al. 2004). Furthermore, increased insulin sensitivity (Liu, Coschigano et al. 2004), reduced IGF-1 levels (Donahue and Beamer 1993; Meyer, Korthaus et al. 2004) and unchanged absolute food intake (Coschigano, Holland et al. 2003) are phenotypical characteristics of these mice. These data show similarities to our observations in *Cadm1*KO mice. However, mice and humans with dysfunctional GH signaling suffer from obesity (Donahue and Beamer 1993; Roemmich, Huerta et al. 2001; Li, Knapp et al. 2003; Meyer, Korthaus et al. 2004). Complete absence of GH signaling is likely to cause obesity, reflecting the lack of lipolytic effects of GH on adipocytes (LeRoith and Yakar 2007). However, in our studies male *Cadm1*KO mice showed decreased and female *Cadm1*KO mice showed unchanged relative body fat content (Figure 10). Thus, *Cadm1*KO mice do not suffer from obesity more than control mice, suggesting that GH signaling is not impaired in these animals. Furthermore, *Cadm1*KO mice display normal *Ghrh, Gh* and *Ghr* expression and respond normally to a GH release challenge (Figure 20), suggesting that synthesis and release of GH is not impaired in *Cadm1*KO mice. It can therefore be suggested that *Cadm1* deficient mice are not deficient in GH or GH signaling and changes in insulin sensitivity and postnatal growth in these mice cannot be explained by changes in GH signaling.

4.6 Conclusions and perspectives

Type 2 diabetes has become a world-wide pandemic disease. The disease is characterized by resistance to insulin, largely caused by overweight and obesity, and subsequent hyperglycemia. Failure of pancreatic β-cells to meet increased insulin demands dramatically increases blood glucose levels and marks the onset of type 2 diabetes.

MiR-375 is the highest expressed miRNA of the pancreas. This miRNA regulates β-cell growth and insulin secretion and was suggested to influence the development of type 2 diabetes. Genes regulated by miR-375 had been identified but their role in the function of this miRNA in pancreatic islets had not been established. Therefore, we studied the role of the miR-375 target *Cadm1* initially in pancreatic β-cells in order to investigate a possible role of CADM1 in growth and function of β-cells. These initial studies also showed increased insulin sensitivity and reduced body weight in *Cadm1*KO mice. Since body weight is a major determent for insulin sensitivity and therefore for the pathogenesis of type 2 diabetes, we also investigated the influence of CADM1 on energy homeostasis.

The initial analyses of glucose homeostasis revealed an increased glucose-stimulated insulin secretion of *Cadm1*KO mice compared to control mice. *In vitro* cell culture data confirmed enhanced glucose-stimulated insulin secretion after *Cadm1* depletion. Furthermore, male *Cadm1*KO mice exhibited increased locomotor activity, reduced body fat content and improved insulin sensitivity after diet and genetic-induced obesity. *Cadm1*KO females showed improved insulin sensitivity, unchanged locomotor activity and body fat content. *Cadm1*KO mice of both genders exhibited reduced postnatal growth and unchanged body weight gain after four weeks of age. Mice deficient for *Cadm1* in neuronal and glia cells confirmed the phenotypical changes in insulin sensitivity, body fat content and body weight.

Our data suggest that deletion of *Cadm1* in mice increases locomotor activity, which reduces body fat content. Reduced body fat content improves insulin sensitivity and

decreases leptin levels in *Cadm1*KO mice. Body weight gain seems to be balanced by enhanced food intake in *Cadm1* deficient mice. We further hypothesized that CADM1 regulates neuronal insulin signaling, which influences insulin sensitivity and locomotor activity. The basis of this postulated mechanism was built on our data showing that IPSC frequency onto hypothalamic *Pomc*-expressing neurons is decreased in *Cadm1*KO mice. CADM1 is hypothesized to be a possible mediator of neurotransmitter signaling between hypothalamic *Agrp*-expressing neurons and second-order neurons and between *Agrp*-expressing neurons and *Pomc*-expressing neurons. The result of this influence would be a decreased HGP, resulting in improved insulin sensitivity, and increased locomotor activity in *Cadm1* deficient mice. An alternative postulated mechanism is based on the role of CADM1 in autism. CADM1 has been linked to the induction of autistic-like behavior before. We hypothesize that increased repetitive behavior, typical for autistic-like behavior, increases locomotor activity and subsequently reduces body fat content and increases insulin sensitivity. Decreased postnatal USVs might lead to impaired caretaking behavior of the mother and cause impaired postnatal growth of *Cadm1*KO mice. However, changes in energy and glucose homeostasis and postnatal growth of *Cadm1* deficient mice cannot be explained by only one of the two mechanisms. We therefore postulate that both mechanisms might be relevant in *Cadm1* deficient mice.

In future studies, the role of the two postulated mechanisms in energy and glucose homeostasis of *Cadm1* deficient mice should be investigated. Euglycemic-hyperinsulinemic clamp studies, as previously used (Konner, Janoschek et al. 2007), can uncover the contribution of each tissue in insulin-mediated glucose uptake. Increased insulin signaling in *Agrp*-expressing neurons results in increased HGP (Konner, Janoschek et al. 2007; Lin, Plum et al. 2010). Acute and chronic exercise is known to enhance insulin-mediated glucose uptake in skeletal muscle (Nuutila, Knuuti et al. 1994; Hardin, Azzarelli et al. 1995; Thorell, Hirshman et al. 1999; Frosig, Roepstorff et al. 2009). Therefore, euglycemic-hyperinsulinemic studies would help to elucidate whether increased insulin sensitivity in *Cadm1*KO mice is caused by enhanced locomotor activity or increased neuronal signaling or both.

In addition, investigations of mice with deletions of *Cadm1* in restricted areas of the brain might help to identify mechanisms of the CADM1 actions. For this purpose, mice carrying a conditional *Cadm1* allele could be crossed to mice carrying a cre-expressing gene under the control of promoters, such as the *PCP-2* promoter. This promoter restricts cre expression to Purkinje cells in the cerebellum and bipolar neurons in the retina (Barski, Dethleffsen et al. 2000). This cre line was used before to identify Purkinje cells of the cerebellum as responsible region for autistic-like behavior caused by mutations in tuberous sclerosis complex (Weber, Egelhoff et al. 2000; Reith, McKenna et al. 2012). A mouse line with deletion of *Cadm1* in cerebellar Purkinje cells might therefore help to elucidate whether the observed changes in glucose and energy homeostasis of *Cadm1*KO mice are caused by *Cadm1* deletion in cerebellar Purkinje cells. Similarities in the phenotype of *Cadm1*KO mice and mice with Purkinje cells-restricted *Cadm1* deletion might suggest that mutation in *Cadm1* cause autistic-like behavior and the observed changes in glucose and energy homeostasis. Similar, mice with *Cadm1* deletions in *Pomc*- or *Agrp/Npy*-expressing or both might help to understand whether CADM1 has a functional role in these neurons. Initial studies with mice carrying a conditional *Cadm1* allele and an allele with cre expression under the control of the *Pomc* promoter (Balthasar, Coppari et al. 2004) did not show changes in body weight, food intake, glucose or insulin sensitivity (own data, data not shown). However, mice with *Cadm1* deletion in *Agrp/Npy*-expressing neurons (Tong, Ye et al. 2008) have not been investigated in depth but might help to understand whether *Cadm1* expression in these neurons plays a role in energy and glucose homeostasis. In addition, we hypothesized that CADM1 might facilitate neurotransmitter trafficking between *Npy*-expressing neurons and second-order neurons and *Npy*-expressing neurons and *Pomc*-expressing neurons (4.3). Since CADM1 also binds to CADM2 (Fogel, Akins et al. 2007), deletion of *Cadm1* on pre- and postsynaptic membranes might be necessary to cause similar phenotypical changes like in *Cadm1*KO mice. Therefore, analyses of mice with *Cadm1* deletions in *Npy*-expressing neurons and *Pomc*-expressing neurons should be included. Of note, CADM1 expression has also been confirmed in non-neuronal cells of the brains, such as glia and granule cells (Thomas, Akins et al.

2008). Since deletion of *Cadm1* in these cell types might be necessary for the full induction of changes in glucose and energy homeostasis, region specific knock-down of *Cadm1*, such as virus-mediated knockdown (Garza, Kim et al. 2008), should be used. Specific knock-down of *Cadm1* in the hypothalamus or cerebellum might help to decide on the contribution of the two postulated mechanisms.

Besides the investigation whether CADM1 might regulate neuronal insulin signaling or influence autistic-like behavior or both, the function of CADM1 in pancreatic β-cells should be investigated in future studies. These studies could include mouse models to elucidate whether CADM1 regulates glucose-mediated insulin secretion directly in β-cells or indirectly by influencing autonomic islet innervation or both as discussed before (4.4). Insulin secretion experiments in mice with *Cadm1* deficiency in pancreatic β-cells (*Cadm1MIPCre*KO) might help to investigate if CADM1 regulates insulin secretion directly in β-cells. Insulin secretion studies in mice with *Cadm1* deletion in neuronal and glia cells might identify an indirect regulation of insulin secretion by CADM1. The deletion of *Cadm1* in neuronal and glia cells is driven by the promoter of the *nestin* gene. Expression of *nestin* was confirmed in early neural crest cells (Lothian and Lendahl 1997), suggesting that neural crest cells of pancreatic islets express *nestin* during development. Pancreatic neural crest cells of *Cadm1NesCre*KO mice are therefore expected to be *Cadm1* deficient. Insulin secretion experiments with these mice would help to understand whether neural crest cells or other *nestin* expressing cells in the CNS contribute to enhanced glucose-stimulated insulin secretion of *Cadm1*KO mice. Furthermore, pharmacologic manipulations of the autonomic system can further establish a possible role of CADM1 in influencing β-cells through the autonomic nervous system and whether CADM1 influences the SNS or PSNS or both.

In addition to the investigation of the putative role of CADM1 in the brain and pancreatic islets, future studies could elucidate the role of possible interaction partners of CADM1. These interaction partners might include MINT1, which was shown to bind to CADM1 (Biederer, Sara et al. 2002) (1.3.1). *Mint1*KO mice show, similar to *Cadm1*KO mice, decreased postnatal growth and alterations in behavior and synaptic GABA

trafficking (Mori, Okuyama et al. 2002; Ho, Morishita et al. 2003). Studies of the energy and glucose homeostasis of *Mint1*KO mice might help to understand whether the molecular mechanism of CADM1 action includes binding to the VELI-CASK-MINT1 complex as discussed before (4.3.5).

Finally, the role of CADM1 pancreatic insulin secretion and whole body insulin sensitivity in the pathogenesis of type 2 diabetes should be investigated. For this purpose, *Cadm1* deficient mice could be crossed to diabetic murine models, such *ob/ob* or *db/db* mice on the C57BL/KsJ-background (Coleman 1978). These data would help to understand whether CADM1 as a regulator of energy and glucose homeostasis contributes to the development of type 2 diabetes.

References

Aguirre, V., T. Uchida, et al. (2000). "The c-Jun NH(2)-terminal kinase promotes insulin resistance during association with insulin receptor substrate-1 and phosphorylation of Ser(307)." J Biol Chem **275**(12): 9047-9054.

Alessi, D. R., M. Andjelkovic, et al. (1996). "Mechanism of activation of protein kinase B by insulin and IGF-1." EMBO J **15**(23): 6541-6551.

Altshuler, D., J. N. Hirschhorn, et al. (2000). "The common PPARgamma Pro12Ala polymorphism is associated with decreased risk of type 2 diabetes." Nat Genet **26**(1): 76-80.

American Psychiatric Association (2011). Diagnostic and Statistical Manual of Mental Disorders (DSM) 5. A 05 Autism Spectrum Disorder, American Psychiatric Association.

Anderson, K. E., J. Coadwell, et al. (1998). "Translocation of PDK-1 to the plasma membrane is important in allowing PDK-1 to activate protein kinase B." Curr Biol **8**(12): 684-691.

Angulo, P. and K. D. Lindor (2002). "Non-alcoholic fatty liver disease." J Gastroenterol Hepatol **17 Suppl**: S186-190.

Araki, E., M. A. Lipes, et al. (1994). "Alternative pathway of insulin signalling in mice with targeted disruption of the IRS-1 gene." Nature **372**(6502): 186-190.

Araki, E., X. J. Sun, et al. (1993). "Human skeletal muscle insulin receptor substrate-1. Characterization of the cDNA, gene, and chromosomal localization." Diabetes **42**(7): 1041-1054.

Arrigoni, E., J. Lu, et al. (2009). "Long-term synaptic plasticity is impaired in rats with lesions of the ventrolateral preoptic nucleus." Eur J Neurosci **30**(11): 2112-2120.

Ashby, J. P. and R. N. Speake (1975). "Insulin and glucagon secretion from isolated islets of Langerhans. The effects of calcium ionophores." Biochem J **150**(1): 89-96.

Ashcroft, F. M. and P. Rorsman (2012). "Diabetes mellitus and the beta cell: the last ten years." Cell **148**(6): 1160-1171.

Autism and Developmental Disabilities Monitoring Network (2012). "Prevalence of autism spectrum disorders--Autism and Developmental Disabilities Monitoring Network, 14 sites, United States, 2008." MMWR Surveill Summ **61**(3): 1-19.

Backer, J. M., M. G. Myers, Jr., et al. (1992). "Phosphatidylinositol 3'-kinase is activated by association with IRS-1 during insulin stimulation." EMBO J **11**(9): 3469-3479.

Baile, C. A. and M. A. Della-Fera (1985). "Central nervous system cholecystokinin and the control of feeding." Ann N Y Acad Sci **448**: 424-430.

Balasubramanian, S., S. R. Fam, et al. (2007). "GABAB receptor association with the PDZ scaffold Mupp1 alters receptor stability and function." J Biol Chem **282**(6): 4162-4171.

Balthasar, N., R. Coppari, et al. (2004). "Leptin receptor signaling in POMC neurons is required for normal body weight homeostasis." Neuron **42**(6): 983-991.

Balthasar, N., L. T. Dalgaard, et al. (2005). "Divergence of melanocortin pathways in the control of food intake and energy expenditure." Cell **123**(3): 493-505.

Banerji, M. A., N. Faridi, et al. (1999). "Body composition, visceral fat, leptin, and insulin resistance in Asian Indian men." J Clin Endocrinol Metab **84**(1): 137-144.

Barski, J. J., K. Dethleffsen, et al. (2000). "Cre recombinase expression in cerebellar Purkinje cells." Genesis **28**(3-4): 93-98.

Bartel, D. P. (2004). "MicroRNAs: genomics, biogenesis, mechanism, and function." Cell **116**(2): 281-297.

Barzilai, N., J. Wang, et al. (1997). "Leptin selectively decreases visceral adiposity and enhances insulin action." J Clin Invest **100**(12): 3105-3110.

Bastard, J. P., M. Maachi, et al. (2002). "Adipose tissue IL-6 content correlates with resistance to insulin activation of glucose uptake both in vivo and in vitro." J Clin Endocrinol Metab **87**(5): 2084-2089.

Baumann, H., K. K. Morella, et al. (1996). "The full-length leptin receptor has signaling capabilities of interleukin 6-type cytokine receptors." Proc Natl Acad Sci U S A **93**(16): 8374-8378.

Belgardt, B. F., J. Mauer, et al. (2010). "Hypothalamic and pituitary c-Jun N-terminal kinase 1 signaling coordinately regulates glucose metabolism." Proc Natl Acad Sci U S A **107**(13): 6028-6033.

Bell, G. I., J. C. Murray, et al. (1989). "Polymorphic human insulin-responsive glucose-transporter gene on chromosome 17p13." Diabetes **38**(8): 1072-1075.

Benoit, S. C., E. L. Air, et al. (2002). "The catabolic action of insulin in the brain is mediated by melanocortins." J Neurosci **22**(20): 9048-9052.

Berthoud, H. R. (2002). "Multiple neural systems controlling food intake and body weight." Neurosci Biobehav Rev **26**(4): 393-428.

Biederer, T. (2006). "Bioinformatic characterization of the SynCAM family of immunoglobulin-like domain-containing adhesion molecules." Genomics **87**(1): 139-150.

Biederer, T., Y. Sara, et al. (2002). "SynCAM, a synaptic adhesion molecule that drives synapse assembly." Science **297**(5586): 1525-1531.

Biederer, T. and T. C. Sudhof (2000). "Mints as adaptors. Direct binding to neurexins and recruitment of munc18." J Biol Chem **275**(51): 39803-39806.

Biesalski, H.-K. (2004). Ernährungsmedizin.

Biesalski, H. K. and P. Grimm (2002). "Taschenatlas der Ernährung." Thieme Verlag **2. aktualis. Aufl.**

Birkenfeld, A. L., H. Y. Lee, et al. (2011). "Deletion of the Mammalian INDY Homolog Mimics Aspects of Dietary Restriction and Protects against Adiposity and Insulin Resistance in Mice." Cell Metab **14**(2): 184-195.

Birnberg, N. C., J. C. Lissitzky, et al. (1983). "Glucocorticoids regulate proopiomelanocortin gene expression in vivo at the levels of transcription and secretion." Proc Natl Acad Sci U S A **80**(22): 6982-6986.

Bjorbaek, C., K. El-Haschimi, et al. (1999). "The role of SOCS-3 in leptin signaling and leptin resistance." J Biol Chem **274**(42): 30059-30065.

Bjorbak, C., H. J. Lavery, et al. (2000). "SOCS3 mediates feedback inhibition of the leptin receptor via Tyr985." J Biol Chem **275**(51): 40649-40657.

Bjornholm, M., A. R. He, et al. (2002). "Absence of functional insulin receptor substrate-3 (IRS-3) gene in humans." Diabetologia **45**(12): 1697-1702.

Bluher, M., M. D. Michael, et al. (2002). "Adipose tissue selective insulin receptor knockout protects against obesity and obesity-related glucose intolerance." Dev Cell **3**(1): 25-38.

Boles, K. S., W. Barchet, et al. (2005). "The tumor suppressor TSLC1/NECL-2 triggers NK-cell and CD8+ T-cell responses through the cell-surface receptor CRTAM." Blood **106**(3): 779-786.

Boni-Schnetzler, M., J. B. Rubin, et al. (1986). "Structural requirements for the transmembrane activation of the insulin receptor kinase." J Biol Chem **261**(32): 15281-15287.

Bonnefond, A., P. Froguel, et al. (2010). "The emerging genetics of type 2 diabetes." Trends Mol Med **16**(9): 407-416.

Bonni, A., A. Brunet, et al. (1999). "Cell survival promoted by the Ras-MAPK signaling pathway by transcription-dependent and -independent mechanisms." Science **286**(5443): 1358-1362.

Bork, P., L. Holm, et al. (1994). "The immunoglobulin fold. Structural classification, sequence patterns and common core." J Mol Biol **242**(4): 309-320.

Boucher, J. (2012). "Research review: structural language in autistic spectrum disorder - characteristics and causes." J Child Psychol Psychiatry **53**(3): 219-233.

Branchi, I., D. Santucci, et al. (2001). "Ultrasonic vocalisation emitted by infant rodents: a tool for assessment of neurobehavioural development." Behav Brain Res **125**(1-2): 49-56.

Braun, M., A. Wendt, et al. (2004). "GABAB receptor activation inhibits exocytosis in rat pancreatic beta-cells by G-protein-dependent activation of calcineurin." J Physiol **559**(Pt 2): 397-409.

Brobeck, J. R. (1946). "Mechanism of the development of obesity in animals with hypothalamic lesions." Physiol Rev **26**(4): 541-559.

Bruning, J. C., D. Gautam, et al. (2000). "Role of brain insulin receptor in control of body weight and reproduction." Science **289**(5487): 2122-2125.

Bruning, J. C., M. D. Michael, et al. (1998). "A muscle-specific insulin receptor knockout exhibits features of the metabolic syndrome of NIDDM without altering glucose tolerance." Mol Cell **2**(5): 559-569.

Bruss, M. D., E. B. Arias, et al. (2005). "Increased phosphorylation of Akt substrate of 160 kDa (AS160) in rat skeletal muscle in response to insulin or contractile activity." Diabetes **54**(1): 41-50.

Butler, A. A. and L. P. Kozak (2010). "A recurring problem with the analysis of energy expenditure in genetic models expressing lean and obese phenotypes." Diabetes **59**(2): 323-329.

Butler, A. E., J. Janson, et al. (2003). "Beta-cell deficit and increased beta-cell apoptosis in humans with type 2 diabetes." Diabetes **52**(1): 102-110.

Cai, D., S. Dhe-Paganon, et al. (2003). "Two new substrates in insulin signaling, IRS5/DOK4 and IRS6/DOK5." J Biol Chem **278**(28): 25323-25330.

Cai, D., M. Yuan, et al. (2005). "Local and systemic insulin resistance resulting from hepatic activation of IKK-beta and NF-kappaB." Nat Med **11**(2): 183-190.

Calegari, V. C., A. S. Torsoni, et al. (2011). "Inflammation of the hypothalamus leads to defective pancreatic islet function." J Biol Chem **286**(15): 12870-12880.

Cali, A. M., C. D. Man, et al. (2009). "Primary defects in beta-cell function further exacerbated by worsening of insulin resistance mark the development of impaired glucose tolerance in obese adolescents." Diabetes Care **32**(3): 456-461.

Campfield, L. A., F. J. Smith, et al. (1995). "Recombinant mouse OB protein: evidence for a peripheral signal linking adiposity and central neural networks." Science **269**(5223): 546-549.

Carey, D. G., A. B. Jenkins, et al. (1996). "Abdominal fat and insulin resistance in normal and overweight women: Direct measurements reveal a strong relationship in subjects at both low and high risk of NIDDM." Diabetes **45**(5): 633-638.

Catlin, E. A., C. J. Cha, et al. (1985). "Postnatal growth and fatty acid synthesis in overgrown rat pups induced by fetal hyperinsulinemia." Metabolism **34**(12): 1110-1114.

Chaithongdi, N., J. S. Subauste, et al. (2011). "Diagnosis and management of hyperglycemic emergencies." Hormones (Athens) **10**(4): 250-260.

Chan, O., M. Lawson, et al. (2007). "ATP-sensitive K(+) channels regulate the release of GABA in the ventromedial hypothalamus during hypoglycemia." Diabetes **56**(4): 1120-1126.

Cheadle, L. and T. Biederer (2012). "The novel synaptogenic protein Farp1 links postsynaptic cytoskeletal dynamics and transsynaptic organization." J Cell Biol.

Chen, C., H. Hosokawa, et al. (1994). "Mechanism of compensatory hyperinsulinemia in normoglycemic insulin-resistant spontaneously hypertensive rats. Augmented enzymatic activity of glucokinase in beta-cells." J Clin Invest **94**(1): 399-404.

Cho, H., J. Mu, et al. (2001). "Insulin resistance and a diabetes mellitus-like syndrome in mice lacking the protein kinase Akt2 (PKB beta)." Science **292**(5522): 1728-1731.

Cho, H., J. L. Thorvaldsen, et al. (2001). "Akt1/PKBalpha is required for normal growth but dispensable for maintenance of glucose homeostasis in mice." J Biol Chem **276**(42): 38349-38352.

Choi, S. J., Z. Yablonka-Reuveni, et al. (2011). "Increased Energy Expenditure and Leptin Sensitivity Account for Low Fat Mass in Myostatin Deficient Mice." Am J Physiol Endocrinol Metab.

Cobb, M. H., B. C. Sang, et al. (1989). "Autophosphorylation activates the soluble cytoplasmic domain of the insulin receptor in an intermolecular reaction." J Biol Chem **264**(31): 18701-18706.

Coleman, D. L. (1978). "Obese and diabetes: two mutant genes causing diabetes-obesity syndromes in mice." Diabetologia **14**(3): 141-148.

Conaway, H. H., M. A. Griffey, et al. (1975). "Characterization of acetylcholine-induced insulin secretion in the isolated perfused dog pancreas." Proc Soc Exp Biol Med **150**(2): 308-312.

Consoli, A., N. Nurjhan, et al. (1989). "Predominant role of gluconeogenesis in increased hepatic glucose production in NIDDM." Diabetes **38**(5): 550-557.

Cook, D. L. and C. N. Hales (1984). "Intracellular ATP directly blocks K+ channels in pancreatic B-cells." Nature **311**(5983): 271-273.

Coschigano, K. T., A. N. Holland, et al. (2003). "Deletion, but not antagonism, of the mouse growth hormone receptor results in severely decreased body weights, insulin, and insulin-like growth factor I levels and increased life span." Endocrinology **144**(9): 3799-3810.

Couturier, C. and R. Jockers (2003). "Activation of the leptin receptor by a ligand-induced conformational change of constitutive receptor dimers." J Biol Chem **278**(29): 26604-26611.

Cowley, M. A., J. L. Smart, et al. (2001). "Leptin activates anorexigenic POMC neurons through a neural network in the arcuate nucleus." Nature **411**(6836): 480-484.

Cross, D. A., D. R. Alessi, et al. (1995). "Inhibition of glycogen synthase kinase-3 by insulin mediated by protein kinase B." Nature **378**(6559): 785-789.

Cusi, K., K. Maezono, et al. (2000). "Insulin resistance differentially affects the PI 3-kinase- and MAP kinase-mediated signaling in human muscle." J Clin Invest **105**(3): 311-320.

Davies, P. S., J. Gregory, et al. (1995). "Physical activity and body fatness in pre-school children." Int J Obes Relat Metab Disord **19**(1): 6-10.

de Alvaro, C., T. Teruel, et al. (2004). "Tumor necrosis factor alpha produces insulin resistance in skeletal muscle by activation of inhibitor kappaB kinase in a p38 MAPK-dependent manner." J Biol Chem **279**(17): 17070-17078.

de Leeuw van Weenen, J. E., E. T. Parlevliet, et al. (2011). "Pharmacological modulation of dopamine receptor D2-mediated transmission alters the metabolic phenotype of diet induced obese and diet resistant C57Bl6 mice." Exp Diabetes Res **2011**: 928523.

De Souza, C. T., E. P. Araujo, et al. (2005). "Consumption of a fat-rich diet activates a proinflammatory response and induces insulin resistance in the hypothalamus." Endocrinology **146**(10): 4192-4199.

De Vos, A., H. Heimberg, et al. (1995). "Human and rat beta cells differ in glucose transporter but not in glucokinase gene expression." J Clin Invest **96**(5): 2489-2495.

DeFalco, J., M. Tomishima, et al. (2001). "Virus-assisted mapping of neural inputs to a feeding center in the hypothalamus." Science **291**(5513): 2608-2613.

DeFronzo, R. A., R. Gunnarsson, et al. (1985). "Effects of insulin on peripheral and splanchnic glucose metabolism in noninsulin-dependent (type II) diabetes mellitus." J Clin Invest **76**(1): 149-155.

Devos, R., Y. Guisez, et al. (1997). "Ligand-independent dimerization of the extracellular domain of the leptin receptor and determination of the stoichiometry of leptin binding." J Biol Chem **272**(29): 18304-18310.

Dhindsa, S., M. G. Miller, et al. (2010). "Testosterone concentrations in diabetic and nondiabetic obese men." Diabetes Care **33**(6): 1186-1192.

Dobbins, R. L., M. W. Chester, et al. (1998). "A fatty acid- dependent step is critically important for both glucose- and non-glucose-stimulated insulin secretion." J Clin Invest **101**(11): 2370-2376.

Dominici, F. P. and D. Turyn (2002). "Growth hormone-induced alterations in the insulin-signaling system." Exp Biol Med (Maywood) **227**(3): 149-157.

Donahue, L. R. and W. G. Beamer (1993). "Growth hormone deficiency in 'little' mice results in aberrant body composition, reduced insulin-like growth factor-I and insulin-like growth factor-binding protein-3 (IGFBP-3), but does not affect IGFBP-2, -1 or -4." J Endocrinol **136**(1): 91-104.

Dong, H., M. Kumar, et al. (2006). "Gamma-aminobutyric acid up- and downregulates insulin secretion from beta cells in concert with changes in glucose concentration." Diabetologia **49**(4): 697-705.

Donner, D. B. and K. Yonkers (1983). "Hormone-induced conformational changes in the hepatic insulin receptor." J Biol Chem **258**(15): 9413-9418.

Dukes, I. D., M. S. McIntyre, et al. (1994). "Dependence on NADH produced during glycolysis for beta-cell glucose signaling." J Biol Chem **269**(15): 10979-10982.

Easton, R. M., H. Cho, et al. (2005). "Role for Akt3/protein kinase Bgamma in attainment of normal brain size." Mol Cell Biol **25**(5): 1869-1878.

El Ouaamari, A., N. Baroukh, et al. (2008). "miR-375 targets 3'-phosphoinositide-dependent protein kinase-1 and regulates glucose-induced biological responses in pancreatic beta-cells." Diabetes **57**(10): 2708-2717.

Emanuelli, B., P. Peraldi, et al. (2001). "SOCS-3 inhibits insulin signaling and is up-regulated in response to tumor necrosis factor-alpha in the adipose tissue of obese mice." J Biol Chem **276**(51): 47944-47949.

Ender, C., A. Krek, et al. (2008). "A human snoRNA with microRNA-like functions." Mol Cell **32**(4): 519-528.

Ernst, M. B., C. M. Wunderlich, et al. (2009). "Enhanced Stat3 activation in POMC neurons provokes negative feedback inhibition of leptin and insulin signaling in obesity." J Neurosci **29**(37): 11582-11593.

Evans, M. L., R. J. McCrimmon, et al. (2004). "Hypothalamic ATP-sensitive K + channels play a key role in sensing hypoglycemia and triggering counterregulatory epinephrine and glucagon responses." Diabetes **53**(10): 2542-2551.

Fabbrini, E., F. Magkos, et al. (2009). "Intrahepatic fat, not visceral fat, is linked with metabolic complications of obesity." Proc Natl Acad Sci U S A **106**(36): 15430-15435.

Fatemi, S. H., T. D. Folsom, et al. (2009). "Expression of GABA(B) receptors is altered in brains of subjects with autism." Cerebellum **8**(1): 64-69.

Fatemi, S. H., A. R. Halt, et al. (2002). "Purkinje cell size is reduced in cerebellum of patients with autism." Cell Mol Neurobiol **22**(2): 171-175.

Felig, P., J. Wahren, et al. (1976). "Insulin, glucagon, and somatostatin in normal physiology and diabetes mellitus." Diabetes **25**(12): 1091-1099.

Figlewicz, D. P., L. J. Stein, et al. (1985). "Acute and chronic gastrin-releasing peptide decreases food intake in baboons." Am J Physiol **248**(5 Pt 2): R578-583.

Fogel, A. I., M. R. Akins, et al. (2007). "SynCAMs organize synapses through heterophilic adhesion." J Neurosci **27**(46): 12516-12530.

Fogel, A. I., M. Stagi, et al. (2011). "Lateral assembly of the immunoglobulin protein SynCAM 1 controls its adhesive function and instructs synapse formation." EMBO J.

Foretz, M., C. Pacot, et al. (1999). "ADD1/SREBP-1c is required in the activation of hepatic lipogenic gene expression by glucose." Mol Cell Biol **19**(5): 3760-3768.

Frayling, T. M., N. J. Timpson, et al. (2007). "A common variant in the FTO gene is associated with body mass index and predisposes to childhood and adult obesity." Science **316**(5826): 889-894.

Freychet, P., J. Roth, et al. (1971). "Insulin receptors in the liver: specific binding of (125 I)insulin to the plasma membrane and its relation to insulin bioactivity." Proc Natl Acad Sci U S A **68**(8): 1833-1837.

Friedman, J. M. and R. L. Leibel (1992). "Tackling a weighty problem." Cell **69**(2): 217-220.

Froguel, P., M. Vaxillaire, et al. (1992). "Close linkage of glucokinase locus on chromosome 7p to early-onset non-insulin-dependent diabetes mellitus." Nature **356**(6365): 162-164.

Frosig, C., C. Roepstorff, et al. (2009). "Reduced malonyl-CoA content in recovery from exercise correlates with improved insulin-stimulated glucose uptake in human skeletal muscle." Am J Physiol Endocrinol Metab **296**(4): E787-795.

Fruhbeck, G. (2001). "A heliocentric view of leptin." Proc Nutr Soc **60**(3): 301-318.

Fujita, E., A. Soyama, et al. (2003). "RA175, which is the mouse ortholog of TSLC1, a tumor suppressor gene in human lung cancer, is a cell adhesion molecule." Exp Cell Res **287**(1): 57-66.

Fujita, E., Y. Tanabe, et al. (2012). "Cadm1-expressing synapses on Purkinje cell dendrites are involved in mouse ultrasonic vocalization activity." PLoS ONE **7**(1): e30151.

Fujita, E., Y. Tanabe, et al. (2012). "A complex of synaptic adhesion molecule CADM1, a molecule related to Autism Spectrum Disorder, with MUPP1 in the cerebellum." J Neurochem.

Fujita, E., K. Urase, et al. (2005). "Distribution of RA175/TSLC1/SynCAM, a member of the immunoglobulin superfamily, in the developing nervous system." Brain Res Dev Brain Res **154**(2): 199-209.

Galichet, C., R. Lovell-Badge, et al. (2010). "Nestin-Cre mice are affected by hypopituitarism, which is not due to significant activity of the transgene in the pituitary gland." PLoS ONE **5**(7): e11443.

Gammelsaeter, R., M. Froyland, et al. (2004). "Glycine, GABA and their transporters in pancreatic islets of Langerhans: evidence for a paracrine transmitter interplay." J Cell Sci **117**(Pt 17): 3749-3758.

Gao, Q., G. Mezei, et al. (2007). "Anorectic estrogen mimics leptin's effect on the rewiring of melanocortin cells and Stat3 signaling in obese animals." Nat Med **13**(1): 89-94.

Gao, Z., D. Hwang, et al. (2002). "Serine phosphorylation of insulin receptor substrate 1 by inhibitor kappa B kinase complex." J Biol Chem **277**(50): 48115-48121.

Garofalo, R. S., S. J. Orena, et al. (2003). "Severe diabetes, age-dependent loss of adipose tissue, and mild growth deficiency in mice lacking Akt2/PKB beta." J Clin Invest **112**(2): 197-208.

Garza, J. C., C. S. Kim, et al. (2008). "Adeno-associated virus-mediated knockdown of melanocortin-4 receptor in the paraventricular nucleus of the hypothalamus promotes high-fat diet-induced hyperphagia and obesity." J Endocrinol **197**(3): 471-482.

Gautam, D., S. J. Han, et al. (2006). "A critical role for beta cell M3 muscarinic acetylcholine receptors in regulating insulin release and blood glucose homeostasis in vivo." Cell Metab **3**(6): 449-461.

Gee, C. E., C. L. Chen, et al. (1983). "Identification of proopiomelanocortin neurones in rat hypothalamus by in situ cDNA-mRNA hybridization." Nature **306**(5941): 374-376.

Ghilardi, N. and R. C. Skoda (1997). "The leptin receptor activates janus kinase 2 and signals for proliferation in a factor-dependent cell line." Mol Endocrinol **11**(4): 393-399.

Ghilardi, N., S. Ziegler, et al. (1996). "Defective STAT signaling by the leptin receptor in diabetic mice." Proc Natl Acad Sci U S A **93**(13): 6231-6235.

Giangreco, A., K. B. Jensen, et al. (2009). "Necl2 regulates epidermal adhesion and wound repair." Development **136**(20): 3505-3514.

Gloyn, A. L., M. N. Weedon, et al. (2003). "Large-scale association studies of variants in genes encoding the pancreatic beta-cell KATP channel subunits Kir6.2 (KCNJ11) and SUR1 (ABCC8) confirm that the KCNJ11 E23K variant is associated with type 2 diabetes." Diabetes **52**(2): 568-572.

Gomperts, B. D., I. M. Kramer, et al. (2003). "Signal transduction." Academic Press: 315-343.

Graf, E. R., X. Zhang, et al. (2004). "Neurexins induce differentiation of GABA and glutamate postsynaptic specializations via neuroligins." Cell **119**(7): 1013-1026.

Grant, S. F., G. Thorleifsson, et al. (2006). "Variant of transcription factor 7-like 2 (TCF7L2) gene confers risk of type 2 diabetes." Nat Genet **38**(3): 320-323.

Grillo, C. A., G. G. Piroli, et al. (2011). "Obesity/hyperleptinemic phenotype adversely affects hippocampal plasticity: effects of dietary restriction." Physiol Behav **104**(2): 235-241.

Guariglia, S. R., E. C. Jenkins, Jr., et al. (2011). "Chlorination byproducts induce gender specific autistic-like behaviors in CD-1 mice." Neurotoxicology **32**(5): 545-553.

Hahn, T. M., J. F. Breininger, et al. (1998). "Coexpression of Agrp and NPY in fasting-activated hypothalamic neurons." Nat Neurosci **1**(4): 271-272.

Halaas, J. L., K. S. Gajiwala, et al. (1995). "Weight-reducing effects of the plasma protein encoded by the obese gene." Science **269**(5223): 543-546.

Halban, P. A. (2004). "Cellular sources of new pancreatic beta cells and therapeutic implications for regenerative medicine." Nat Cell Biol **6**(11): 1021-1025.

Hamaguchi, T., H. Fukushima, et al. (1991). "Abnormal glucagon response to arginine and its normalization in obese hyperinsulinaemic patients with glucose intolerance: importance of insulin action on pancreatic alpha cells." Diabetologia **34**(11): 801-806.

Hami, J., A. Sadr-Nabavi, et al. (2012). "Sex differences and left-right asymmetries in expression of insulin and insulin-like growth factor-1 receptors in developing rat hippocampus." Brain Struct Funct **217**(2): 293-302.

Hardin, D. S., B. Azzarelli, et al. (1995). "Mechanisms of enhanced insulin sensitivity in endurance-trained athletes: effects on blood flow and differential expression of GLUT 4 in skeletal muscles." J Clin Endocrinol Metab **80**(8): 2437-2446.

Haskell-Luevano, C., P. Chen, et al. (1999). "Characterization of the neuroanatomical distribution of agouti-related protein immunoreactivity in the rhesus monkey and the rat." Endocrinology **140**(3): 1408-1415.

Havrankova, J., J. Roth, et al. (1978). "Insulin receptors are widely distributed in the central nervous system of the rat." Nature **272**(5656): 827-829.

Hawkins, P. T., T. R. Jackson, et al. (1992). "Platelet-derived growth factor stimulates synthesis of PtdIns(3,4,5)P3 by activating a PtdIns(4,5)P2 3-OH kinase." Nature **358**(6382): 157-159.

Heim, M. H., I. M. Kerr, et al. (1995). "Contribution of STAT SH2 groups to specific interferon signaling by the Jak-STAT pathway." Science **267**(5202): 1347-1349.

Herder, C. and M. Roden (2011). "Genetics of type 2 diabetes: pathophysiologic and clinical relevance." Eur J Clin Invest **41**(6): 679-692.

Herman, W. H., S. S. Fajans, et al. (1997). "Diminished insulin and glucagon secretory responses to arginine in nondiabetic subjects with a mutation in the hepatocyte nuclear factor-4alpha/MODY1 gene." Diabetes **46**(11): 1749-1754.

Hileman, S. M., D. D. Pierroz, et al. (2002). "Characterizaton of short isoforms of the leptin receptor in rat cerebral microvessels and of brain uptake of leptin in mouse models of obesity." Endocrinology **143**(3): 775-783.

Hillebrand, J. J., D. de Wied, et al. (2002). "Neuropeptides, food intake and body weight regulation: a hypothalamic focus." Peptides **23**(12): 2283-2306.

Ho, A., W. Morishita, et al. (2003). "A role for Mints in transmitter release: Mint 1 knockout mice exhibit impaired GABAergic synaptic transmission." Proc Natl Acad Sci U S A **100**(3): 1409-1414.

Hong, J., M. H. Gui, et al. (2008). "Differences in insulin resistance and pancreatic B-cell function in obese subjects with isolated impaired glucose tolerance and isolated impaired fasting glucose." Diabet Med **25**(1): 73-79.

Horvath, T. L., B. Sarman, et al. (2010). "Synaptic input organization of the melanocortin system predicts diet-induced hypothalamic reactive gliosis and obesity." Proc Natl Acad Sci U S A **107**(33): 14875-14880.

Hotamisligil, G. S., P. Peraldi, et al. (1996). "IRS-1-mediated inhibition of insulin receptor tyrosine kinase activity in TNF-alpha- and obesity-induced insulin resistance." Science **271**(5249): 665-668.

Hotamisligil, G. S., N. S. Shargill, et al. (1993). "Adipose expression of tumor necrosis factor-alpha: direct role in obesity-linked insulin resistance." Science **259**(5091): 87-91.

Hoy, J. L., J. R. Constable, et al. (2009). "SynCAM1 recruits NMDA receptors via protein 4.1B." Mol Cell Neurosci **42**(4): 466-483.

Hu, F. B., R. J. Sigal, et al. (1999). "Walking compared with vigorous physical activity and risk of type 2 diabetes in women: a prospective study." JAMA **282**(15): 1433-1439.

Hummel, K. P., M. M. Dickie, et al. (1966). "Diabetes, a new mutation in the mouse." Science **153**(740): 1127-1128.

Ingalls, A. M., M. M. Dickie, et al. (1950). "Obese, a new mutation in the house mouse." J Hered **41**(12): 317-318.

Ito, A., M. Hagiyama, et al. (2008). "Nerve-mast cell and smooth muscle-mast cell interaction mediated by cell adhesion molecule-1, CADM1." J Smooth Muscle Res **44**(2): 83-93.

Ito, A., N. Ichiyanagi, et al. (2012). "Adhesion molecule CADM1 contributes to gap junctional communication among pancreatic islet alpha-cells and prevents their excessive secretion of glucagon." Islets **4**(1).

Ito, A., T. Jippo, et al. (2003). "SgIGSF: a new mast-cell adhesion molecule used for attachment to fibroblasts and transcriptionally regulated by MITF." Blood **101**(7): 2601-2608.

Jacobowitz, D. M. and T. L. O'Donohue (1978). "alpha-Melanocyte stimulating hormone: immunohistochemical identification and mapping in neurons of rat brain." Proc Natl Acad Sci U S A **75**(12): 6300-6304.

James, D. E., K. M. Burleigh, et al. (1985). "Time dependence of insulin action in muscle and adipose tissue in the rat in vivo. An increasing response in adipose tissue with time." Diabetes **34**(10): 1049-1054.

Jetton, T. L., J. Lausier, et al. (2005). "Mechanisms of compensatory beta-cell growth in insulin-resistant rats: roles of Akt kinase." Diabetes **54**(8): 2294-2304.

Jetton, T. L., Y. Liang, et al. (1994). "Analysis of upstream glucokinase promoter activity in transgenic mice and identification of glucokinase in rare neuroendocrine cells in the brain and gut." J Biol Chem **269**(5): 3641-3654.

Jin, T. and L. Liu (2008). "The Wnt signaling pathway effector TCF7L2 and type 2 diabetes mellitus." Mol Endocrinol **22**(11): 2383-2392.

Johnson, J. H., C. B. Newgard, et al. (1990). "The high Km glucose transporter of islets of Langerhans is functionally similar to the low affinity transporter of liver and has an identical primary sequence." J Biol Chem **265**(12): 6548-6551.

Kaczmarski, R. S. and G. J. Mufti (1991). "The cytokine receptor superfamily." Blood Rev **5**(3): 193-203.

Kahn, B. B. and J. S. Flier (2000). "Obesity and insulin resistance." J Clin Invest **106**(4): 473-481.

Kahn, S. E. (2003). "The relative contributions of insulin resistance and beta-cell dysfunction to the pathophysiology of Type 2 diabetes." Diabetologia **46**(1): 3-19.

Kaiyala, K. J., G. J. Morton, et al. (2010). "Identification of body fat mass as a major determinant of metabolic rate in mice." Diabetes **59**(7): 1657-1666.

Kasuga, M., Y. Zick, et al. (1982). "Insulin stimulation of phosphorylation of the beta subunit of the insulin receptor. Formation of both phosphoserine and phosphotyrosine." J Biol Chem **257**(17): 9891-9894.

Kasuga, M., Y. Zick, et al. (1982). "Insulin stimulates tyrosine phosphorylation of the insulin receptor in a cell-free system." Nature **298**(5875): 667-669.

Kawano, S., W. Ikeda, et al. (2009). "Silencing of ErbB3/ErbB2 signaling by immunoglobulin-like Necl-2." J Biol Chem **284**(35): 23793-23805.

Keahey, H. H., A. S. Rajan, et al. (1989). "Characterization of voltage-dependent Ca2+ channels in beta-cell line." Diabetes **38**(2): 188-193.

Kellerer, M., M. Koch, et al. (1997). "Leptin activates PI-3 kinase in C2C12 myotubes via janus kinase-2 (JAK-2) and insulin receptor substrate-2 (IRS-2) dependent pathways." Diabetologia **40**(11): 1358-1362.

Kennedy, G. C. (1953). "The role of depot fat in the hypothalamic control of food intake in the rat." Proc R Soc Lond B Biol Sci **140**(901): 578-596.

King, P. J., P. S. Widdowson, et al. (1999). "Regulation of neuropeptide Y release by neuropeptide Y receptor ligands and calcium channel antagonists in hypothalamic slices." J Neurochem **73**(2): 641-646.

Kitamura, T., Y. Feng, et al. (2006). "Forkhead protein FoxO1 mediates Agrp-dependent effects of leptin on food intake." Nat Med **12**(5): 534-540.

Klip, A. and M. R. Paquet (1990). "Glucose transport and glucose transporters in muscle and their metabolic regulation." Diabetes Care **13**(3): 228-243.

Koma, Y., T. Furuno, et al. (2008). "Cell adhesion molecule 1 is a novel pancreatic-islet cell adhesion molecule that mediates nerve-islet cell interactions." Gastroenterology **134**(5): 1544-1554.

Kong, D., Q. Tong, et al. (2012). "GABAergic RIP-Cre Neurons in the Arcuate Nucleus Selectively Regulate Energy Expenditure." Cell **151**(3): 645-657.

Konner, A. C., S. Hess, et al. (2011). "Role for insulin signaling in catecholaminergic neurons in control of energy homeostasis." Cell Metab **13**(6): 720-728.

Konner, A. C., R. Janoschek, et al. (2007). "Insulin action in AgRP-expressing neurons is required for suppression of hepatic glucose production." Cell Metab **5**(6): 438-449.

Korner, J., E. Savontaus, et al. (2001). "Leptin regulation of Agrp and Npy mRNA in the rat hypothalamus." J Neuroendocrinol **13**(11): 959-966.

Kralisch, S., J. Klein, et al. (2005). "Isoproterenol, TNFalpha, and insulin downregulate adipose triglyceride lipase in 3T3-L1 adipocytes." Mol Cell Endocrinol **240**(1-2): 43-49.

Kraniou, G. N., D. Cameron-Smith, et al. (2006). "Acute exercise and GLUT4 expression in human skeletal muscle: influence of exercise intensity." J Appl Physiol **101**(3): 934-937.

Krapivinsky, G., I. Medina, et al. (2004). "SynGAP-MUPP1-CaMKII synaptic complexes regulate p38 MAP kinase activity and NMDA receptor-dependent synaptic AMPA receptor potentiation." Neuron **43**(4): 563-574.

Kriska, A. M., A. Saremi, et al. (2003). "Physical activity, obesity, and the incidence of type 2 diabetes in a high-risk population." Am J Epidemiol **158**(7): 669-675.

Krol, J., I. Loedige, et al. (2010). "The widespread regulation of microRNA biogenesis, function and decay." Nat Rev Genet **11**(9): 597-610.

Krude, H., H. Biebermann, et al. (1998). "Severe early-onset obesity, adrenal insufficiency and red hair pigmentation caused by POMC mutations in humans." Nat Genet **19**(2): 155-157.

Kublaoui, B. M., T. Gemelli, et al. (2008). "Oxytocin deficiency mediates hyperphagic obesity of Sim1 haploinsufficient mice." Mol Endocrinol **22**(7): 1723-1734.

Kubota, N., Y. Terauchi, et al. (2002). "Disruption of adiponectin causes insulin resistance and neointimal formation." J Biol Chem **277**(29): 25863-25866.

Kulkarni, R. N., J. C. Bruning, et al. (1999). "Tissue-specific knockout of the insulin receptor in pancreatic beta cells creates an insulin secretory defect similar to that in type 2 diabetes." Cell **96**(3): 329-339.

Kurose, T., Y. Seino, et al. (1990). "Mechanism of sympathetic neural regulation of insulin, somatostatin, and glucagon secretion." Am J Physiol **258**(1 Pt 1): E220-227.

Lage, R., C. Dieguez, et al. (2008). "AMPK: a metabolic gauge regulating whole-body energy homeostasis." Trends Mol Med **14**(12): 539-549.

Larue, C. G. and J. Le Magnen (1972). "The olfactory control of meal pattern in rats." Physiol Behav **9**(5): 817-821.

Lavan, B. E., M. R. Kuhne, et al. (1992). "The association of insulin-elicited phosphotyrosine proteins with src homology 2 domains." J Biol Chem **267**(16): 11631-11636.

Lee, G. H., R. Proenca, et al. (1996). "Abnormal splicing of the leptin receptor in diabetic mice." Nature **379**(6566): 632-635.

Leibel, R. L., W. K. Chung, et al. (1997). "The molecular genetics of rodent single gene obesities." J Biol Chem **272**(51): 31937-31940.

Leibiger, B., I. B. Leibiger, et al. (2001). "Selective insulin signaling through A and B insulin receptors regulates transcription of insulin and glucokinase genes in pancreatic beta cells." Mol Cell **7**(3): 559-570.

LeRoith, D. (2002). "Beta-cell dysfunction and insulin resistance in type 2 diabetes: role of metabolic and genetic abnormalities." Am J Med **113 Suppl 6A**: 3S-11S.

LeRoith, D. and S. Yakar (2007). "Mechanisms of disease: metabolic effects of growth hormone and insulin-like growth factor 1." Nat Clin Pract Endocrinol Metab **3**(3): 302-310.

Levine, J. A. (2004). "Non-exercise activity thermogenesis (NEAT)." Nutr Rev **62**(7 Pt 2): S82-97.

Li, S., J. H. Zhao, et al. (2011). "Genetic predisposition to obesity leads to increased risk of type 2 diabetes." Diabetologia **54**(4): 776-782.

Li, Y., J. R. Knapp, et al. (2003). "Enlargement of interscapular brown adipose tissue in growth hormone antagonist transgenic and in growth hormone receptor gene-disrupted dwarf mice." Exp Biol Med (Maywood) **228**(2): 207-215.

Lin, H. V., L. Plum, et al. (2010). "Divergent regulation of energy expenditure and hepatic glucose production by insulin receptor in agouti-related protein and POMC neurons." Diabetes **59**(2): 337-346.

List, E. O., L. Sackmann-Sala, et al. (2011). "Endocrine parameters and phenotypes of the growth hormone receptor gene disrupted (GHR-/-) mouse." Endocr Rev **32**(3): 356-386.

Liu, J. L., K. T. Coschigano, et al. (2004). "Disruption of growth hormone receptor gene causes diminished pancreatic islet size and increased insulin sensitivity in mice." Am J Physiol Endocrinol Metab **287**(3): E405-413.

Liu, S. C., Q. Wang, et al. (1999). "Insulin receptor substrate 3 is not essential for growth or glucose homeostasis." J Biol Chem **274**(25): 18093-18099.

Liu, Y. F., K. Paz, et al. (2001). "Insulin stimulates PKCzeta -mediated phosphorylation of insulin receptor substrate-1 (IRS-1). A self-attenuated mechanism to negatively regulate the function of IRS proteins." J Biol Chem **276**(17): 14459-14465.

Liu, Y. Q., T. L. Jetton, et al. (2002). "beta-Cell adaptation to insulin resistance. Increased pyruvate carboxylase and malate-pyruvate shuttle activity in islets of nondiabetic Zucker fatty rats." J Biol Chem **277**(42): 39163-39168.

Loeffler, J. P., B. A. Demeneix, et al. (1986). "GABA differentially regulates the gene expression of proopiomelanocortin in rat intermediate and anterior pituitary." Peptides **7**(2): 253-258.

Löffler, G. and P. E. Petrides (2003). Biochemie & Pathobiochemie.

Lothian, C. and U. Lendahl (1997). "An evolutionarily conserved region in the second intron of the human nestin gene directs gene expression to CNS progenitor cells and to early neural crest cells." Eur J Neurosci **9**(3): 452-462.

Louis, G. W., G. M. Leinninger, et al. (2010). "Direct innervation and modulation of orexin neurons by lateral hypothalamic LepRb neurons." J Neurosci **30**(34): 11278-11287.

Lovis, P., E. Roggli, et al. (2008). "Alterations in microRNA expression contribute to fatty acid-induced pancreatic beta-cell dysfunction." Diabetes **57**(10): 2728-2736.

MacDonald, M. J. (1993). "Glucose enters mitochondrial metabolism via both carboxylation and decarboxylation of pyruvate in pancreatic islets." Metabolism **42**(10): 1229-1231.

MacDonald, P. E., S. Obermuller, et al. (2005). "Regulated exocytosis and kiss-and-run of synaptic-like microvesicles in INS-1 and primary rat beta-cells." Diabetes **54**(3): 736-743.

Maehama, T. and J. E. Dixon (1998). "The tumor suppressor, PTEN/MMAC1, dephosphorylates the lipid second messenger, phosphatidylinositol 3,4,5-trisphosphate." J Biol Chem **273**(22): 13375-13378.

Maffei, M., H. Fei, et al. (1995). "Increased expression in adipocytes of ob RNA in mice with lesions of the hypothalamus and with mutations at the db locus." Proc Natl Acad Sci U S A **92**(15): 6957-6960.

Maffei, M., J. Halaas, et al. (1995). "Leptin levels in human and rodent: measurement of plasma leptin and ob RNA in obese and weight-reduced subjects." Nat Med **1**(11): 1155-1161.

Maisonnette, S., S. Morato, et al. (1993). "Role of resocialization and of 5-HT1A receptor activation on the anxiogenic effects induced by isolation in the elevated plus-maze test." Physiol Behav **54**(4): 753-758.

Malecki, M. T., U. S. Jhala, et al. (1999). "Mutations in NEUROD1 are associated with the development of type 2 diabetes mellitus." Nat Genet **23**(3): 323-328.

Mao, J., T. Yang, et al. (2009). "aP2-Cre-mediated inactivation of acetyl-CoA carboxylase 1 causes growth retardation and reduced lipid accumulation in adipose tissues." Proc Natl Acad Sci U S A **106**(41): 17576-17581.

Marks, J. L., D. Porte, Jr., et al. (1990). "Localization of insulin receptor mRNA in rat brain by in situ hybridization." Endocrinology **127**(6): 3234-3236.

Martin, L. A., D. Goldowitz, et al. (2010). "Repetitive behavior and increased activity in mice with Purkinje cell loss: a model for understanding the role of cerebellar pathology in autism." Eur J Neurosci **31**(3): 544-555.

Masuda, M., M. Yageta, et al. (2002). "The tumor suppressor protein TSLC1 is involved in cell-cell adhesion." J Biol Chem **277**(34): 31014-31019.

Mauras, N., S. Welch, et al. (1998). "Ovarian hyperandrogenism is associated with insulin resistance to both peripheral carbohydrate and whole-body protein metabolism in postpubertal young females: a metabolic study." J Clin Endocrinol Metab **83**(6): 1900-1905.

Maximov, A., T. C. Sudhof, et al. (1999). "Association of neuronal calcium channels with modular adaptor proteins." J Biol Chem **274**(35): 24453-24456.

May, T., K. Cornish, et al. (2012). "Gender Profiles of Behavioral Attention in Children With Autism Spectrum Disorder." J Atten Disord.

McGowan, M. K., K. M. Andrews, et al. (1992). "Chronic intrahypothalamic infusions of insulin or insulin antibodies alter body weight and food intake in the rat." Physiol Behav **51**(4): 753-766.

McInnes, C., J. Wang, et al. (1998). "Structure-based minimization of transforming growth factor-alpha (TGF-alpha) through NMR analysis of the receptor-bound ligand. Design, solution structure, and activity of TGF-alpha 8-50." J Biol Chem **273**(42): 27357-27363.

Melkman-Zehavi, T., R. Oren, et al. (2011). "miRNAs control insulin content in pancreatic beta-cells via downregulation of transcriptional repressors." EMBO J **30**(5): 835-845.

Mertz, R. J., J. F. Worley, et al. (1996). "Activation of stimulus-secretion coupling in pancreatic beta-cells by specific products of glucose metabolism. Evidence for privileged signaling by glycolysis." J Biol Chem **271**(9): 4838-4845.

Meur, G., Q. Qian, et al. (2011). "Nucleo-cytosolic shuttling of FoxO1 directly regulates mouse Ins2 but not Ins1 gene expression in pancreatic beta cells (MIN6)." J Biol Chem **286**(15): 13647-13656.

Meyer, C., H. J. Woerle, et al. (2004). "Abnormal renal, hepatic, and muscle glucose metabolism following glucose ingestion in type 2 diabetes." Am J Physiol Endocrinol Metab **287**(6): E1049-1056.

Meyer, C. W., D. Korthaus, et al. (2004). "A novel missense mutation in the mouse growth hormone gene causes semidominant dwarfism, hyperghrelinemia, and obesity." Endocrinology **145**(5): 2531-2541.

Meyer, C. W., J. Neubronner, et al. (2007). "Expanding the body mass range: associations between BMR and tissue morphology in wild type and mutant dwarf mice (David mice)." J Comp Physiol B **177**(2): 183-192.

Michael, M. D., R. N. Kulkarni, et al. (2000). "Loss of insulin signaling in hepatocytes leads to severe insulin resistance and progressive hepatic dysfunction." Mol Cell **6**(1): 87-97.

Mignogna, P. and D. Viggiano (2010). "Brain distribution of genes related to changes in locomotor activity." Physiol Behav **99**(5): 618-626.

Minokoshi, Y., T. Alquier, et al. (2004). "AMP-kinase regulates food intake by responding to hormonal and nutrient signals in the hypothalamus." Nature **428**(6982): 569-574.

Mitrakou, A., D. Kelley, et al. (1990). "Contribution of abnormal muscle and liver glucose metabolism to postprandial hyperglycemia in NIDDM." Diabetes **39**(11): 1381-1390.

Miyazaki, J., K. Araki, et al. (1990). "Establishment of a pancreatic beta cell line that retains glucose-inducible insulin secretion: special reference to expression of glucose transporter isoforms." Endocrinology **127**(1): 126-132.

Mizuno, T. M., S. P. Kleopoulos, et al. (1998). "Hypothalamic pro-opiomelanocortin mRNA is reduced by fasting and [corrected] in ob/ob and db/db mice, but is stimulated by leptin." Diabetes **47**(2): 294-297.

Mori, A., K. Okuyama, et al. (2002). "Alteration of methamphetamine-induced striatal dopamine release in mint-1 knockout mice." Neurosci Res **43**(3): 251-257.

Mori, H., R. Hanada, et al. (2004). "Socs3 deficiency in the brain elevates leptin sensitivity and confers resistance to diet-induced obesity." Nat Med **10**(7): 739-743.

Murakami, Y. (2005). "Involvement of a cell adhesion molecule, TSLC1/IGSF4, in human oncogenesis." Cancer Sci **96**(9): 543-552.

Muraoka, O., B. Xu, et al. (2003). "Leptin-induced transactivation of NPY gene promoter mediated by JAK1, JAK2 and STAT3 in the neural cell lines." Neurochem Int **42**(7): 591-601.

Myers, M. G., Jr., J. M. Backer, et al. (1992). "IRS-1 activates phosphatidylinositol 3'-kinase by associating with src homology 2 domains of p85." Proc Natl Acad Sci U S A **89**(21): 10350-10354.

Nakanishi, S., A. Inoue, et al. (1979). "Nucleotide sequence of cloned cDNA for bovine corticotropin-beta-lipotropin precursor." Nature **278**(5703): 423-427.

Nakashima, K., Y. Kanda, et al. (2009). "MIN6 is not a pure beta cell line but a mixed cell line with other pancreatic endocrine hormones." Endocr J **56**(1): 45-53.

Nakazato, M., N. Murakami, et al. (2001). "A role for ghrelin in the central regulation of feeding." Nature **409**(6817): 194-198.

Nesher, R., I. E. Karl, et al. (1985). "Dissociation of effects of insulin and contraction on glucose transport in rat epitrochlearis muscle." Am J Physiol **249**(3 Pt 1): C226-232.

Nguyen, K. T., P. Tajmir, et al. (2006). "Essential role of Pten in body size determination and pancreatic beta-cell homeostasis in vivo." Mol Cell Biol **26**(12): 4511-4518.

Niklasson, M., P. Daneryd, et al. (2000). "Effects of exercise on insulin distribution and action in testosterone-treated oophorectomized female rats." J Appl Physiol **88**(6): 2116-2122.

Nolan, C. J., P. Damm, et al. (2011). "Type 2 diabetes across generations: from pathophysiology to prevention and management." Lancet **378**(9786): 169-181.

Nuutila, P., M. J. Knuuti, et al. (1994). "Different alterations in the insulin-stimulated glucose uptake in the athlete's heart and skeletal muscle." J Clin Invest **93**(5): 2267-2274.

Obici, S., Z. Feng, et al. (2002). "Decreasing hypothalamic insulin receptors causes hyperphagia and insulin resistance in rats." Nat Neurosci **5**(6): 566-572.

Obici, S., B. B. Zhang, et al. (2002). "Hypothalamic insulin signaling is required for inhibition of glucose production." Nat Med **8**(12): 1376-1382.

Ohshige, T., M. Iwata, et al. (2011). "Association of new loci identified in European genome-wide association studies with susceptibility to type 2 diabetes in the Japanese." PLoS ONE **6**(10): e26911.

Olszewski, P. K., R. Fredriksson, et al. (2011). "Fto colocalizes with a satiety mediator oxytocin in the brain and upregulates oxytocin gene expression." Biochem Biophys Res Commun **408**(3): 422-426.

Olszewski, P. K., R. Fredriksson, et al. (2009). "Hypothalamic FTO is associated with the regulation of energy intake not feeding reward." BMC Neurosci **10**: 129.

Osborn, O., M. Sanchez-Alavez, et al. (2010). "Metabolic characterization of a mouse deficient in all known leptin receptor isoforms." Cell Mol Neurobiol **30**(1): 23-33.

Osei, K., S. Rhinesmith, et al. (2004). "Impaired insulin sensitivity, insulin secretion, and glucose effectiveness predict future development of impaired glucose tolerance

and type 2 diabetes in pre-diabetic African Americans: implications for primary diabetes prevention." Diabetes Care **27**(6): 1439-1446.

Osundiji, M. A., D. D. Lam, et al. (2012). "Brain glucose sensors play a significant role in the regulation of pancreatic glucose-stimulated insulin secretion." Diabetes **61**(2): 321-328.

Ozes, O. N., H. Akca, et al. (2001). "A phosphatidylinositol 3-kinase/Akt/mTOR pathway mediates and PTEN antagonizes tumor necrosis factor inhibition of insulin signaling through insulin receptor substrate-1." Proc Natl Acad Sci U S A **98**(8): 4640-4645.

Pan, D. A., S. Lillioja, et al. (1997). "Skeletal muscle triglyceride levels are inversely related to insulin action." Diabetes **46**(6): 983-988.

Paranjape, S. A., O. Chan, et al. (2011). "Chronic reduction of insulin receptors in the ventromedial hypothalamus produces glucose intolerance and islet dysfunction in the absence of weight gain." Am J Physiol Endocrinol Metab **301**(5): E978-983.

Park, K. S., B. D. Rhee, et al. (1991). "Intra-abdominal fat is associated with decreased insulin sensitivity in healthy young men." Metabolism **40**(6): 600-603.

Paz, K., R. Hemi, et al. (1997). "A molecular basis for insulin resistance. Elevated serine/threonine phosphorylation of IRS-1 and IRS-2 inhibits their binding to the juxtamembrane region of the insulin receptor and impairs their ability to undergo insulin-induced tyrosine phosphorylation." J Biol Chem **272**(47): 29911-29918.

Pelletier, G. and L. Desy (1979). "Localization of ACTH in the human hypothalamus." Cell Tissue Res **196**(3): 525-530.

Persico, A. M. and T. Bourgeron (2006). "Searching for ways out of the autism maze: genetic, epigenetic and environmental clues." Trends Neurosci **29**(7): 349-358.

Pietri, T., C. Easley-Neal, et al. (2008). "Six cadm/SynCAM genes are expressed in the nervous system of developing zebrafish." Dev Dyn **237**(1): 233-246.

Pilkis, S. J. and D. K. Granner (1992). "Molecular physiology of the regulation of hepatic gluconeogenesis and glycolysis." Annu Rev Physiol **54**: 885-909.

Pinheiro Volp, A. C., F. C. Esteves de Oliveira, et al. (2011). "Energy expenditure: components and evaluation methods." Nutr Hosp **26**(3): 430-440.

Pinto, S., A. G. Roseberry, et al. (2004). "Rapid rewiring of arcuate nucleus feeding circuits by leptin." Science **304**(5667): 110-115.

Plata-Salaman, C. R. (1995). "Cytokines and feeding suppression: an integrative view from neurologic to molecular levels." Nutrition **11**(5 Suppl): 674-677.

Poitout, V., J. Amyot, et al. (2010). "Glucolipotoxicity of the pancreatic beta cell." Biochim Biophys Acta **1801**(3): 289-298.

Posey, K. A., D. J. Clegg, et al. (2009). "Hypothalamic proinflammatory lipid accumulation, inflammation, and insulin resistance in rats fed a high-fat diet." Am J Physiol Endocrinol Metab **296**(5): E1003-1012.

Poy, M. N., L. Eliasson, et al. (2004). "A pancreatic islet-specific microRNA regulates insulin secretion." Nature **432**(7014): 226-230.

Poy, M. N., J. Hausser, et al. (2009). "miR-375 maintains normal pancreatic α- and β-cell mass " Proc Natl Acad Sci U S A.

Prentki, M. and C. J. Nolan (2006). "Islet beta cell failure in type 2 diabetes." J Clin Invest **116**(7): 1802-1812.

Puigserver, P., J. Rhee, et al. (2003). "Insulin-regulated hepatic gluconeogenesis through FOXO1-PGC-1alpha interaction." Nature **423**(6939): 550-555.

Purkayastha, S., H. Zhang, et al. (2011). "Neural dysregulation of peripheral insulin action and blood pressure by brain endoplasmic reticulum stress." Proc Natl Acad Sci U S A **108**(7): 2939-2944.

Reetz, A., M. Solimena, et al. (1991). "GABA and pancreatic beta-cells: colocalization of glutamic acid decarboxylase (GAD) and GABA with synaptic-like microvesicles suggests their role in GABA storage and secretion." EMBO J **10**(5): 1275-1284.

Reith, R. M., J. McKenna, et al. (2012). "Loss of Tsc2 in Purkinje cells is associated with autistic-like behavior in a mouse model of tuberous sclerosis complex." Neurobiol Dis.

Rhodes, C. J. (2005). "Type 2 diabetes-a matter of beta-cell life and death?" Science **307**(5708): 380-384.

Ritvo, E. R., B. J. Freeman, et al. (1986). "Lower Purkinje cell counts in the cerebella of four autistic subjects: initial findings of the UCLA-NSAC Autopsy Research Report." Am J Psychiatry **143**(7): 862-866.

Robbins, E. M., A. J. Krupp, et al. (2010). "SynCAM 1 adhesion dynamically regulates synapse number and impacts plasticity and learning." Neuron **68**(5): 894-906.

Robertson, R. P., J. Harmon, et al. (2004). "Beta-cell glucose toxicity, lipotoxicity, and chronic oxidative stress in type 2 diabetes." Diabetes **53 Suppl 1**: S119-124.

Robertson, R. P., J. Harmon, et al. (2003). "Glucose toxicity in beta-cells: type 2 diabetes, good radicals gone bad, and the glutathione connection." Diabetes **52**(3): 581-587.

Roemmich, J. N., M. G. Huerta, et al. (2001). "Alterations in body composition and fat distribution in growth hormone-deficient prepubertal children during growth hormone therapy." Metabolism **50**(5): 537-547.

Rorsman, P. and G. Trube (1985). "Glucose dependent K+-channels in pancreatic beta-cells are regulated by intracellular ATP." Pflugers Arch **405**(4): 305-309.

Rosen, O. M., R. Herrera, et al. (1983). "Phosphorylation activates the insulin receptor tyrosine protein kinase." Proc Natl Acad Sci U S A **80**(11): 3237-3240.

Ruderman, N. B., R. Kapeller, et al. (1990). "Activation of phosphatidylinositol 3-kinase by insulin." Proc Natl Acad Sci U S A **87**(4): 1411-1415.

Rung, J., S. Cauchi, et al. (2009). "Genetic variant near IRS1 is associated with type 2 diabetes, insulin resistance and hyperinsulinemia." Nat Genet **41**(10): 1110-1115.

Saghizadeh, M., J. M. Ong, et al. (1996). "The expression of TNF alpha by human muscle. Relationship to insulin resistance." J Clin Invest **97**(4): 1111-1116.

Saltiel, A. R. and C. R. Kahn (2001). "Insulin signalling and the regulation of glucose and lipid metabolism." Nature **414**(6865): 799-806.

Saltzman, E. and S. B. Roberts (1995). "The role of energy expenditure in energy regulation: findings from a decade of research." Nutr Rev **53**(8): 209-220.

Sandau, U. S., A. E. Mungenast, et al. (2011). "SynCAM1, a Synaptic Adhesion Molecule, Is Expressed in Astrocytes and Contributes to erbB4 Receptor-Mediated Control of Female Sexual Development." Endocrinology.

Sandau, U. S., A. E. Mungenast, et al. (2011). "The Synaptic Cell Adhesion Molecule, SynCAM1, Mediates Astrocyte-to-Astrocyte and Astrocyte-to-GnRH Neuron Adhesiveness in the Mouse Hypothalamus." Endocrinology.

Sano, H., S. Kane, et al. (2003). "Insulin-stimulated phosphorylation of a Rab GTPase-activating protein regulates GLUT4 translocation." J Biol Chem **278**(17): 14599-14602.

Satoh, H., M. T. Nguyen, et al. (2004). "Adenovirus-mediated chronic "hyper-resistinemia" leads to in vivo insulin resistance in normal rats." J Clin Invest **114**(2): 224-231.

Satoh, N., Y. Ogawa, et al. (1997). "The arcuate nucleus as a primary site of satiety effect of leptin in rats." Neurosci Lett **224**(3): 149-152.

Saxena, R., L. Gianniny, et al. (2006). "Common single nucleotide polymorphisms in TCF7L2 are reproducibly associated with type 2 diabetes and reduce the insulin response to glucose in nondiabetic individuals." Diabetes **55**(10): 2890-2895.

Schmidt, R. F., G. Thews, et al. (2000). "Physiologie des Menschen." Springer Verlag **28. Auflage**.

Schwartz, G. J. and T. H. Moran (1996). "Sub-diaphragmatic vagal afferent integration of meal-related gastrointestinal signals." Neurosci Biobehav Rev **20**(1): 47-56.

Schwartz, M. W. and D. Porte, Jr. (2005). "Diabetes, obesity, and the brain." Science **307**(5708): 375-379.

Schwartz, M. W., R. J. Seeley, et al. (1996). "Identification of targets of leptin action in rat hypothalamus." J Clin Invest **98**(5): 1101-1106.

Schwartz, M. W., R. J. Seeley, et al. (1997). "Leptin increases hypothalamic pro-opiomelanocortin mRNA expression in the rostral arcuate nucleus." Diabetes **46**(12): 2119-2123.

Schwartz, M. W., A. J. Sipols, et al. (1992). "Inhibition of hypothalamic neuropeptide Y gene expression by insulin." Endocrinology **130**(6): 3608-3616.

Sciacchitano, S. and S. I. Taylor (1997). "Cloning, tissue expression, and chromosomal localization of the mouse IRS-3 gene." Endocrinology **138**(11): 4931-4940.

Shah, P., A. Vella, et al. (2000). "Lack of suppression of glucagon contributes to postprandial hyperglycemia in subjects with type 2 diabetes mellitus." J Clin Endocrinol Metab **85**(11): 4053-4059.

Shih, D. Q., S. Screenan, et al. (2001). "Loss of HNF-1alpha function in mice leads to abnormal expression of genes involved in pancreatic islet development and metabolism." Diabetes **50**(11): 2472-2480.

Shimada, K., T. Tachibana, et al. (2012). "Temporal and Spatial Cellular Distribution of Neural Crest Derivatives and Alpha Cells during Islet Development." Acta Histochem Cytochem **45**(1): 65-75.

Shimomura, I., M. Matsuda, et al. (2000). "Decreased IRS-2 and increased SREBP-1c lead to mixed insulin resistance and sensitivity in livers of lipodystrophic and ob/ob mice." Mol Cell **6**(1): 77-86.

Shingai, T., W. Ikeda, et al. (2003). "Implications of nectin-like molecule-2/IGSF4/RA175/SgIGSF/TSLC1/SynCAM1 in cell-cell adhesion and transmembrane protein localization in epithelial cells." J Biol Chem **278**(37): 35421-35427.

Shoelson, S. E., S. Chatterjee, et al. (1992). "YMXM motifs of IRS-1 define substrate specificity of the insulin receptor kinase." Proc Natl Acad Sci U S A **89**(6): 2027-2031.

Shuto, Y., T. Shibasaki, et al. (2002). "Hypothalamic growth hormone secretagogue receptor regulates growth hormone secretion, feeding, and adiposity." J Clin Invest **109**(11): 1429-1436.

Sipols, A. J., D. G. Baskin, et al. (1995). "Effect of intracerebroventricular insulin infusion on diabetic hyperphagia and hypothalamic neuropeptide gene expression." Diabetes **44**(2): 147-151.

Skoglund, G., I. Lundquist, et al. (1988). "Selective alpha 2-adrenoceptor activation by clonidine: effects on 45Ca2+ efflux and insulin secretion from isolated rat islets." Acta Physiol Scand **132**(3): 289-296.

Skolnik, E. Y., C. H. Lee, et al. (1993). "The SH2/SH3 domain-containing protein GRB2 interacts with tyrosine-phosphorylated IRS1 and Shc: implications for insulin control of ras signalling." EMBO J **12**(5): 1929-1936.

Skyler, J. S. (2004). "Diabetes mellitus: pathogenesis and treatment strategies." J Med Chem **47**(17): 4113-4117.

Smith, S. B., H. Watada, et al. (2000). "Autoregulation and maturity onset diabetes of the young transcription factors control the human PAX4 promoter." J Biol Chem **275**(47): 36910-36919.

Sohn, J. W., Y. Xu, et al. (2011). "Serotonin 2C receptor activates a distinct population of arcuate pro-opiomelanocortin neurons via TRPC channels." Neuron **71**(3): 488-497.

Stack, C. M., M. A. Lim, et al. (2008). "Deficits in social behavior and reversal learning are more prevalent in male offspring of VIP deficient female mice." Exp Neurol **211**(1): 67-84.

Stagi, M., A. I. Fogel, et al. (2010). "SynCAM 1 participates in axo-dendritic contact assembly and shapes neuronal growth cones." Proc Natl Acad Sci U S A **107**(16): 7568-7573.

Steele-Perkins, G., J. Turner, et al. (1988). "Expression and characterization of a functional human insulin-like growth factor I receptor." J Biol Chem **263**(23): 11486-11492.

Stephens, T. W., M. Basinski, et al. (1995). "The role of neuropeptide Y in the antiobesity action of the obese gene product." Nature **377**(6549): 530-532.

Stoffers, D. A., N. T. Zinkin, et al. (1997). "Pancreatic agenesis attributable to a single nucleotide deletion in the human IPF1 gene coding sequence." Nat Genet **15**(1): 106-110.

Stolar, M. (2010). "Glycemic control and complications in type 2 diabetes mellitus." Am J Med **123**(3 Suppl): S3-11.

Stumvoll, M. and H. Haring (2002). "The peroxisome proliferator-activated receptor-gamma2 Pro12Ala polymorphism." Diabetes **51**(8): 2341-2347.

Suckow, A. T., D. Comoletti, et al. (2008). "Expression of neurexin, neuroligin, and their cytoplasmic binding partners in the pancreatic beta-cells and the involvement of neuroligin in insulin secretion." Endocrinology **149**(12): 6006-6017.

Sun, X. J., L. M. Wang, et al. (1995). "Role of IRS-2 in insulin and cytokine signalling." Nature **377**(6545): 173-177.

Swallow, J. G., P. Koteja, et al. (2001). "Food consumption and body composition in mice selected for high wheel-running activity." J Comp Physiol B **171**(8): 651-659.

Szarek, E., P. S. Cheah, et al. (2010). "Molecular genetics of the developing neuroendocrine hypothalamus." Mol Cell Endocrinol **323**(1): 115-123.

Takahashi, Y., Y. Okimura, et al. (1997). "Leptin induces mitogen-activated protein kinase-dependent proliferation of C3H10T1/2 cells." J Biol Chem **272**(20): 12897-12900.

Takayanagi, Y., E. Fujita, et al. (2010). "Impairment of social and emotional behaviors in Cadm1-knockout mice." Biochem Biophys Res Commun **396**(3): 703-708.

Tamemoto, H., T. Kadowaki, et al. (1994). "Insulin resistance and growth retardation in mice lacking insulin receptor substrate-1." Nature **372**(6502): 182-186.

Tartaglia, L. A., M. Dembski, et al. (1995). "Identification and expression cloning of a leptin receptor, OB-R." Cell **83**(7): 1263-1271.

Tennese, A. A. and R. Wevrick (2011). "Impaired hypothalamic regulation of endocrine function and delayed counterregulatory response to hypoglycemia in Magel2-null mice." Endocrinology **152**(3): 967-978.

Thomas-Reetz, A., J. W. Hell, et al. (1993). "A gamma-aminobutyric acid transporter driven by a proton pump is present in synaptic-like microvesicles of pancreatic beta cells." Proc Natl Acad Sci U S A **90**(11): 5317-5321.

Thomas, L. A., M. R. Akins, et al. (2008). "Expression and adhesion profiles of SynCAM molecules indicate distinct neuronal functions." J Comp Neurol **510**(1): 47-67.

Thorell, A., M. F. Hirshman, et al. (1999). "Exercise and insulin cause GLUT-4 translocation in human skeletal muscle." Am J Physiol **277**(4 Pt 1): E733-741.

Tobe, K., K. Matuoka, et al. (1993). "Insulin stimulates association of insulin receptor substrate-1 with the protein abundant Src homology/growth factor receptor-bound protein 2." J Biol Chem **268**(15): 11167-11171.

Tokunaga, K., M. Fukushima, et al. (1986). "Effect of vagotomy on serum insulin in rats with paraventricular or ventromedial hypothalamic lesions." Endocrinology **119**(4): 1708-1711.

Tomita, T., V. Doull, et al. (1992). "Pancreatic islets of obese hyperglycemic mice (ob/ob)." Pancreas **7**(3): 367-375.

Tong, Q., C. P. Ye, et al. (2008). "Synaptic release of GABA by AgRP neurons is required for normal regulation of energy balance." Nat Neurosci **11**(9): 998-1000.

Tronche, F., C. Kellendonk, et al. (1999). "Disruption of the glucocorticoid receptor gene in the nervous system results in reduced anxiety." Nat Genet **23**(1): 99-103.

Tsai, P. T., C. Hull, et al. (2012). "Autistic-like behaviour and cerebellar dysfunction in Purkinje cell Tsc1 mutant mice." Nature **488**(7413): 647-651.

Tsanov, M., S. D. Vann, et al. (2011). "Differential regulation of synaptic plasticity of the hippocampal and the hypothalamic inputs to the anterior thalamus." Hippocampus **21**(1): 1-8.

Tschop, M. H., J. R. Speakman, et al. (2011). "A guide to analysis of mouse energy metabolism." Nat Methods **9**(1): 57-63.

Tschopp, O., Z. Z. Yang, et al. (2005). "Essential role of protein kinase B gamma (PKB gamma/Akt3) in postnatal brain development but not in glucose homeostasis." Development **132**(13): 2943-2954.

Tung, Y. C., E. Ayuso, et al. (2010). "Hypothalamic-specific manipulation of Fto, the ortholog of the human obesity gene FTO, affects food intake in rats." PLoS ONE **5**(1): e8771.

Tung, Y. C., S. J. Piper, et al. (2006). "A comparative study of the central effects of specific proopiomelancortin (POMC)-derived melanocortin peptides on food intake and body weight in pomc null mice." Endocrinology **147**(12): 5940-5947.

Turek, F. W., C. Joshu, et al. (2005). "Obesity and metabolic syndrome in circadian Clock mutant mice." Science **308**(5724): 1043-1045.

Tuttle, R. L., N. S. Gill, et al. (2001). "Regulation of pancreatic beta-cell growth and survival by the serine/threonine protein kinase Akt1/PKBalpha." Nat Med **7**(10): 1133-1137.

Uchida, T., M. G. Myers, Jr., et al. (2000). "IRS-4 mediates protein kinase B signaling during insulin stimulation without promoting antiapoptosis." Mol Cell Biol **20**(1): 126-138.

Vaisse, C., J. L. Halaas, et al. (1996). "Leptin activation of Stat3 in the hypothalamus of wild-type and ob/ob mice but not db/db mice." Nat Genet **14**(1): 95-97.

van de Wall, E., R. Leshan, et al. (2008). "Collective and individual functions of leptin receptor modulated neurons controlling metabolism and ingestion." Endocrinology **149**(4): 1773-1785.

van den Hoek, A. M., P. J. Voshol, et al. (2004). "Intracerebroventricular neuropeptide Y infusion precludes inhibition of glucose and VLDL production by insulin." Diabetes **53**(10): 2529-2534.

van der Weyden, L., M. J. Arends, et al. (2006). "Loss of TSLC1 causes male infertility due to a defect at the spermatid stage of spermatogenesis." Mol Cell Biol **26**(9): 3595-3609.

van Houten, M., B. I. Posner, et al. (1979). "Insulin-binding sites in the rat brain: in vivo localization to the circumventricular organs by quantitative radioautography." Endocrinology **105**(3): 666-673.

van Houten, M., B. I. Posner, et al. (1980). "Insulin binding sites localized to nerve terminals in rat median eminence and arcuate nucleus." Science **207**(4435): 1081-1083.

Viggiano, D. (2008). "The hyperactive syndrome: metanalysis of genetic alterations, pharmacological treatments and brain lesions which increase locomotor activity." Behav Brain Res **194**(1): 1-14.

Vionnet, N., M. Stoffel, et al. (1992). "Nonsense mutation in the glucokinase gene causes early-onset non-insulin-dependent diabetes mellitus." Nature **356**(6371): 721-722.

Vong, L., C. Ye, et al. (2011). "Leptin action on GABAergic neurons prevents obesity and reduces inhibitory tone to POMC neurons." Neuron **71**(1): 142-154.

Wallberg-Henriksson, H. and J. O. Holloszy (1985). "Activation of glucose transport in diabetic muscle: responses to contraction and insulin." Am J Physiol **249**(3 Pt 1): C233-237.

Wang, D. and H. S. Sul (1998). "Insulin stimulation of the fatty acid synthase promoter is mediated by the phosphatidylinositol 3-kinase pathway. Involvement of protein kinase B/Akt." J Biol Chem **273**(39): 25420-25426.

Watanabe, M., H. Hayasaki, et al. (1998). "Histologic distribution of insulin and glucagon receptors." Braz J Med Biol Res **31**(2): 243-256.

Weber, A. M., J. C. Egelhoff, et al. (2000). "Autism and the cerebellum: evidence from tuberous sclerosis." J Autism Dev Disord **30**(6): 511-517.

Weir, G. C., S. D. Knowlton, et al. (1974). "Glucagon secretion from the perfused rat pancreas. Studies with glucose and catecholamines." J Clin Invest **54**(6): 1403-1412.

Weir, J. B. (1949). "New methods for calculating metabolic rate with special reference to protein metabolism." J Physiol **109**(1-2): 1-9.

Weisberg, S. P., D. McCann, et al. (2003). "Obesity is associated with macrophage accumulation in adipose tissue." J Clin Invest **112**(12): 1796-1808.

Wellen, K. E. and G. S. Hotamisligil (2005). "Inflammation, stress, and diabetes." J Clin Invest **115**(5): 1111-1119.

Wendt, A., B. Birnir, et al. (2004). "Glucose inhibition of glucagon secretion from rat alpha-cells is mediated by GABA released from neighboring beta-cells." Diabetes **53**(4): 1038-1045.

Whitney, E. R., T. L. Kemper, et al. (2009). "Density of cerebellar basket and stellate cells in autism: evidence for a late developmental loss of Purkinje cells." J Neurosci Res **87**(10): 2245-2254.

WHO (2012). "Diabetes." Fact sheet N°312.

Wicksteed, B., M. Brissova, et al. (2010). "Conditional gene targeting in mouse pancreatic ss-Cells: analysis of ectopic Cre transgene expression in the brain." Diabetes **59**(12): 3090-3098.

Williams, K. W., L. O. Margatho, et al. (2010). "Segregation of acute leptin and insulin effects in distinct populations of arcuate proopiomelanocortin neurons." J Neurosci **30**(7): 2472-2479.

Williams, M. D. and G. M. Mitchell (2012). "MicroRNAs in Insulin Resistance and Obesity." Exp Diabetes Res **2012**: 484696.

Withers, D. J., J. S. Gutierrez, et al. (1998). "Disruption of IRS-2 causes type 2 diabetes in mice." Nature **391**(6670): 900-904.

Woods, A., K. Dickerson, et al. (2005). "Ca2+/calmodulin-dependent protein kinase kinase-beta acts upstream of AMP-activated protein kinase in mammalian cells." Cell Metab **2**(1): 21-33.

Woods, S. C., E. C. Lotter, et al. (1979). "Chronic intracerebroventricular infusion of insulin reduces food intake and body weight of baboons." Nature **282**(5738): 503-505.

Xu, W. H., R. Huber, et al. (2007). "Gender- and region-specific expression of insulin receptor protein in mouse brain: effect of mild inhibition of oxidative phosphorylation." J Neural Transm **114**(3): 373-377.

Yang, Q., T. E. Graham, et al. (2005). "Serum retinol binding protein 4 contributes to insulin resistance in obesity and type 2 diabetes." Nature **436**(7049): 356-362.

Yaswen, L., N. Diehl, et al. (1999). "Obesity in the mouse model of pro-opiomelanocortin deficiency responds to peripheral melanocortin." Nat Med **5**(9): 1066-1070.

Yeargin-Allsopp, M., C. Rice, et al. (2003). "Prevalence of autism in a US metropolitan area." JAMA **289**(1): 49-55.

Yecies, J. L., H. H. Zhang, et al. (2011). "Akt stimulates hepatic SREBP1c and lipogenesis through parallel mTORC1-dependent and independent pathways." Cell Metab **14**(1): 21-32.

Yki-Jarvinen, H. and V. A. Koivisto (1983). "Effects of body composition on insulin sensitivity." Diabetes **32**(10): 965-969.

Zhang, X., G. Zhang, et al. (2008). "Hypothalamic IKKbeta/NF-kappaB and ER stress link overnutrition to energy imbalance and obesity." Cell **135**(1): 61-73.

Zhang, Y., R. Proenca, et al. (1994). "Positional cloning of the mouse obese gene and its human homologue." Nature **372**(6505): 425-432.

Zhao, A. Z., M. M. Shinohara, et al. (2000). "Leptin induces insulin-like signaling that antagonizes cAMP elevation by glucagon in hepatocytes." J Biol Chem **275**(15): 11348-11354.

Zhao, E., M. P. Keller, et al. (2009). "Obesity and genetics regulate microRNAs in islets, liver, and adipose of diabetic mice." Mamm Genome **20**(8): 476-485.

Zhao, H., J. Guan, et al. (2010). "Up-regulated pancreatic tissue microRNA-375 associates with human type 2 diabetes through beta-cell deficit and islet amyloid deposition." Pancreas **39**(6): 843-846.

Zhao, T. J., G. Liang, et al. (2010). "Ghrelin O-acyltransferase (GOAT) is essential for growth hormone-mediated survival of calorie-restricted mice." Proc Natl Acad Sci U S A **107**(16): 7467-7472.

Zhiling, Y., E. Fujita, et al. (2008). "Mutations in the gene encoding CADM1 are associated with autism spectrum disorder." Biochem Biophys Res Commun **377**(3): 926-929.

Zhou, D., H. Liu, et al. (2012). "Common variant (rs9939609) in the FTO gene is associated with metabolic syndrome." Mol Biol Rep **39**(6): 6555-6561.

Zhu, W., D. Czyzyk, et al. (2010). "Glucose prevents the fall in ventromedial hypothalamic GABA that is required for full activation of glucose counterregulatory responses during hypoglycemia." Am J Physiol Endocrinol Metab **298**(5): E971-977.

Acknowledgments

I am sincerely grateful to Dr. Matthew Poy for providing me with this project, giving me the opportunity to work in his lab and his tremendous support. Furthermore, I would like to thank Allan Bradley and Louise van der Weyden for kindly providing *Cadm1* null and conditional *Cadm1* mice.

I would also like to thank Prof. Thomas Sommer, Prof. Mathias Treier and Prof. Thomas Willnow for their advice in the project planning and for agreeing to form my thesis committee.

Special thanks go to all members of the group of Matthew Poy for stimulating discussions and help with experimental work and proofreading this thesis. Special thanks go to Sudhir Gopal Tattikota, AG Poy, MDC Berlin-Buch, who conducted gene expression analysis by qRT-PCR. In addition, I would like to thank all members of the group of Prof. Thomas Willnow and Dr. Jan Siemens for their generous technical advice. My special thanks got to Kun Song and Dr. Mirko Moroni, who kindly provided confocal images and electrophysiological analyses for the project.

Lastly, I would like to acknowledge Dr. Petra Wiedmer for her great advice in data analysis and thesis writing.